LA-13189-T
Thesis

UC-701
Issued: November 1996

Modeling Interfacial Area Transport in Multi-Fluid Systems

Stephen Lee Yarbro

Los Alamos
NATIONAL LABORATORY
Los Alamos, New Mexico 87545

DISCLAIMER

ACKNOWLEDGMENT

I want to thank my colleages, Dana Christensen, Keith Fife and Joel Williams for their support and commiseration during this effort. A special thanks to the faculty at the New Mexico State University Chemical Engineering department, Dr. James Eakman, Dr. Stan Holbrook, Dr. Richard Long, and Dr. Stuart Munson-McGee for their hard work and willingness to make this 'novel', distance-learning graduate program a success. I also appreciate the efforts of Dr. Brian VanderHeyden, who kindly reviewed the draft and gave me the benefit of his expertise and experience.

In particular, I want to thank my advisor, Dr. Richard Long. He spent hours patiently explaining many technical details that I probably should have known at my age and stage of scholastic development. With much 'lively' discussion on the finer points of mathematics and transport phenomena, he actually helped me to learn something of this subject in spite of myself.

TABLE OF CONTENTS

APPENDICES

LIST OF TABLES

LIST OF APPENDIX TABLES

LIST OF FIGURES

LIST OF APPENDIX FIGURES

NOMENCLATURE

A = cross-sectional area, L^2

A_d = cross-sectional area of dispersed phase inlet, L^2

A_T = total channel cross-sectional area, L^2

a_{ii} = initial interfacial area concentration, L^2/L^3

a_i = interfacial area concentration, L^2/L^3

a_{ic} = calculated interfacial area, L^2/L^3

a_{im} = measured interfacial area, L^2/L^3

C_d = drag coefficient

C_{vm} = virtual mass coefficient

D = channel diameter, L

D_{32} = Sauter Mean Drop Diameter, L

Do = nominal Pipe Diameter, L

Dd = inlet pipe diameter for dispersed phase, L

Dc = inlet pipe diameter for continuous phase, L

D_T = outside pipe diameter either Kenics mixer of viewing section, L

F = force, $M\text{-}L/t^2$

F_d = drag force, $M\text{-}L/t^2$

F_{vm} = force, $M\text{-}L/t^2$

f_k = friction factor for phase k, dimensionless

f_d = friction factor for dispersed phase, dimensionless

f_m = friction factor multiplier similar to K factor or equivalent length, L_e/D

f = friction factor

$f(\mu)$ = probability function for the ensemble average

g = body force due to gravity, L/t^2

M_k = interfluid momentum transfer, $M/L\text{-}t^2$

G_g = Gas mass velocity, $M/L^2\text{-}t$

G_l = Liquid mass velocity, M/L^2-t

$\underline{n_i}$ = unit normal vector for the interface between two fluids

$\underline{n_s}$ = unit normal vector for the external surface of a volume

p_k = pressure of phase k, M/L- t^2

p_{ki} = pressure of phase k at interface, M/L- t^2

p_d = pressure of dispersed phase, M/L- t^2

p_c = pressure of continuous phase, M/L- t^2

Q_c = volumetric flow rate of continuous phase, L^3/t

Q_d = volumetric flow rate of dispersed phase, L^3/t

q_f = heat flux within phase k

q_i = heat flux at the interface between phase k and phase k+1

q_r = heat generation from reaction

r_a = reaction rate of species a, moles/t

$\underline{\underline{R}}_k$ = Reynold's Stress within phase k (defined in text), M/L- t^2

$\underline{\underline{R}}_c$ = Reynold's Stress within continuous phase (defined in text), M/L- t^2

S_i = Surface where two fluids meet within a volume, L^2

S_k = External surface boundary for the volume, L^2

$\underline{\underline{S}}$ = Interfluid Reynold's Stress (defined in text) , M/L- t^2

$\underline{\underline{T}}_k$ = Stress within phase k, M/L-t^2

$\underline{\underline{T}}_i$ = Stress at interface between phase k and phase k+1, M/L-t^2

T = temperature, K

t = time, t

U_k = internal energy of phase k

V_k = volume of a particular fluid phase k, L^3

V_{co} = initial axial linear velocity of continuous phase, L/t

V_{do} = initial axial linear velocity of dispersed phase, L/t

$\underline{v_k}$ = velocity of phase k, L/t

v_{cz} = z-component of velocity of continuous phase, L/t

v_{dz} = z-component of velocity of dispersed phase, L/t

$\underline{v}_k'$ = velocity fluctuation of phase k from the ensemble average, L/t

$\underline{v}_{ki}$ = velocity of phase k at the interface, L/t

$\underline{v}_{ki}'$ = velocity fluctuation of phase k at the interface from the ensemble average, L/t

$\underline{v}_i$ = interface velocity, L/t

$\underline{v}_i'$ = interface velocity fluctuation from the ensemble average, L/t

X = phase indicator (either 0 or 1)

$\underline{x}$ = spatial coordinates, L

Greek Letters

α_k = volume fraction of phase k

α_c = volume fraction of continuous phase

α_d = volume fraction of dispersed phase

μ_k = viscosity of phase k, M/L-t

μ_c = viscosity of continuous phase, M/L-t

μ_d = viscosity of dispersed phase, M/L-t

θ = inclination angle or contact angle, degrees

ρ_k = density of phase k, M/L^3

ρ_{ki} = density of phase k at interface, M/L^3

ρ_c = density of continuous phase , M/L^3

ρ_d = density of dispersed phase , M/L^3

σ = surface tension, M/t^2

ϕ_k = diffusion of general property of phase k

ϕ_i = diffusion of general property of phase k at the interface

ϕ_k' = fluctuation of diffusion of general property of phase k

ϕ_{ki} = diffusion of general property of phase k at the interface

ϕ_{ki}' = fluctuation of diffusion of general property of phase k at the interface

$\underline{\underline{\tau}}$ = stress in phase k (defined in text)

$\underline{\underline{\tau}}_k^{Re}$ = Reynold's stress in phase k (defined in text)

ξ = dynamic pressure coefficient

ψ_k = general property of phase k

ψ_g = generation of general property of phase k

ψ_k' = fluctuation from the ensemble average of a general property of phase k

ψ_{ki}' = fluctuation from the ensemble average of a general property of phase k at the interface

ψ_{ki} = general property of phase k at the interface

Ψ_i = general property specific to interface

Ψ_{ig} = generation of a general property specific to interface

ζ = general property for the population balance

$$\lambda = \left[\left(\frac{\rho_L}{0.075}\right)\left(\frac{\rho_g}{62.4}\right)\right]^{1/2}, \text{ for Baker flow regime plot}$$

$$\phi = \left(\frac{73}{\sigma}\right)\left[\mu_l\left(\frac{62.3}{\rho_L}\right)^2\right]^{1/3}, \text{ for Baker flow regime plot}$$

Mathematica Notation (unless otherwise noted in the comments for the specific program)

ai[z] = calculated interfacial area concentration, L^2/L^3

aio = inlet interfacial area concentration, L^2/L^3

area = cross-sectional area of the pipe, L^2

areac = cross-sectional inlet area of the continuous phase, L^2

aread = cross-sectional inlet area of the dispersed phase, L^2

areaf = inlet flow area, L^2

Cd = drag coefficient, dimensionless

Cvm = virtual mass coefficient, dimensionless

delp = calculated pressure drop, $M/L\text{-}t^2$

Dh = hydraulic diameter, L

Dia = diameter of the outer pipe, L

Diac = diameter of continuous phase inlet, L

Diad = diameter of dispersed phase inlet, L

DynP = dynamic pressure, $M/L\text{-}t^2$

f = friction factor, dimensionless

fd = dispersed phase friction factor, dimensionless

fm = friction factor multiplier, dimensionless

fphid = constant in interfacial drag equation, dimensionless

Fd = interfacial drag, $M/L\text{-}t^2$

Fw = wall drag, $M/L\text{-}t^2$

Fvw = virtual mass, $M/L\text{-}t^2$

Hc = height of flow area, L

L = length of mixer, L

mu = mixture viscosity, M/L-t

muc = continuous phase viscosity, M/L-t

mud = dispersed phase viscosity, M/L-t

nre = calculated Reynold's No., dimensionless

phic[z] = calculated continuous phase fraction, dimensionless

phid[z] = calculated dispersed phase fraction, dimensionless

phidi = inlet dispersed phase fraction, dimensionless

phido = average dispersed phase fraction, dimensionless

phico = average continuous phase fraction, dimensionless

Qc = given inlet continuous phase flowrate, L^3/t

Qd = given inlet dispersed phase flowrate, L^3/t

Qco = inlet continuous phase flowrate, L^3/t

Qdo = inlet dispersed phase flowrate, L^3/t

R = radius of outer pipe, L

re = given Reynold's No., dimensionless

rho = mixture density, M/L^3

rhoc = continuous phase density, M/L^3

rhod = dispersed phase density, M/L^3

ST = surface tension, M/t^2

theta = contact angle for Tee mixer, radians

Tzz = bubble-induced turbulence, $M/L\text{-}t^2$

Vc[z] = calculated continuous phase velocity, L/t

Vd[z] = calculated dispersed phase velocity, L/t

Vco = inlet continuous phase velocity, L/t

Vdo = inlet dispersed phase velocity, L/t

Vf = average mixture velocity, L/t

Vol = volume of mixer, L^3

Wc = width of flow area, L

we = Weber No., dimensionless

Wi = rate of surface work, $M/L^2\text{-}t^3$

Other Notation

$\langle\ \rangle$ = ensemble average (defined in text)

$\langle\ \rangle_V$ = ensemble/volume average (defined in text)

$\underline{\ }$ = vector

$\underline{\underline{\ }}$ = 2nd order tensor

$(\ )^T$ = transpose

= dimensionless variable

Notation Specific to Chapter 1 and Chapter 2

a_i = interfacial area concentration, 1/L

$A(V)$ = probability density of droplet size V in vessel

$A(V')$ = probability density of droplet size V' in vessel

$A(V - V')$ = probability density of droplet size V - V' in vessel

$A_o(V)$ = probability density of droplet size V in feed

B = 'birth' term for eqn 2.2 and eqn 2.3

C_1, C_2 = adjustable breakage constants

C_3, C_4 = adjustable coalescence constants

C_5 = adjustable turbulence constant

C_A = concentration of species A, M/L^3

d_I = impeller diameter, L

D = 'death' term eqn 2.2 and eqn 2.3

D_i = diffusion coefficient of species A, L^2/t

D_{32} = sauter mean drop diameter, L

D_o = characteristic length typically pipe diameter, L

$f, f(x_i)$ = complex unknown function for Monte Carlo approach

$f(V)$ = escape frequency of drops of volume V

$g(V')$ = breakage frequency of drops of volume V

$h(V,V')$ = collision frequency of drops of volumes V and V'

k = mass transfer coefficient, M/L^2-t

n_o = number feed rate of drops, 1/t

N = total number of drops for eqn 2.3 and eqn 2.4, number of samples eqn 2.9 to eqn 2.11

N^* = revolutions per second, 1/t

r_a = generation of species A by reaction, M/L^3-t

R = phase space for Monte Carlo approach

U = symbol for element uranium, figure 1.1, overall heat transfer coefficient, $M/T\text{-}t^3$

V = drop volume different from V' or system volume, L^3

V' = drop volume different from V, L^3

V_{max} = maximum drop volume, L^3

$\underline{v}$,v= linear velocity, L/t

$\underline{v_i}$ = interfacial velocity, L/t

$\langle v \rangle$ = average linear velocity, L/t

$\nu(V)$ = number of drops formed per breakage of drop of volume V

We = Weber No. , $\rho v^2 L/\sigma$, dimensionless

Greek Symbols Specific to Chapter 1 and Chapter 2

$\beta(V',V)$ = number fraction of drops with volume V to V + dV from by breakage of drop with volume V'

$\lambda(V-V',V)$, $\lambda(V,V')$ = coalescence efficiency of drops of volume V - V' to V and V to V'

ψ = number density distribution for eqn 2.2

ϕ = dispersed phase holdup fraction

ϕ_{dis} = particle disintegration source term

ϕ_{co} = particle coalescence source term

ϕ_{ph} = phase change source term

μ_c = continuous phase viscosity, M/L-t

μ_d = dispersed phase viscosity, M/L-t

σ = surface tension, M/t^2

ρ_c = continuous phase density, M/L^3

ρ_d = dispersed phase density, M/L^3

ζ = 'internal' coordinate (size, concentration, etc.) for eqn 2.2 and Monte Carlo approach

MODELING INTERFACIAL AREA TRANSPORT IN MULTI-FLUID SYSTEMS

BY

STEPHEN L. YARBRO

ABSTRACT

Many typical chemical engineering operations are multi-fluid systems. They are carried out in distillation columns (vapor/liquid), liquid-liquid contactors (liquid/liquid) and other similar devices. An important parameter is interfacial area concentration, which determines the rate of interfluid heat, mass and momentum transfer and ultimately, the overall performance of the equipment. In many cases, the models for determining interfacial area concentration are empirical and can only describe the cases for which there is experimental data. In an effort to understand multiphase reactors and the mixing process better, a multi-fluid model has been developed as part of a research effort to calculate interfacial area transport in several different types of in-line static mixers. For this work, the ensemble-averaged property conservation equations have been derived for each fluid and for the mixture. These equations were then combined to derive a transport equation for the interfacial area concentration. The final, one-dimensional model was compared to interfacial area concentration data from two sizes of Kenics in-line mixer, two sizes of co-current jet and a Tee mixer. In all cases, the calculated and experimental data compared well with the highest scatter being with the Tee mixer comparison.

Chapter 1

INTRODUCTION

1.1 Background

In the chemical process industry, inefficient mixing wastes $ 10 billion dollars each year (Long, 1994). A lack of process knowledge results in over-design to compensate or under-design with recycle or high reagent losses. Most design procedures are empirical correlations or use 'ideal' models that ignore the realities of actual equipment. Therefore, it is economically justifiable to examine methods of extending these models to include actual system effects.

For design, interfacial area must be known to calculate the transfer rate for mass, heat and momentum. This study focuses on a two-phase system of immiscible fluids typically used for liquid-liquid extraction. For these systems, empirical design equations are normally developed for specific equipment such as packed columns or mixer-settlers (Thornton, 1956a, 1956b). This restricts the design to systems that are within the experimental data. Consequently, a more fundamental approach is needed.

1.2 Applications

In the nuclear industry, liquid-liquid extraction is an important unit operation for a variety of applications including fuel reprocessing, waste treatment, and

recovering fissile material from spent fuel. The Plutonium-URanium EXtraction (PUREX) process, shown in Figure 1.1, recovers plutonium and uranium from a variety of different reactor fuels. In the PUREX process, tributyl phosphate (TBP) dissolved in a hydrocarbon diluent, binds with plutonium and uranium to remove them from a high-acid aqueous stream. A suitable contacting device mixes and separates the organic and aqueous phases. Because of the particular chemistry of plutonium and uranium, TBP is reasonably selective and separates the fissile material from the non-fissile fission products.

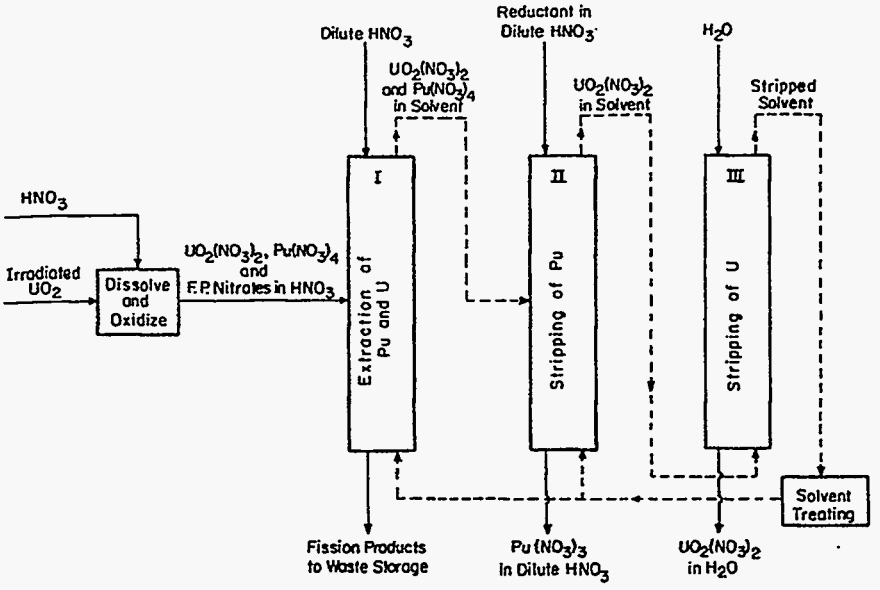

Figure 1.1 PUREX Process Flow Diagram (Benedict, 1981)

Achieving separation factors that exceed 10^8 is necessary for a successful operation (Wish, 1959). Economics drives these high separation factors.

Most of the fissile material is used in either defense or commercial power programs. Since automated, remote handling operations are extremely expensive, it is

cheaper to handle plutonium and uranium directly, in gloveboxes, instead of using heavily shielded, remote operations. Even though the chemistry of the process helps to provide excellent separation factors and good recovery of materials, good equipment design is critical to good process performance.

More recently, with the demise of the nuclear power industry and the end of the "Cold War," a high priority is being assigned to cleaning up nuclear waste. At many of the production sites, underground tanks containing process wastes from spent fuel recovery are scheduled for processing.

Also included in this clean-up effort is the processing of residues produced in support of defense programs. Many actinide-containing residues such as ash from incinerated combustibles, salt residues from oxide conversion processes, glass, plastics and other materials will require processing before storage or disposal. Most of this material has enough radioactive material to classify it as transuranic (TRU) waste. This is waste material with more than 100 nCi/g of radioactive material with atomic numbers greater than 92 and half-lives greater than 20 years. Because the residues have low initial actinide concentrations, processing generates fairly large volumes of dilute acid waste. Unfortunately, the concentration of fissile material in these residues is high enough that packaging it without processing will over-fill the Waste Isolation Pilot Plant (WIPP) which is the only repository in the United States for emplacement of TRU waste. Table 1.1 details the current estimates of TRU generation. Also, increasing the number of shipments required to send material causes the risk associated with these shipments to rise accordingly. Certification, packaging and

transportation costs are also much higher for TRU waste than for Low Level Waste (LLW), i.e., waste that is below the 100 nCi/g requirement. Currently, there are three sites in the United States that can dispose of LLW. South Carolina, Nevada and Idaho all have operating LLW burial sites.

If the material is processed, then the lean acid waste produced will require further processing to ensure that the overall volume of TRU waste decreases. The current processing method for initial recovery of the plutonium from the residues is anion exchange. Column effluents are evaporated to reduce the volume. The acid distillate is neutralized with lime and precipitated with ferric hydroxide. The

Table1.1 Current WIPP Capacity and Proposed Emplacement Volumes (Pillay, 1993)

Department of Energy's (DOE) TRU Waste Inventory

- **Stored TRU (1992).....2.2 x 10^6 ft^3**
- **Stored LLW (1992).....1.4 x 10^6 ft^3**
- **Buried (1990).....6.7 x 10^6 ft^3**

Total **10.3 x 10^6 ft^3**

- **Projected Generation Rate of Additional TRU by 2010.....1.6 x 10^6 ft^3**
- **Contaminated Soil.....5 to 64 x 10^6 ft^3**

Total WIPP Emplacement Capacity.....6.45 x 10^6 ft^3

evaporator bottoms, still containing the majority of radioactivity, are neutralized with caustic and cemented. These cement drums will be sent to WIPP. Current cost figures

are approximately $10,000 per TRU cement drum. Estimated costs for a similar LLW drum are approximately $200-$500. Therefore, further treatment to reduce the number of TRU cement drums is economically justified.

Also, while anion exchange is selective for plutonium, it does not recover americium. ^{241}Am is generated through decay of the ^{241}Pu isotope that is present in the original plutonium. Removing americium reduces the volume of TRU liquid waste. Because ^{241}Am has a half-life of 438 years, it has a specific activity of 3.43 Ci/g.

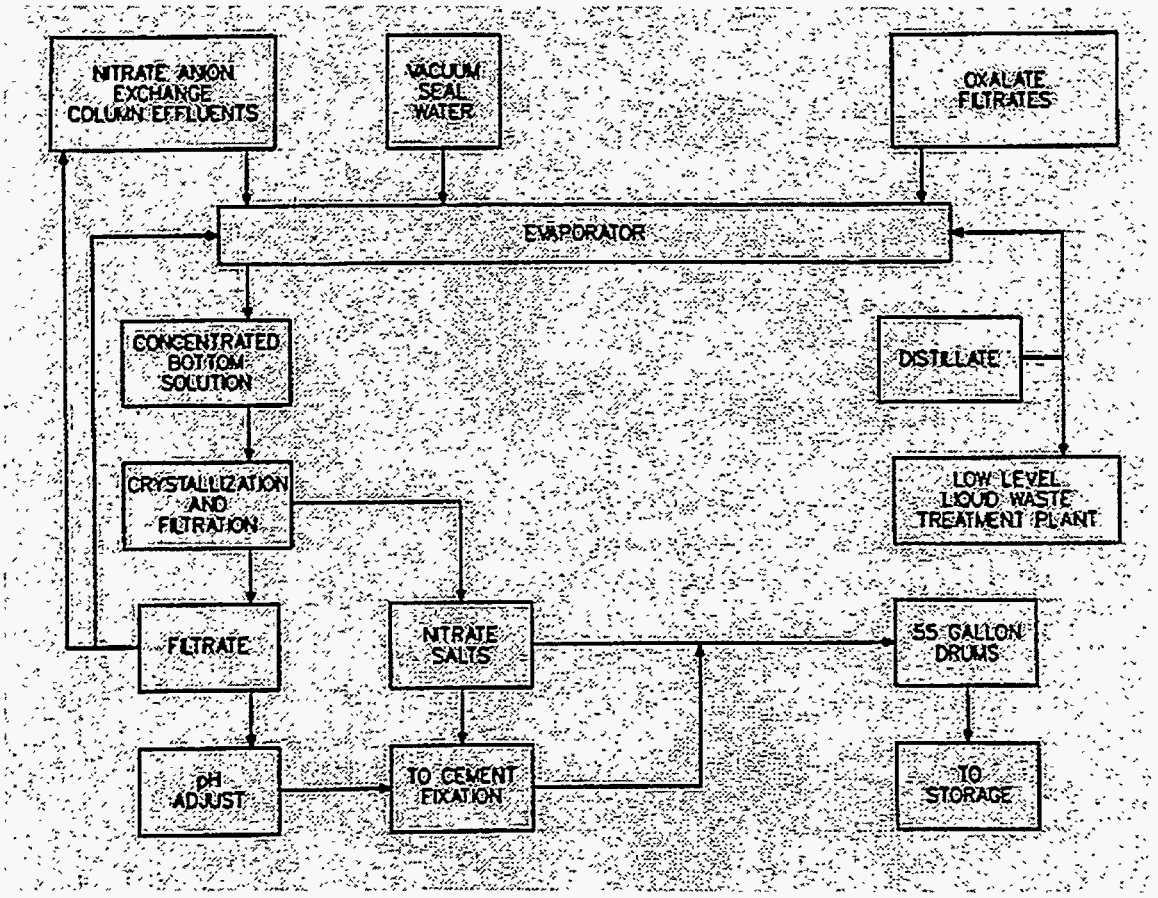

Figure 1.2 Flowsheet of the Current Plutonium Residue Process

This means that any recovery process, such as the one shown in Figure 1.2, will have to have a high recovery efficiency. Continuous or semi-continuous processes will be necessary to process large volumes of lean material. The process will have to mechanically simple. Any remote or glovebox process enormously complicates maintenance procedures. Radiation exposures to maintenance and operations personnel also have to be considered.

Problems with radioactive waste disposal are unique to the nuclear industry, but similar waste disposal problems are encountered elsewhere. Mining, electroplating and foundry industries are having to solve the problem of processing large volumes of wastes that contain toxic metals, such as chromium, lead, cadmium and others to meet state and federal environmental requirements. While in these industries, simple equipment is not required for remote handling but to reduce capital and operating costs.

1.3 Motionless Mixers as Liquid-Liquid Contacting Equipment

In an effort to design simple, robust and efficient equipment for liquid-liquid extraction (LLE) operations, motionless mixers (MM) have been evaluated for several different systems (Leacock,1961, Li, 1983, Merchuk, 1980a, 1980b, Tunison, 1976, 1978, Tse,1978). Motionless mixers come in many different designs. The Kenics mixer consists of left-hand and right-hand helical sections which mix the fluids. Koch mixers (Koch, 1991) have similar elements, with the difference of "corrugation" or extra bends in the mixing elements to enhance turbulence. Simple motionless

mixers or "static" mixers can be made by filling a pipe with packing material, such as glass beads or ceramic saddles to increase mixing efficiency.

Leacock (1961) examined the extraction of isobutanol and water in cocurrent flow in a packed column. He used different lengths of glass columns packed with 3 mm glass beads. Then, mass transfer coefficients at several different phase ratios and column lengths were measured. The conclusion was that the packed column was a very efficient means of contacting two phases. Equilibrium was obtained in only a few inches of packing. The mass transfer coefficients increased with higher fluid velocities and flooding conditions, as are encountered with conventional liquid-liquid contacting devices, were not found. The only limitation was the pressure drop allowable by the glass tubing.

In the most recent studies, the extraction of copper with various organic extractants was evaluated. Merchuk (1980a,1980b) empirically examined the efficiencies of copper sulfate extraction by LIX-64N comparing a Kenics mixer, Koch mixer, tubes packed with ceramic and polypropylene Intalox saddles, empty pipes, and a baffled tank stirred with a turbine impeller.

The conclusion was that the Koch mixer design was more efficient than the Kenics mixer for similar residence times. However, packed tubes are as efficient as Koch mixers but there is a strong relationship to the wetting characteristics of the continuous phase and the packing materials in the mixer. Depending on which phase is continuous, the wetting characteristics of the packing can give different efficiencies. When compared to stirred tanks, the power required for dispersion is approximately

equal, but the volume required for the static mixers is about two orders of magnitude smaller than that required for stirred tanks.

Tunison (1976) measured the extraction of copper sulfate with Kelex 100 in a Kenics mixer. He estimated the interfacial area between the two phases using photographs of the mixture. Using the interfacial area along with estimates of the reaction rate, he was able to define a volumetric rate constant, the product of the reaction-rate constant and the interfacial area to help define the hydrodynamic behavior of the reactor. He then wrote material balances for a one-dimensional plug-flow reactor. Solving the material balance allowed calculation of the overall conversion in the reactor. Because the reaction kinetics of the copper sulfate with Kelex 100 are slow, this system is an example of a rate-controlled system.

Tse (1978) used Tunison's one-dimensional model to evaluate the extraction of copper and zinc chlorides with tri-isooctylamine (TIOA). Because the reaction kinetics of this system are fast, this system is mass-transfer controlled. Unfortunately, the model only qualitatively predicted the metal extraction behavior when both metals were extracting simultaneously.

1.4 Role and Importance of Interfacial Area

Interfacial area concentration is one of the most important parameters in analyzing multi-fluid flow with multi-fluid, separated flow models (Kataoka, 1986). Because multi-fluid models are currently the most accurate, they are the basis for

most of the current commercial and academic fluid dynamics codes such as PHOENICS, CFDLIB, FLOW-3D (CFX), STAR-3D and FLUENT (Versteeg, 1995).

Multi-fluid models are based on formulating 'instantaneous' momentum, energy and mass equations for each separate phase. Because the instantaneous equations are still beyond the current state-of-the-art to solve, they are averaged according to various techniques similar to the approach employed for single-fluid turbulence. The multi-fluid formulation is more accurate than mixture or drift-flux models because it contains information on the interaction of the fluids at the interface in addition to interactions within the fluid. These interfacial interactions typically are represented as constitutive equations based on either empirical or semi-theoretical methods. In the present state-of-the-art, the interfacial interaction terms are the weakest and least understood portions of the multi-fluid model.

The interfacial area concentration is an important parameter because most of the inter-fluid interactions occur across an interfacial contact surface. Therefore, most of these terms can be modeled as (Ishii, 1975)

(Interfacial transfer term) ~ (Interfacial area concentration, a_i) x (Driving force) (1.1)

In this equation, interfacial area concentration is the interfacial contact area divided by the volume of the fluid mixture. It is related to the geometric structure of the interface, which is related to the flow parameters of the system. The driving force is related to the system parameters through turbulent and molecular effects. Hence, the interfacial area concentration should be specified by the appropriate constitutive relation or transport equation (Ishii, 1980). Consequently, a knowledge of the

interfacial area concentration is extremely important to formulating accurate multi-fluid models.

1.5 Problem Statement and Objectives

1.5.1 Objectives

The objectives of this research are to

1. Examine the literature to determine the current state-of-the-art in multi-fluid modeling and interfacial area transport

2. Use an appropriate averaging method, develop the appropriate general property balance equations which include interfacial area concentration in the interfacial transfer terms and derive an interfacial area transport equation based on system flow parameters

3. Define appropriate constitutive equations and by inserting them into the general equations, derive a specific multi-fluid model including interfacial area concentration transport

4. Use the model to calculate the interfacial area concentration for different types of static mixers with liquid-liquid sytems

5. Compare the numerical and experimental results, draw conclusions and propose future work

1.5.2 Outline of the Dissertation

In this chapter we have presented a background, justification and specific objectives for this research.

Chapter 2 is a survey of previous work on various approaches to multi-fluid modeling and the current state of interfacial area knowledge.

Chapter 3 introduces the instantaneous general property balance, and then the selected averaging method to produce the proper 'averaged' general property balances. Specific balances for mass, momentum, mechanical energy, total energy and entropy are derived. Mixture equations are introduced to isolate the interfacial energy and interfacial area concentration. The appropriate general property balance is then combined with the total energy mixture equation to derive a general transport equation for interfacial area concentration.

Chapter 4 introduces specific constituitive equations and a one-dimensional model is derived and solved for the interfacial area concentrations produced in Kenics static mixers, a co-current jet, and tee mixer.

Chapter 5 presents conclusions and proposes further research.

Chapter 2

SURVEY OF PREVIOUS WORK ON DISPERSED PHASE SYSTEMS AND INTERFACIAL AREA

2.1 Introduction

The modeling and characterization of two-phase, dispersed processes has received a tremendous amount of attention. Particularly, gas-liquid processes have been the object of the most study. Distillation, gas scrubbing and many catalytic reactions have been researched to discover the nature of the process. As a result, this work has been used as a model to study multi-fluid interactions in many different situations.

Traditional design procedures for gas-liquid and liquid-liquid processes are usually based on the McCabe-Thiele approach (Treybal, 1963 and Yarbro, 1987). Equilibrium data is plotted and used to predict the number of ideal stages required for the desired separation. However, this approach is difficult to use for the transfer of more than one species. This is especially true if the transfer of one species effects the transfer of another. Therefore, a graphical iterative procedure has to be employed.

First, the equilibrium data for all transferring species are plotted separately. Then, operating lines are calculated based on the design criteria and overall material balance for the system. Stages are stepped off for one species, and this concentration

profile is used to estimate the concentration of the second. The process is repeated until the two concentration profiles do not change within a specified error.

The procedure is time-consuming and also does not account for physical characteristics of the system. It is also only appropriate for staged systems or systems that can be treated as staged. It does not account for chemical reaction or heat generation. For this approach to be accurate, the system has to be at equilibrium at each stage. If this assumption is not valid, because of the physical traits of the system, such as slow kinetics or mass transfer, a correction factor is used. Typically, this correction factor is a stage efficiency and allows for more stages to be added to account for non-idealities.

This approach is an overall approach. It does not allow individual equipment characteristics to be designed. Also, certain characteristics of the system, which could allow significant performance improvement, are not studied. For example, slow kinetics of one species may allow higher selectivities to be obtained by just adjusting the residence time of contact. Mass or heat transfer effects could be adjusted by increasing the contact area. Therefore, a more complete approach to design and characterization of multi-phase systems is desirable and needs to include studies of the physical aspects of the system, particularly interfacial area.

For these reasons, many investigators have developed other models of multi-phase processes. Excellent reviews on multi-fluid CSTR's have been presented by Tavlarides and Stamatoudis (Tavlarides, 1981) and Tavlarides and Bapat (Tavlarides, 1983). For homogeneous reaction mixtures, convective models based on velocity

profiles, dispersion models, compartments models, statistical models, empirical models and micromixing models have been proposed. Because of the large volume of work on homogeneous fluids, many heterogeneous models are adaptations of the homogeneous case.

For multi-phase or heterogeneous fluid reactors, the models can be grouped into four main areas (Tunison, 1976): drop-size or residence time distribution, population-balance, Monte Carlo, and macroscopic/multi-fluid models.

2.2 Modeling of Multi-Phase Processes

2.2.1 Drop Size Distribution (Spherical Cell/Rigid Drop)

Because the actual droplet behavior can affect the reactor performance, many investigators have factored that behavior into their models. One method has been to derive the equations of change for the individual phases and assume the drops behave as rigid, spherical particles. The equations are solved for an individual drop and the results averaged over the entire reactor volume (Barnea, 1978). In this work, drop size was correlated using dimensional analysis as a function of physical parameters and the Weber number.

Gal-Or (Gal-Or, 1966) and Tavlarides (Tavlarides, 1969) examine the effect of drop size on conversions for unsteady-state mass transfer in a continuous stirred tank reactor (CSTR). They used the following approach. By assuming each drop to be surrounded by the continuous phase or 'shell', they were able to develop diffusion equations using the substantial time derivative as follows.

$$\frac{DC_A}{Dt} = D_i \nabla^2 C_A + r_A \qquad (2.1)$$

Using a single drop as the control volume, they solved the diffusion equation and then averaged drop concentrations over an assumed drop size distribution. Interactions in dense dispersions were accounted for by increasing the number of droplets. Coalescence and dispersion processes were not accounted for in the model. They concluded that the drop-size distribution could be replaced by an average drop size without introducing a large error in the predicted conversions. The rigid drop allows the boundary conditions to be specified to allow solution of the differential equations.

In support of Gal-Or, Barnea, Hoffer and Resnick (Barnea, 1978), as discussed earlier, concluded that an average drop size could be used to predict conversions for steady-state conditions and the drop size had a strong effect on conversion. This was especially true in cases where interphase mass transfer was the rate-controlling step.

2.2.2 Drop Interaction Models

2.2.2.1 Population Balance Models (PBM)

Because droplet coalescence and dispersion is a random process, statistical or probability approaches have been used to predict reactor performance. These methods are called population balance models. Curl (Curl, 1963), Hulbert and Katz (Hulbert, 1964), Eakman, Tsuchiya, and Fredickson (Eakman, 1965), Valentas and Amundson (Valentas, 1966a), Valentas, Bilous and Amundson (Valentas, 1966b), Bayens and Laurence (Bayens, 1969), Shah and Ramkrishna (Shah, 1973),

Ramkrishna and Borwanker (Ramkrishna, 1973, 1974a), Park and Blair (Park, 1975), Coulaloglou and Tavlarides (Coulaloglou, 1977), Min and Ray (Min, 1978), Jeon and Lee (Jeon, 1986), Laso, Steiner, and Hartland (Laso, 1987), Guimares and Cruz-Pinto (Guimares, 1988), Al Khani, Gourdon, and Casamatta (Al Khani, 1989), Tsouris and Tavlarides (Tsouris, 1994), Jacob, (Jacob, 1995), Ramkrishna, Sathyagal, and Narsimhan (Ramkrishna, 1995) and Lam, Sathyagal, Kumar, and Ramkrishna (Lam, 1996) have presented both theoretical approaches and experimental work validating various population balance models.

For multi-fluid dispersions, each drop can be described by using its position within the reactor, drop concentration and age. A population balance is then derived by equating the rate of change of the number of drops per volume with the rate of drop formation at that particular place in the reactor. The microscopic population balance is shown below

$$\frac{\partial \psi}{\partial t} = \underline{\nabla} \cdot \underline{v}\psi + \underline{\nabla} \cdot \left(\frac{d\zeta}{dt} \psi \right) + B - D = 0 \tag{2.2}$$

where $\underline{\nabla} \cdot \underline{v}\psi$ represents the spatial coordinates of the drop and $\underline{\nabla} \cdot \left(\frac{d\zeta}{dt} \psi \right)$ is the internal coordinates such as the drop concentration or drop volume. Many different effects can cause a drop to change its state or position in the reactor, such as, change in physical properties, mass transfer effects or drop coalescence or dispersion.

Ramkrishna (Ramkrishna, 1974b) has examined the experimental work required to obtain information to apply a population balance model. He used data

from batch mixing experiments to derive a power law expression for the probability of drop breakage. He concluded that batch experiments can provide a considerable amount of data to allow prediction of drop size distributions in non-coalescing dispersions.

Curl (1963) was one of the first to attempt to use a population balance method to predict conversions in dispersed phase systems. He derived a model which allowed the drops to interact with each other instead of a hypothetical drop of some assumed concentration. With this assumption, he was able to produce a complicated integro-differential equation that was only analytically solvable by assuming zero-order kinetics. Others, such as Bayens and Laurence (1969), have extended Curl's work to other CSTR's and to spray columns. Park and Blair (1975) have also presented more general models of droplet coalescence and dispersion frequencies.

For the PBM, models are necessary for droplet behavior in the reactor. A vast amount of work has been presented for CSTR's for drop breakage and coalescence. Hinze (Hinze, 1955), Shinnar and Church (Shinnar, 1960), Madden and Damerell (Madden, 1962), Howarth (Howarth, 1964, 1967), Chen and Middleman (Chen, 1967), Ramkrishna (Ramkrishna, 1974b), Coulaloglou and Tavlarides (Coulaloglou, 1976), Delichatsios and Probstein (Delichatsios, 1976), Verhoff, Ross, and Curl (Verhoff, 1977), Cruz-Pinto and Korchinsky (Cruz-Pinto, 1981), Narsimhan, Nejfelt, and Ramkrishna (Narsimhan, 1984), Davies (Davies, 1985), Muralidhar and Ramkrishna (Muralidhar, 1986), Calabrese, Chang, and Dang (Calabrese, 1986a), Wang and Calabrese (Wang, 1986), Calabrese, Wang, and Bryner (Calabrese, 1986b),

Das and Kumar (Das, 1987), Muralidhar, Ramkrishna, Das, and Kumar (Muralidhar, 1988), Tobin, Muralidhar, Wright, and Ramkrishna (Tobin, 1990), Tsouris and Tavlarides (Tsouris, 1994) and Lam, Sathyagal, Kumar, and Ramkrishna (Lam, 1996) have studied the breakage and coalescence of drops in dispersions.

Typically, these workers have worked in dilute dispersions to eliminate either drop breakage or coalescence events and have usually made the following assumptions:

1. There is isotropic turbulent flow.
2. Drop size is within the inertial subrange eddies at steady state.
3. Energy spectrum function has a -5/3 dependence on the wave number k.
4. Viscous effects are negligible.
5. Drop deforms due to local pressure change.
6. Kinetic energy distribution of the drops is the same as the turbulent eddies.

As an example of the PBM approach, Coulaloglou and Tavlarides (Coulaloglou, 1977) have developed the following expression for the PBM for a batch CSTR at steady state with no mass transfer.

$$NA(V) = B - D \tag{2.3}$$

Expanding the birth and death terms as functions of breakage frequency, breakage distribution function, coalescence rate and efficiency and assuming that the number of daughter drops formed during breakage is two give the following relationship

$$NA(V)=\frac{\left[\begin{array}{l} n_o A_o(V)+\int_V^{V_{max}} \beta(V',V)v(V')g(V')NA(V')dV+ \\ \int_0^{V/2}\lambda(V-V',V)h(V,V')NA(V-V')NA(V')dV' \end{array}\right]}{g(V)+\int_0^{V_{max}-V}\lambda(V,V')h(V,V')NA(V')dV'+f(V)} \tag{2.4}$$

These investigators assumed that the dispersion was homogeneous and therefore the drop properties do not change with position within the reactor. They derived the following relationships for breakage frequency, breakage distribution, collision frequency and coalescence efficiency based on the phenomenological properties of the system.

$$g(V)=C_1V^{-2/9}d_I^{2/3}\frac{N^*}{1+\phi}\exp\left[-\frac{C_2\sigma(1+\phi)^2}{\rho_d V^{5/9}d_I^{4/3}N^{*2}}\right] \tag{2.5}$$

$$\beta(V',V)=\frac{2C_3}{V'(2\pi)^{1/2}}\exp\left[-\frac{(2V-V')^2C_3^2}{2V'^2}\right] \tag{2.6}$$

$$h(V',V)=C_4\left(V'^{2/3}+V^{2/3}\right)\left(V'^{2/9}+V^{2/9}\right)^{1/2}\frac{N^*}{1+\phi}d_I^{2/3} \tag{2.7}$$

$$\lambda(V',V)=\exp\left[-\frac{C_5\mu_c\rho_c d_I^2N^{*3}}{\sigma(1+\phi)^3}\left(\frac{V'^{1/3}V^{1/3}}{V'^{1/3}+V^{1/3}}\right)^4\right] \tag{2.8}$$

However, with this approach, complicated numerical expressions are required and the more general models have several adjustable parameters which require extensive experimentation for determination. The main problem is properly defining functions that describe drop breakage and coalescence. Particularly, with situations

that have non-linear transfer characteristics, these approaches are extremely difficult to calculate numerically.

2.2.2.2 Monte Carlo Models

Monte Carlo (MC) techniques appear to be a natural extension of statistical methods. In multi-phase systems, mixing and mass transfer effects can have a strong influence on the overall performance of the reactor. Because of the complexity of multi-fluid interactions, MC approaches have the advantage of using direct, microscopic drop interaction, controlled by the physical aspects of the system to predict the overall behavior of the reactor using statistical techniques. However, they have the disadvantage of extensive computing time and effort to calculate large enough samples to accurately model the system.

Originally proposed by Laplace, MC techniques were developed at Los Alamos during the late 1940's to describe the enormously complicated neutron and radiation diffusion processes occurring in nuclear systems. Monte Carlo methods use random sampling procedures to predict outcomes of stochastic processes. Given N random points, $x_1, x_2, \ldots, x_N$, uniformly distributed in a known volume V, integration of a complex function, f, can be approximated as shown below

$$\iiint_V f dV \approx V\langle f\rangle \pm V\left[\frac{\langle f^2\rangle - \langle f\rangle^2}{N}\right]^{1/2} \tag{2.9}$$

where f is defined as

$$\langle f \rangle = \frac{1}{N} \sum_{i=1}^{N} f(x_i) \tag{2.10}$$

$$\langle f^2 \rangle = \frac{1}{N} \sum_{i=1}^{N} f(x_i)^2 \tag{2.11}$$

and the value is the 'mean value' of a function of a random variable bounded by the limits of integration. Stochastic processes are those processes whose behavior is determined by random events. Mixing and droplet formation and coalescence are inherently random events and are therefore stochastic.

Ramkrishna (Ramkrishna, 1980) has shown that there is a precise mathematical connection between the two approaches. The basis for PBM is that over a phase space R, the probability that a drop with characteristics described by ζ will exist in R at time t is given below

$$\int_R \zeta dR = 1 \tag{2.12}$$

Monte Carlo methods, given a function ζ, can then estimate values within the phase space and average them to get values of ζ over the boundaries of R. Probabilities calculated from physical system properties can be used to eliminate events of low probability. Monte Carlo methods are attractive when ζ is a complicated function difficult to integrate analytically or by conventional methods.

2.2.3 Macroscopic and Multi-Fluid Models

Conventional macroscopic models (Pavlica, 1970) attempt to characterize the overall behavior of the reactor and do not account for fluid mixing on the droplet

level. Typically, only property transfer between phases is calculated. The contact area is assumed to be the interfacial area of the dispersed phase. Given the difficulty of estimating the interfacial area, a normalized area per unit volume is used (Levenspiel, 1972) as an estimate.

Current macroscopic models begin with a material balance over a fixed volume and assume that the interfacial area is constant and that the property transfer effects can be described with an overall transfer factor such as U or k. Usually, simplifying assumptions such as plug flow and equal phase velocities are used to reduce the complexity of the problem.

More advanced types of macroscopic models are the multi-fluid models. In this approach, separate property balances are written for each fluid in the system. With this method, it is important to have the constitutive equations properly defined for the individual fluids and for the property transfer between fluids.

In addition, it is typical to perform some type of averaging of the equations to allow calculation in the multi-fluid system. There are a variety of approaches, such as ensemble, space and time, and various combinations. Many researchers have been studying the averaging problem, Standart (Standart, 1964), Drew and Segal (Drew, 1971), Travis, Harlow, and Amsden (Travis, 1974), Delhaye (Delhaye, 1974), Ishii (Ishii, 1975), Harlow and Amsden (Harlow, 1975), Nigmatulin (Nigmatulin, 1979), Drew and Lahey, (Drew, 1979a), Hassanizadeh and Gray (Hassanizadeh, 1979), Banerjee and Chan (Banerjee, 1980), Ishii and Mishima (Ishii, 1984), Stewart and Wendorff (Stewart, 1984), Dobran (Dobran, 1984, 1985), Kashiwa (Kashiwa, 1987),

Kashiwa and Rauenzahn (Kashiwa, 1994), Pauchon and Banerjee (Pauchon, 1986, 1988), Arnold, Drew, and Lahey (Arnold, 1988), Lahey (Lahey, 1989, 1990, 1991), Lahey, Park, and Drew (Lahey, 1993) and Grau and Cantero (Grau, 1994). It is interesting to note that the basic forms of the various mass, momentum and energy equations are similar. Most of the controversy is over the various forms of the final constitutive equations, particularly for the property transport from one fluid to another. It is evident that the fluid-to-fluid property transport is extremely important for the multi-fluid formulation to be accurate. However, the property transfer has to occur across an internal surface area, which can be enormously complex depending on the flow regime. Most researchers acknowledge the importance of interfacial area to enable correct multi-fluid models (Ishii, 1980, 1995; Kataoka, 1986a,1986b, 1990; Lahey, 1993), but the complexity of the problem (Stewart, 1984) has forced most to either use an empirical correlation or assume a constant contact area or particle size (Kashiwa, 1987). Therefore, a method to calculate interfacial area is important to advanced multi-fluid models.

2.2.4 Calculating Interfacial Area

An excellent review of empirical correlations for predicting interfacial area in a variety of systems up to 1981 has been done by Tavlarides (1981). Most of the work completed until then was based on a dimensional analysis of the important variables coupled with Kolmogoroff theory to enable some estimate of the turbulent forces that should contribute to drop formation.

In an attempt to provide a more fundamental basis, Ishii and Mishima (Ishii, 1980) used a multi-fluid model to begin to determine the interfacial area. They looked at the constitutive equations for drag and virtual mass and used the various forms for the different flow regimes to guide the empirical correlation of more than a 1000 data points.

Building on this approach Kataoka, Ishii, and Serizawa (Kataoka, 1986a) attempted to combine Ishii's multi-fluid model and geometrical arguments to allow experimental measurement of interfacial area using a single electrical resistivity probe. This work was continued (Kataoka, 1990) with an improved multi-point sensor and more robust experimental data correlation techniques. They examined the effect of the inlet conditions on interfacial area and derived a relationship between interfacial area and their measurement technique. In addition, they developed an empirical correlation that correctly predicted interfacial area concentration as a function of velocity and phase fraction.

Kalkach, Lahey, Drew and Meyder (Kalkach, 1993) have extended Kataoka's experimental work with an improved multi-point probe and reported data at a variety of different phase fractions and velocities for gas-liquid flow. However, they did not attempt to correlate the data.

Recently, Delhaye and Bricard (Delhaye, 1994) have attempted to correlate a variety of gas-liquid data with several different empirical correlations. None of the existing correlations fit all of the data, so they developed a new correlation based on

the superficial velocity of the gas and liquid. The non-dimensional form of their proposed equation fits all of the data within an error of 30%.

All of the above work was focused on gas-liquid systems, but there has been a corresponding interest in liquid-liquid systems. Experimental and empirical work on CSTR's has been done by Calabrese, Chang and Dang (Calabrese, 1986a), Wang and Calabrese (Wang, 1986) and Calabrese, Wang and Bryner (Calabrese, 1986b). They correlated their data using Kolmogoroff theory and included the effect of viscosity.

Motionless mixers such as Kenics mixers, tees and co-current jets have also been studied. Middleman (Middleman, 1974) measured drop size distributions for several systems with viscosity's ranging from 0.6 to 26 cp and interfacial tensions from 5 to 46 dynes/cm in a Kenics mixer. He correlated his data as follows

$$\frac{D_{32}}{D_o} = 0.49We^{-3/5} \tag{2.13}$$

Middleman derived this equation by using the Kolmogoroff theory. Middleman assumed that the dispersive energy causing drop breakage was due to the inertial subrange eddies and that the drop was stabilized only by the interfacial tension. The above correlation begins to fail as the drop viscosity increases, although it is accurate for systems of relatively inviscid fluids. His work also showed that drop size distribution was independent of dispersed phase fractions up to 25%.

Berkman (Berkman, 1988) extended these correlations by examining the effects of viscosity and hydrodynamic conditions on drop size distributions produced by a Kenics mixer. He found a slight dependence on hydrodynamic conditions for Re >

12,000 and a measurable dependence on viscosity, when viscosity is greater than 20 cp. He fit his data to the following relationship

$$\frac{D_{32}}{D_o} = 0.49We^{-3/5}\left[1+1.38\left(\left(\frac{\mu_d\langle v\rangle}{\sigma}\right)\left(\frac{\rho_c}{\rho_d}\right)^{1/2}\left(\frac{D_{32}}{D_o}\right)^{1/3}\right)\right]^{3/5} \tag{2.14}$$

He concluded that residence time and energy dissipation rate were important to the drop production in the contactor.

Al Taweel and Walker (Al Taweel, 1983) measured drop size distributions for dilute mixtures in a Lightnin "In-Line" mixer. They were able to correlate their data in terms of an energy dissipation rate or Weber number. They, along with Long (Long, 1983), discovered that the assumption of equilibrium for two-phase mixing systems is not always correct. Long and Reimus (Long, 1988a, 1988b,1992a) and Long, et.al. (1992b, 1993) observed that equations (2.13) and (2.14) do not fully account for the effects noted at a tee junction. In particular, they observed that equations (2.13) and (2.14) must be corrected by additive terms that were proportional to dispersed phase volume fraction. They attributed this effect to the geometry of their system, where one would expect the breakage time to be large compared to the residence time. This is an important effect in such systems because it implies that even when the Weber number increases without bound, it is impossible to drive the droplet size to zero. Rather an additive term reflecting the lower limit must be included. It is possible that Al Taweel and Walker did not discover this effect

because all of their work was done at a constant and low dispersed phase fraction of 1%.

Yarbro and Long (Yarbro, 1995) examined a simple two-fluid model based on prior work by Lahey (Lahey, 1991) to estimate the energy dissipation for a liquid-liquid system in a Kenics mixer. For the purpose of this model, it was assumed that the system was at steady-state, the fluids were incompressible and gravity effects could be neglected. Because there is no phase change, the pressure difference between the fluids was negligible and not included.

To develop the constitutive equations for shear, it was assumed that the flow was turbulent and therefore simple friction factor correlations could be used to predict wall and interfacial shear. Specifically for the interfacial shear, an approach used for submerged objects (Bird, 1960) was used. In the turbulent limit near the entrance of the reactor, the friction factor becomes equal to approximately 0.44. Other forces such as the Basset and lift forces were assumed to be small with regard to the interfacial shear especially for small phase fractions. Viscosity effects were assumed to be small for inviscid fluids.

Drop coalescence was assumed to be negligible for small phase fractions and only drop breakage was considered. Based on previous work, drop breakage appears to be a function of the energy dissipated by the continuous phase and the contact time. Because of the large velocity difference between the two fluids at the entrance of the reactor, interfacial shear along with wall shear, would be an important drop production mechanism. With this assumption and the assumption that the drop size is a function of

drop surface energy and surface turbulent forces, an energy balance for drop size was derived.

However, this approach only allowed average interfacial area concentrations to be derived and did not explain the drop production mechanism or to the actual distribution of interfacial area within the reactor. Kocamustafaogullari and Ishii (Kocamustafaogullari, 1995) took a large step and derived an interfacial area transport equation of the following form

$$\frac{\partial}{\partial t} a_i + \underline{\nabla} \cdot \left(a_i \underline{v}_i \right) = \phi_{dis} - \phi_{co} + \phi_{ph} \tag{2.15}$$

from a population balance on the particle number density. They proposed that the source terms, ϕ_{dis}, (the particle disintegration), ϕ_{co}, (the particle coalescence), and ϕ_{ph}, (the phase change) could be calculated based on the phenomenological models of Coulaloglou and Tavlarides (Coulaloglou, 1977) and Prince and Blanch (Prince, 1990) or on earlier empirical relationships based on Weber and Reynold's numbers. Unfortunately, they did not present any calculations in their paper.

2.2.5 Conclusion

A careful survey of the literature has revealed that there are several approaches to modeling multi-fluid systems. It appears that the most fundamental method at present is to use an appropriate macroscopic/multi-fluid model because the physics can be represented by various constitutive equations and the assumptions for choosing the equations can be linked to the situation under study. Statistical methods are attractive because they can handle the complexity of dispersed phase systems, but they do not

necessarily help to understand the phenomena involved. Unfortunately, for multi-fluid models to be successful, a better understanding of the property transport from fluid to fluid has to occur. Because this happens across an interfacial boundary, a method for predicting interfacial area is needed. The literature survey has indicated that there are reasonable approaches to deriving a transport equation, but a satisfactory equation for area transport has not been demonstrated. Therefore, the remainder of this work will focus on deriving and demonstrating a relationship for the transport of interfacial area concentration.

Chapter 3

DERIVING THE BASIC EQUATIONS FOR MULTI-FLUID SYSTEMS

3.1 The Phase k Local Instantaneous General Property Balance

Consider an arbitrary volume in space containing two fluids as shown below in Figure 3.1.

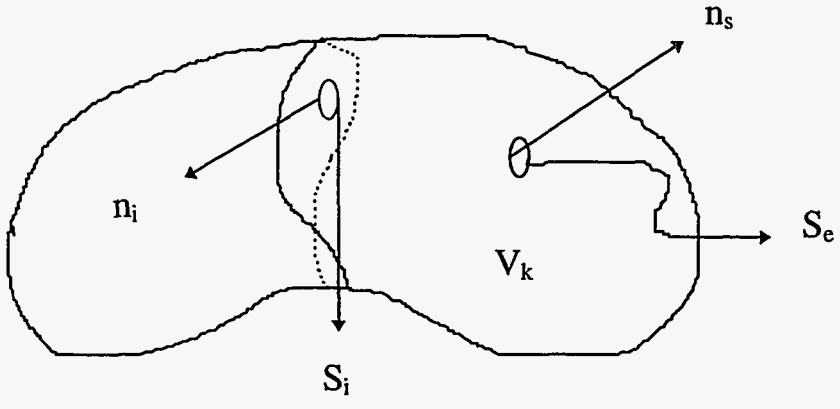

Figure 3.1 General Two-Fluid System

An instantaneous general property balance can be written for the volume (Bird, 1960, Standart, 1964) as follows

$$\iiint_V \frac{\partial}{\partial t}\psi_k dV + \iint_{S_e}\left[\psi_k \underline{v}_k + \phi_k\right]\cdot \underline{n}_s dS_e + \iiint_V \psi_g dV = \iint_{S_i}\left[\psi_{ki}\left[\underline{v}_{ki} - \underline{v}_i\right] + \phi_i\right]\cdot \underline{n}_i dS_i \quad (3.1)$$

where $\dim\phi_k = \dim\psi_k + 1$ and $\dim\phi_{ki} = \dim\psi_{ki} + 1$ because the general property is multiplied by the velocity vector.

Writing the balance for each phase k of the volume allows property transfer across either of two boundaries. The boundary, S_e, is the external boundary that could

be a vessel wall or the entrance or exit of the volume. This is the boundary through which the fluids in the volume can exchange mass, momentum or energy with the surroundings. The internal boundary, S_i, is the surface through which the fluids can exchange mass, momentum or energy with each other.

3.2 Averaging the Phase k Local Property Balance

Because in multi-fluid systems many properties, such as density, are discontinuous across internal surfaces, eqn (3.1) cannot be used without 'smoothing' the equation to remove the discontinuities. This can be achieved by defining a phase indicator (Drew and Wood, 1985) as follows

$$X(\underline{x},t;\mu) = \begin{cases} 1: \text{If phase k is present at } (\underline{x}, t) \\ 0: \text{If phase k is not present at } (\underline{x}, t) \end{cases}$$

The phase indicator has the mathematical properties of a unit step function and it follows that the phase indicator is changing at the interface, S_i, of the two fluids so that we can define an interface indicator function

$$\Delta X(\underline{x},t;\mu) = \begin{cases} 0: \text{If phase k is present at } (\underline{x}, t) \\ 1: \text{If } S_i \text{ is present at } (\underline{x}, t) \\ 0: \text{If phase j is present at } (\underline{x}, t) \end{cases}$$

In most engineering systems of interest, instantaneous values are too difficult to calculate with current computer technology. Since they are often not required for

design or evaluation, an appropriate averaging procedure is applied. In this case, a statistical or ensemble averaging procedure is used. The 'ensemble average' will be the statistical average over all values of a property measured in a single experiment over a given volume and time. Therefore, the average is defined

$$\langle \psi(\underline{x},t) \rangle = \int_{\mu} \psi(\underline{x},t;\mu) f(\mu) d\mu \tag{3.2}$$

where f is a probability density function, i.e., $f(\mu)$ greater or equal to zero and

$$\int_a^b f(\mu) = 1 \tag{3.3}$$

With this definition, instantaneous values can be defined as the sum of an average value and a fluctuation from the average (Bird, 1960)

$$\psi_k = \langle \psi_k \rangle + \psi_k' \tag{3.4}$$

so eqn (3.1) can be re-written

$$\begin{aligned} &\iiint_V \frac{\partial}{\partial t}\left[\left(\langle \psi_k \rangle + \psi_k'\right)X\right]dV + \iint_{S_e}\left[\left(\langle \psi_k \rangle + \psi_k'\right)\left(\langle \underline{v}_k \rangle + \underline{v}_k'\right) + \left(\langle \phi_k \rangle + \phi_k'\right)\right]X \cdot \underline{n}_s dS_e \\ &+ \iiint_V \left(\langle \psi_g \rangle + \psi_g'\right)X dV = \iint_{S_i}\left\{\left(\langle \psi_{ki} \rangle + \psi_{ki}'\right)\left[\left(\langle \underline{v}_k \rangle + \underline{v}_k'\right) - \left(\langle \underline{v}_{ki} \rangle + \underline{v}_{ki}'\right)\right] + \left(\langle \phi_i \rangle + \phi_i'\right)\right\}\Delta X \cdot \underline{n}_i dS_i \end{aligned} \tag{3.5}$$

Carrying out the multiplication produces this equation

$$\begin{aligned} &\iiint_V \frac{\partial}{\partial t}\left[\left(\langle \psi_k \rangle + \psi_k'\right)X\right]dV + \iint_{S_e}\left[\langle \psi_k \rangle\langle \underline{v}_k \rangle + \langle \psi_k \rangle v_k' + \psi_k'\langle \underline{v}_k \rangle + \psi_k'\underline{v}_k' + \langle \phi_k \rangle + \phi_k'\right]X \cdot \underline{n}_s dS_e \\ &+ \iiint_V \left(\langle \psi_g \rangle + \psi_g'\right)X dV \\ &= \iint_{S_i}\left[\begin{array}{l}\langle \psi_{ki} \rangle\langle \underline{v}_k \rangle + \langle \psi_{ki} \rangle\underline{v}_k' - \langle \psi_{ki} \rangle\langle \underline{v}_i \rangle - \langle \psi_{ki} \rangle\underline{v}_i' + \psi_{ki}'\langle \underline{v}_k \rangle \\ +\psi_{ki}'\underline{v}_k' - \psi_{ki}'\langle \underline{v}_i \rangle - \psi_{ki}'\underline{v}_i' + \langle \phi_i \rangle + \phi_i'\end{array}\right]\Delta X \cdot \underline{n}_i dS_i \end{aligned} \tag{3.6}$$

Because of the many unknown fluctuations, eqn (3.6) will be averaged using eqn (3.2). Since the integration limits are arbitrary and the total control volume is continuous, the order of integration can be changed and eqn (3.6) can be written term-by-term

$$\iiint_V \frac{\partial}{\partial t}\left[\int_\mu \left(\langle\psi_k\rangle + \psi_k'\right) X f(\mu) d\mu\right] dV = \iiint_V \frac{\partial}{\partial t}\langle\langle\psi_k\rangle X\rangle dV \tag{3.7a}$$

$$\begin{aligned}&\iint_{S_e}\left\{\int_\mu\left[\left(\langle\psi_k\rangle\langle\underline{v}_k\rangle + \langle\psi_k\rangle\underline{v}_k' + \psi_k'\langle\underline{v}_k\rangle + \psi_k'\underline{v}_k' + \langle\phi_k\rangle + \phi_k'\right) X\cdot\underline{n}_s\right] f(\mu)d\mu\right\} dS_e \\ &= \iint_{S_e}\left[\langle\langle\psi_k\rangle\langle\underline{v}_k\rangle X\rangle + \langle\langle\psi_k'\underline{v}_k'\rangle X\rangle + \langle\langle\phi_k\rangle X\rangle\right]\cdot\underline{n}_s dS_e\end{aligned} \tag{3.7b}$$

$$\begin{aligned}&\iint_{S_i}\left\{\int_\mu\left[\left\{\begin{pmatrix}\langle\psi_{ki}\rangle\langle\underline{v}_k\rangle + \langle\psi_{ki}\rangle\underline{v}_k' - \langle\psi_{ki}\rangle\langle\underline{v}_i\rangle - \langle\psi_{ki}\rangle\underline{v}_i' + \psi_{ki}'\langle\underline{v}_k\rangle \\ + \psi_{ki}'\underline{v}_k' - \psi_{ki}'\langle\underline{v}_i\rangle - \psi_{ki}'\underline{v}_i' + \langle\phi_i\rangle + \phi_i'\end{pmatrix}\Delta X\right\}\cdot\underline{n}_i\right] f(\mu)d\mu\right\} dS_i \\ &= \iint_{S_i}\left[\left(\langle\langle\psi_{ki}\rangle\langle\underline{v}_k\rangle\rangle - \langle\langle\psi_{ki}\rangle\langle\underline{v}_i\rangle\rangle + \langle\psi_{ki}'\underline{v}_k'\rangle - \langle\psi_{ki}'\underline{v}_i'\rangle + \langle\langle\phi_i\rangle\rangle\right)\Delta X\right]\cdot\underline{n}_i dS_i\end{aligned} \tag{3.7c}$$

$$\iiint_V \left[\int_\mu \left(\langle\psi_g\rangle + \psi_g'\right) X f(\mu) d\mu\right] dV = \iiint_V \langle\langle\psi_g\rangle X\rangle dV \tag{3.7d}$$

Combining eqns (3.7a-d) and treating averaged terms as constants so that they can be brought outside the averaging brackets (Brodkey, 1967) give

$$\begin{aligned}&\iiint_V \frac{\partial}{\partial t}\left(\langle\psi_k\rangle\langle X\rangle\right) dV + \iint_{S_e}\left\{\left[\langle\psi_k\rangle\langle\underline{v}_k\rangle + \langle\phi_k\rangle\right]\langle X\rangle + \langle\psi_k'\underline{v}_k' X\rangle\right\}\cdot\underline{n}_s dS_e + \iiint_V \langle\psi_g\rangle\langle X\rangle dV \\ &= \iint_{S_i}\left\{\left[\langle\psi_{ki}\rangle\left(\langle\underline{v}_k\rangle - \langle\underline{v}_i\rangle\right) + \langle\phi_i\rangle\right]\langle\Delta X\rangle + \langle\psi_{ki}'\underline{v}_k'\Delta X\rangle - \langle\psi_{ki}'\underline{v}_i'\Delta X\rangle\right\}\cdot\underline{n}_i dS_i\end{aligned} \tag{3.8}$$

Now, because most engineering measurements produce data that is time and volume averaged, eqn (3.8) will be volume-averaged (Hestroni, 1982)

$$\langle \psi_k \rangle_V = \frac{1}{V} \iiint_V \langle \psi_k \rangle dV \tag{3.9}$$

after applying the Gauss Divergence theorem to the external surface term to give the following

$$\begin{aligned} &\iiint_V \left\{ \frac{\partial \langle \psi_k \rangle \langle X \rangle}{\partial t} + \underline{\nabla} \cdot \left\{ \left[\langle \psi_k \rangle \langle \underline{v}_k \rangle + \langle \phi_k \rangle \right] \langle X \rangle + \langle \psi'_k \underline{v}'_k X \rangle \right\} + \langle \psi_g \rangle \langle X \rangle \right\} dV \\ &= \iint_{S_i} \left\{ \left[\langle \psi_{ki} \rangle \left(\langle \underline{v}_k \rangle - \langle \underline{v}_i \rangle \right) + \langle \phi_i \rangle \right] \langle \Delta X \rangle + \langle \psi'_{ki} \underline{v}'_k \Delta X \rangle - \langle \psi'_{ki} \underline{v}'_i \Delta X \rangle \right\} \cdot \underline{n}_i dS_i \end{aligned} \tag{3.10}$$

Now the volume averaging operator can be applied in a natural way

$$\begin{aligned} &\frac{1}{V} \iiint_V \left\{ \frac{\partial \langle \psi_k \rangle \langle X \rangle}{\partial t} + \underline{\nabla} \cdot \left\{ \left[\langle \psi_k \rangle \langle \underline{v}_k \rangle + \langle \phi_k \rangle \right] \langle X \rangle + \langle \psi'_k \underline{v}'_k X \rangle \right\} + \langle \psi_g \rangle \langle X \rangle \right\} dV \\ &= \frac{1}{V} \left\{ \iint_{S_i} \left\{ \left[\langle \psi_{ki} \rangle \left(\langle \underline{v}_k \rangle - \langle \underline{v}_i \rangle \right) + \langle \phi_i \rangle \right] \langle \Delta X \rangle + \langle \psi'_{ki} \underline{v}'_k \Delta X \rangle - \langle \psi'_{ki} \underline{v}'_i \Delta X \rangle \right\} \cdot \underline{n}_i dS_i \right\} \end{aligned} \tag{3.11}$$

As V -> 0, the left-hand side (LHS) of eqn (3.11) reduces to its integrand, but the right-hand side (RHS) remains in integral form:

$$\begin{aligned} &\frac{\partial}{\partial t} \langle \psi_k \rangle \langle X \rangle + \underline{\nabla} \cdot \left\{ \left[\langle \psi_k \rangle \langle \underline{v}_k \rangle + \langle \phi_k \rangle \right] \langle X \rangle + \langle \psi'_k \underline{v}'_k X \rangle \right\} + \langle \psi_g \rangle \langle X \rangle \\ &= \frac{1}{V} \left\{ \iint_{S_i} \left\{ \left[\langle \psi_{ki} \rangle \left(\langle \underline{v}_k \rangle - \langle \underline{v}_i \rangle \right) + \langle \phi_i \rangle \right] \langle \Delta X \rangle + \langle \psi'_{ki} \underline{v}'_k \Delta X \rangle - \langle \psi'_{ki} \underline{v}'_i \Delta X \rangle \right\} \cdot \underline{n}_i dS_i \right\} \end{aligned} \tag{3.12}$$

Up to this point, the approach has been completely general. However, because of the complexity of the internal surface, we need to simplify the equation. **We will extend the definition of isotropy to allow the property exchange rates over the internal surface to be constant such that they are independent of the direction of S_i. We will assume that the property exchange rate on the interface is the same**

everywhere on the interface at a particular location in the fluid, relative to the interface, regardless of the interface orientation. This is a "generalized isotropy" condition for the interface. With this restriction and defining the following

$$\alpha_k = \langle X \rangle \tag{3.13a}$$

as the ensemble averaged phase fraction and

$$a_i = \frac{S_i \Delta X}{V} \tag{3.13b}$$

as the interfacial area concentration, the integrand on the right-hand side of eqn (3.12) can be factored out, because the "generalized isotropy" restriction implies this integrand is a constant. Therefore,

$$\left\{\left[\langle \psi_{ki} \rangle \left(\langle \underline{v}_k \rangle - \langle \underline{v}_i \rangle\right) + \langle \phi_i \rangle\right]\langle \Delta X \rangle + \langle \psi'_{ki} \underline{v}'_k \Delta X \rangle - \langle \psi'_{ki} \underline{v}'_i \Delta X \rangle\right\} \cdot \underline{n}_i = \text{constant} \tag{3.14}$$

Inserting these definitions into eqn (3.12) and taking the limit as V -> 0 on the RHS, where S_i is arbitrary, eqn (3.12) becomes

$$\begin{aligned} &\frac{\partial}{\partial t}\alpha_k \langle \psi_k \rangle + \underline{\nabla} \cdot \left\{\alpha_k \left[\langle \psi_k \rangle \langle \underline{v}_k \rangle + \langle \phi_k \rangle\right] + \langle \alpha_k \psi'_k \underline{v}'_k \rangle\right\} + \alpha_k \langle \psi_g \rangle \\ &= \left\{a_i \left[\langle \psi_{ki} \rangle \left(\langle \underline{v}_k \rangle - \langle \underline{v}_i \rangle\right) + \langle \phi_i \rangle\right] + \langle a_i \psi'_{ki} \underline{v}'_k \rangle - \langle a_i \psi'_{ki} \underline{v}'_i \rangle\right\} \cdot \underline{n}_i \end{aligned} \tag{3.15}$$

as the ensemble-averaged general multi-fluid property balance with turbulent fluctuations. In eqn (3.15), the interfacial area concentration has been left inside the ensemble averaging brackets of the interfacial turbulence terms and the phase fraction has been left inside the ensemble averaging brackets of the phase k turbulence term. Even though the assumption of "generalized isotropy" allows the terms to be brought

outside the averaging signs, they will be left inside until the closure relationships are defined. As an example, Kataoka, et.al. (Kataoka, 1992) have suggested dividing the interfacial area concentration into a sum of "large scale" and "small scale" terms. This could be readily accommodated in eqn (3.15).

Again, note that this general differential balance assumes "generalized isotropy" is true. It would have to be modified for cases where eqn (3.14) breaks down.

Several limiting cases can be examined to check the form of this equation. First, allow α_k-> 1 and a_i -> 0 so that

$$\frac{\partial\langle\psi\rangle}{\partial t}+\underline{\nabla}\cdot\left[\langle\psi\rangle\langle\underline{v}\rangle+\langle\psi'\underline{v}'\rangle+\langle\phi\rangle\right]+\langle\psi_s\rangle=0 \qquad (3.16)$$

which is the proper form for the ensemble/volume-averaged general property balance for the single fluid case. Conversely, if we allow α_k -> 0 and a_i -> A, a constant value of interfacial surface area, so that it can be brought outside the averaging signs and factored out, then

$$\left[\langle\psi_{ki}\rangle\left(\langle\underline{v}_k\rangle-\langle\underline{v}_i\rangle\right)+\langle\psi'_{ki}\underline{v}'_k\rangle-\langle\psi'_{ki}\underline{v}'_i\rangle+\langle\phi_i\rangle\right]=0 \qquad (3.17)$$

which is the local general property 'jump' condition (Standart, 1964, Ishii, 1975, Delhaye, 1974)

3.3 Mass, Momentum and Energy Balances for Phase k

With the general multi-fluid property balance it is possible to begin to derive equations for mass, momentum, mechanical energy, thermal energy and entropy.

3.3.1 Mass

For mass, define the following

$$\psi_k = \rho_k \tag{3.18a}$$

$$\phi_k = 0 \tag{3.18b}$$

$$\phi_i = 0 \tag{3.18c}$$

$$\psi_g = 0 \tag{3.18d}$$

where ρ_k is the total mass concentration of phase k, and because we are only interested in total mass conservation at this point, we will set the mass diffusion within phase k, ϕ_k, and the mass diffusion as a result of an interface, ϕ_i, equal to zero. As a further simplification, we will restrict the system by having no mass generation, so ψ_g is set to zero. Now, these definitions are inserted into the general property balance equation, eqn (3.15), to obtain

$$\begin{aligned}&\frac{\partial}{\partial t}\left(\alpha_k\langle\rho_k\rangle\right)+\left(\underline{\nabla}\cdot\left[\alpha_k\langle\rho_k\rangle\langle\underline{v_k}\rangle+\langle\alpha_k\rho_k'\underline{v_k'}\rangle\right]\right)\\&=\left(a_i\langle\rho_{ki}\rangle\left[\langle\underline{v_k}\rangle-\langle\underline{v_i}\rangle\right]\right)+\left(\langle a_i\rho_{ki}'\underline{v_k'}\rangle-\langle a_i\rho_{ki}'\underline{v_i'}\rangle\right)\cdot\underline{n_i}\end{aligned} \tag{3.19}$$

Note that the RHS of eqn (3.19) employs the "generalized isotropy" condition defined in eqn (3.14b).

Equation (3.19) can be simplified for incompressible fluids by assuming the density is constant so that there are no density fluctuations

$$\rho_k' = 0 \tag{3.20}$$

for all of the averaged single fluctuation terms. Also, for systems of fluids that are relatively insoluble we can assume that (Ishii, 1975)

$$\rho_{ki} \approx \rho_k \tag{3.21}$$

therefore, eqn (3.19) becomes

$$\frac{\partial}{\partial t}(\alpha_k \rho_k) + \left(\underline{\nabla} \cdot \alpha_k \rho_k \langle \underline{v_k} \rangle\right) = \left(a_i \left[\rho_k \left(\langle \underline{v_k} \rangle - \langle \underline{v_i} \rangle\right)\right]\right) \cdot \underline{n}_i = (a_i \underline{\Gamma}_k) \cdot \underline{n}_i \tag{3.22}$$

where $\underline{\Gamma}_k$ is defined as the mass flux at the interface caused by phase change or reaction (Drew, 1985). For incompressible systems where $\underline{\Gamma}_k$ is zero, the mass balance for phase k can be simplified further

$$\frac{\partial}{\partial t}\alpha_k + \left(\underline{\nabla} \cdot \alpha_k \langle \underline{v_k} \rangle\right) = 0 \tag{3.23}$$

3.3.2 Momentum

For momentum, define the following

$$\psi_k = \rho_k \underline{v}_k \tag{3.24a}$$

$$\phi_k = \underline{\underline{T}}_k \tag{3.24b}$$

$$\phi_i = \underline{\underline{T}}_i \tag{3.24c}$$

$$\psi_g = \rho_k \underline{g} \tag{3.24d}$$

where $\rho_k \underline{v}_k$ is the momentum of phase k, $\underline{\underline{T}}_k$ is the momentum diffusion from viscosity effects within phase k, and $\underline{\underline{T}}_i$ is the momentum diffusion because of the interaction of two fluids at an interface. Momentum generation from body forces, which in this case is only gravity, is $\rho_k \underline{g}$.

$$\frac{\partial}{\partial t}\left[\alpha_k\left\langle\rho_k \underline{v}_k\right\rangle\right]+\left[\underline{\nabla}\cdot\left\{\alpha_k\left\{\left\langle\rho_k \underline{v}_k\right\rangle\left\langle\underline{v}_k\right\rangle+\left\langle\underline{\underline{T}}_k\right\rangle\right\}+\left\langle\alpha_k\rho_k^{'}\underline{v}_k^{'}\underline{v}_k^{'}\right\rangle\right\}\right]-\alpha_k\left\langle\rho_k \underline{g}\right\rangle$$
$$=\left(\left[a_i\left\{\left\langle\rho_{ki}\underline{v}_{ki}\right\rangle\left(\left\langle\underline{v}_k\right\rangle-\left\langle\underline{v}_i\right\rangle\right)+\left\langle\underline{\underline{T}}_i\right\rangle\right\}\right]+\left[\left\langle a_i\rho_{ki}^{'}\underline{v}_{ki}^{'}\underline{v}_k^{'}\right\rangle-\left\langle a_i\rho_{ki}^{'}\underline{v}_{ki}^{'}\underline{v}_i^{'}\right\rangle\right]\right)\cdot\underline{n}_i \tag{3.25}$$

Assuming an incompressible fluid and using the simplifications in eqns (3.20-3.21), the momentum balance can be written as

$$\frac{\partial}{\partial t}\left[\alpha_k\rho_k\left\langle\underline{v}_k\right\rangle\right]+\left[\underline{\nabla}\cdot\left\{\alpha_k\left\{\rho_k\left\langle\underline{v}_k\right\rangle\left\langle\underline{v}_k\right\rangle+\left\langle\underline{\underline{T}}_k\right\rangle\right\}+\rho_k\left\langle\alpha_k\underline{v}_k^{'}\underline{v}_k^{'}\right\rangle\right\}\right]-\alpha_k\rho_k\left\langle\underline{g}\right\rangle$$
$$=\left(\left[a_i\left\{\left\langle\underline{v}_{ki}\right\rangle\Gamma_k+\left\langle\underline{\underline{T}}_i\right\rangle\right\}\right]+\rho_k\left[\left\langle a_i\underline{v}_{ki}^{'}\underline{v}_k^{'}\right\rangle-\left\langle a_i\underline{v}_{ki}^{'}\underline{v}_i^{'}\right\rangle\right]\right)\cdot\underline{n}_i \tag{3.26}$$

For systems with no phase change or reaction, the momentum can be further simplified

$$\frac{\partial}{\partial t}\left[\alpha_k\rho_k\left\langle\underline{v}_k\right\rangle\right]+\left[\underline{\nabla}\cdot\left\{\alpha_k\left\{\rho_k\left\langle\underline{v}_k\right\rangle\left\langle\underline{v}_k\right\rangle+\left\langle\underline{\underline{T}}_k\right\rangle\right\}+\rho_k\left\langle\alpha_k\underline{v}_k^{'}\underline{v}_k^{'}\right\rangle\right\}\right]-\alpha_k\rho_k\left\langle\underline{g}\right\rangle$$
$$=\left\{\left[a_i\left\langle\underline{\underline{T}}_i\right\rangle\right]+\rho_k\left[\left\langle a_i\underline{v}_{ki}^{'}\underline{v}_k^{'}\right\rangle-\left\langle a_i\underline{v}_{ki}^{'}\underline{v}_i^{'}\right\rangle\right]\right\}\cdot\underline{n}_i \tag{3.27}$$

Equation (3.27) is the general momentum balance for an incompressible phase k in a multi-fluid system, given the "generalized isotropy" condition.

If we examine eqn (3.27), all of the terms on the left-hand side (LHS) are the familiar terms from a single-phase momentum balance and are the time-rate of momentum accumulation, momentum convection (inertial terms), momentum diffusion by viscous and Reynold's stresses and momentum generation by body forces (gravity). However, on the RHS, there are additional terms which arise from the interaction of one fluid with another across an interface. The first term represents the diffusion of momentum from one fluid to another and is similar to the viscous stress

single-phase analog. Physically, this term accounts for the transfer of momentum due to the relative motion between fluids. The turbulence term is similar to the single-phase Reynold's stress except that it contains the interfacial area concentration term and therefore accounts for the turbulent interaction between two fluids.

3.3.3 Mechanical Energy

Similar to Bird (1960), the scalar product of the average velocity of phase k will be taken with the momentum balance, eqn (3.26), to obtain a balance equation for mechanical energy.

$$\begin{aligned}&\frac{\partial}{\partial t}\left(\alpha_k\rho_k\frac{\langle v_k^2\rangle}{2}\right)+\left(\underline{\nabla}\cdot\rho_k\alpha_k\frac{\langle v_k^2\rangle}{2}\langle\underline{v}_k\rangle\right)+\left(\langle\underline{v}_k\rangle\cdot\left[\underline{\nabla}\cdot\langle\alpha_k\underline{v}_k'\underline{v}_k'\rangle\right]\right)\\&+\left(\langle\underline{v}_k\rangle\cdot\left[\underline{\nabla}\cdot\alpha_k\langle\underline{\underline{T}}_k\rangle\right]\right)-\left(\langle\underline{v}_k\rangle\cdot\alpha_k\rho_k\langle\underline{g}\rangle\right)\\&=\left[\langle\underline{v}_k\rangle\cdot\left[a_i\left\{\langle\underline{v}_{ki}\rangle\underline{\Gamma}_k+\langle\underline{\underline{T}}_i\rangle\right\}+\rho_k\left\{\langle a_i\underline{v}_{ki}'\underline{v}_k'\rangle-\langle a_i\underline{v}_{ki}'\underline{v}_i'\rangle\right\}\right]\right]\cdot\underline{n}_i\end{aligned}\tag{3.28}$$

Using the following identities (Bird, 1960)

$$\langle\underline{v}_k\rangle\cdot\left[\underline{\nabla}\cdot\alpha_k\langle\underline{\underline{T}}_k\rangle\right]=\underline{\nabla}\cdot\left[\alpha_k\langle\underline{\underline{T}}_k\rangle\cdot\langle\underline{v}_k\rangle\right]-\alpha_k\underline{\underline{T}}_k:\underline{\nabla}\langle\underline{v}_k\rangle\tag{3.29}$$

$$\langle\underline{v}_k\rangle\cdot\left[\underline{\nabla}\cdot\langle\underline{\underline{R}}_k\rangle\right]=\underline{\nabla}\cdot\left[\langle\underline{\underline{R}}_k\rangle\cdot\langle\underline{v}_k\rangle\right]-\underline{\underline{R}}_k:\underline{\nabla}\langle\underline{v}_k\rangle\tag{3.30}$$

and defining the following

$$\underline{\underline{R}}_k=\rho_k\langle\alpha_k\underline{v}_k'\underline{v}_k'\rangle\tag{3.31}$$

$$\underline{\underline{S}}=\rho_k\left[\langle a_i\underline{v}_{ki}'\underline{v}_k'\rangle-\langle a_i\underline{v}_{ki}'\underline{v}_i'\rangle\right]\tag{3.32}$$

where $\underline{\underline{R}}_k$ is the Reynold's stress tensor for the turbulence stress within phase k and $\underline{\underline{S}}$ is an interfluid turbulent correlation tensor, we can re-write the mechanical energy balance. In the mechanical energy balance this allows the total work done by one fluid on the other to be split into an interfacial work term that includes $\underline{\underline{T}}_i$ and an interfluid turbulent work term which includes $\underline{\underline{S}}$. Equation (3.28) can be re-written

$$\begin{aligned}
&\frac{\partial}{\partial t}\left(\alpha_k\rho_k\frac{\langle v_k^2\rangle}{2}\right)+\left(\underline{\nabla}\cdot\alpha_k\rho_k\frac{\langle v_k^2\rangle}{2}\langle\underline{v}_k\rangle\right)+\underline{\nabla}\cdot\left[\langle\underline{\underline{R}}_k\rangle\cdot\langle\underline{v}_k\rangle\right]-\underline{\underline{R}}_k:\underline{\nabla}\langle\underline{v}_k\rangle\\
&+\underline{\nabla}\cdot\left[\alpha_k\langle\underline{\underline{T}}_k\rangle\cdot\langle\underline{v}_k\rangle\right]-\alpha_k\underline{\underline{T}}_k:\underline{\nabla}\langle\underline{v}_k\rangle-\langle\underline{v}_k\rangle\cdot\alpha_k\rho_k\langle\underline{g}\rangle \qquad (3.33)\\
&=\left[\langle\underline{v}_k\rangle\cdot\left[a_i\left\{\langle\underline{v}_{ki}\rangle\Gamma_k+\langle\underline{\underline{T}}_i\rangle\right\}+\underline{\underline{S}}\right]\right]\cdot\underline{n}_i
\end{aligned}$$

A further simplification can be made by assuming no phase change or reaction

$$\begin{aligned}
&\frac{\partial}{\partial t}\left(\alpha_k\rho_k\frac{\langle v_k^2\rangle}{2}\right)+\left(\underline{\nabla}\cdot\alpha_k\rho_k\frac{\langle v_k^2\rangle}{2}\langle\underline{v}_k\rangle\right)+\underline{\nabla}\cdot\left[\langle\underline{\underline{R}}_k\rangle\cdot\langle\underline{v}_k\rangle\right]-\underline{\underline{R}}_k:\underline{\nabla}\langle\underline{v}_k\rangle\\
&+\underline{\nabla}\cdot\left[\alpha_k\langle\underline{\underline{T}}_k\rangle\cdot\langle\underline{v}_k\rangle\right]-\alpha_k\underline{\underline{T}}_k:\underline{\nabla}\langle\underline{v}_k\rangle-\langle\underline{v}_k\rangle\cdot\alpha_k\rho_k\langle\underline{g}\rangle \qquad (3.34)\\
&=\left[\langle\underline{v}_k\rangle\cdot\left[a_i\langle\underline{\underline{T}}_i\rangle+\underline{\underline{S}}\right]\right]\cdot\underline{n}_i
\end{aligned}$$

In this equation, the terms on the LHS represent the time-rate of accumulation of kinetic energy, the convection of kinetic energy for phase k from the surrounding, work from turbulent fluctuations within phase k, energy dissipation from turbulent fluctuations, viscous work from the viscosity of phase k, energy dissipation from phase k viscosity and gravity work (potential energy). On the RHS, the work done by one fluid on the other has been split into a contribution from the relative motion of the

fluids and the turbulent fluctuations that interact between fluids. Again, on the RHS, we note the use of the "generalized isotropy" condition.

3.3.4 Total Energy

For total energy of phase k, define the following

$$\psi_k = \rho_k\left(U_k + \frac{v_k^2}{2}\right) \tag{3.35a}$$

$$\phi_k = \left[\underline{\underline{T}}_k \cdot \langle \underline{v}_k \rangle\right] + \underline{q}_f \tag{3.35b}$$

$$\phi_i = \left[\underline{\underline{T}}_i \cdot \langle \underline{v}_k \rangle\right] + \underline{q}_i \tag{3.35c}$$

$$\psi_g = -\left(\underline{g} \cdot \langle \underline{v}_k \rangle\right) + q_r \tag{3.35d}$$

where ψ_k is the sum of the phase k internal and kinetic energies, ϕ_k is the diffusion of energy by work accomplished by viscous forces and the heat flux to phase k from the external surroundings, ϕ_i is the diffusion of energy from the work done from the relative motion of the fluids at an interface and heat flux across the interface and ψ_g is the generation of energy from gravity and heat of reaction.

Inserting these into the general property balance, eqn (3.15), gives

$$\frac{\partial}{\partial t}\left\langle \rho_k\left(U_k+\frac{v_k^2}{2}\right)\right\rangle+\underline{\nabla}\cdot\left[\alpha_k\left[\left\langle \rho_k\left(U_k+\frac{v_k^2}{2}\right)\right\rangle\langle \underline{v}_k\rangle+\left\langle \underline{\underline{T}}_k\cdot\langle \underline{v}_k\rangle+\underline{q}_f\right\rangle\right]+\left\langle \alpha_k\rho_k^{'}\left(U_k^{'}+\frac{v_k^{'2}}{2}\right)\underline{v}_k^{'}\right\rangle\right]$$
$$+\alpha_k\left\langle -\underline{g}\cdot\langle \underline{v}_k\rangle+q_r\right\rangle \tag{3.36}$$
$$=\left[\begin{array}{l}\left[\left(a_i\left[\left\langle \rho_{ki}\left(U_{ki}+\frac{v_{ki}^2}{2}\right)\right\rangle\left(\langle \underline{v}_k\rangle-\langle \underline{v}_i\rangle\right)+\left\langle \underline{\underline{T}}_i\cdot\langle \underline{v}_k\rangle+\underline{q}_i\right\rangle\right]\right)\right] \\ +\left(\left\langle a_i\rho_{ki}^{'}\left(U_{ki}^{'}+\frac{v_{ki}^{'2}}{2}\right)\underline{v}_k^{'}\right\rangle-\left\langle a_i\rho_{ki}^{'}\left(U_{ki}^{'}+\frac{v_{ki}^{'2}}{2}\right)\underline{v}_i^{'}\right\rangle\right)\end{array}\right]\cdot\underline{n}_i$$

Assuming an incompressible fluid and that averaged variables are constants gives

$$\frac{\partial}{\partial t}\rho_k\left(\langle U_k\rangle+\frac{\langle v_k^2\rangle}{2}\right)+\underline{\nabla}\cdot\left[\alpha_k\left[\rho_k\left(\langle U_k\rangle+\frac{\langle v_k^2\rangle}{2}\right)\langle \underline{v}_k\rangle+\langle \underline{\underline{T}}_k\rangle\cdot\langle \underline{v}_k\rangle+\langle \underline{q}_f\rangle\right]+\rho_k\left\langle \alpha_k\left(U_k^{'}+\frac{v_k^{'2}}{2}\right)\underline{v}_k^{'}\right\rangle\right]$$
$$+\alpha_k\left(-\langle \underline{g}\rangle\cdot\langle \underline{v}_k\rangle+\langle q_r\rangle\right) \tag{3.37}$$
$$=\left[\left(a_i\left[\left(\langle U_{ki}\rangle+\frac{\langle v_{ki}^2\rangle}{2}\right)\underline{\Gamma}_k+\langle \underline{\underline{T}}_i\rangle\cdot\langle \underline{v}_k\rangle+\langle \underline{q}_i\rangle\right]\right)+\rho_k\left(\left\langle a_i\left(U_{ki}^{'}+\frac{v_{ki}^{'2}}{2}\right)\underline{v}_k^{'}\right\rangle-\left\langle a_i\left(U_{ik}^{'}+\frac{v_{ki}^{'2}}{2}\right)\underline{v}_i^{'}\right\rangle\right)\right]\cdot\underline{n}_i$$

Equation (3.37) can be further simplified by assuming no phase change or reaction

$$\frac{\partial}{\partial t}\rho_k\left(\langle U_k\rangle+\frac{\langle v_k^2\rangle}{2}\right)+\underline{\nabla}\cdot\left[\alpha_k\left[\rho_k\left(\langle U_k\rangle+\frac{\langle v_k^2\rangle}{2}\right)\langle \underline{v}_k\rangle+\langle \underline{\underline{T}}_k\rangle\cdot\langle \underline{v}_k\rangle+\langle \underline{q}_f\rangle\right]+\rho_k\left\langle \alpha_k\left(U_k^{'}+\frac{v_k^{'2}}{2}\right)\underline{v}_k^{'}\right\rangle\right]$$
$$-\alpha_k\left(\langle \underline{g}\rangle\cdot\langle \underline{v}_k\rangle\right) \tag{3.38}$$
$$=\left[\left(a_i\left[\langle \underline{\underline{T}}_i\rangle\cdot\langle \underline{v}_k\rangle+\langle \underline{q}_i\rangle\right]\right)+\rho_k\left(\left\langle a_i\left(U_{ik}^{'}+\frac{v_{ki}^{'2}}{2}\right)\underline{v}_k^{'}\right\rangle-\left\langle a_i\left(U_{ki}^{'}+\frac{v_{ki}^{'2}}{2}\right)\underline{v}_i^{'}\right\rangle\right)\right]\cdot\underline{n}_i$$

Again, the LHS is similar to the single-phase total energy balance and represents the time-rate accumulation of total energy, energy convection, diffusion of energy from viscous work and heat flux and energy generation from gravity and reaction. On the RHS, the terms account for energy transfer across an interface from

relative motion, heat flux and turbulent fluctuations. Once more, the "generalized isotropy" condition is employed on the RHS.

3.3.5 Thermal Energy

The equation for thermal energy in a two-fluid system can be obtained in a manner similar to Bird (1960), by subtracting the mechanical energy balance from the total energy balance. Therefore, subtracting eqn (3.34) from eqn (3.38) gives

$$\begin{aligned}&\frac{\partial}{\partial t}\left(\left\langle \rho_k U_k \right\rangle\right)+\underline{\nabla}\cdot\left[\alpha_k\left[\left\langle \rho_k U_k \right\rangle\left\langle \underline{v}_k \right\rangle+\left\langle \underline{q}_f \right\rangle\right]+\left\langle \alpha_k \rho_k' U_k' \underline{v}_k' \right\rangle\right] \\ &+\alpha_k\left\langle q_r \right\rangle+\alpha_k \underline{\underline{T}}_k:\underline{\nabla}\left\langle \underline{v}_k \right\rangle+\underline{\underline{R}}_k:\underline{\nabla}\left\langle \underline{v}_k \right\rangle \\ &=\left[\begin{array}{l}\left(a_i\left[\left\langle \rho_{ki} U_{ki} \right\rangle\left(\left\langle \underline{v}_k \right\rangle-\left\langle \underline{v}_i \right\rangle\right)+\left\langle \underline{q}_i \right\rangle\right]\right) \\ +\left(\left\langle a_i \rho_{ki}'\left(U_{ki}'+\frac{v_{ki}'^2}{2}\right)\underline{v}_k' \right\rangle-\left\langle a_i \rho_{ki}'\left(U_{ki}'+\frac{v_{ki}'^2}{2}\right)\underline{v}_i' \right\rangle\right)-\left(\left\langle \underline{v}_k \right\rangle\cdot\underline{\underline{S}}\right)\end{array}\right]\cdot\underline{n}_i\end{aligned} \tag{3.39}$$

Assuming an incompressible fluid and the definitions in eqns (3.20-3.21) gives

$$\begin{aligned}&\frac{\partial}{\partial t}\left(\rho_k\left\langle U_k \right\rangle\right)+\underline{\nabla}\cdot\left[\alpha_k\left[\rho_k\left\langle U_k \right\rangle\left\langle \underline{v}_k \right\rangle+\left\langle \underline{q}_f \right\rangle\right]+\rho_k\left\langle \alpha_k U_k' \underline{v}_k' \right\rangle\right] \\ &+\alpha_k\left\langle q_r \right\rangle+\alpha_k \underline{\underline{T}}_k:\underline{\nabla}\left\langle \underline{v}_k \right\rangle+\underline{\underline{R}}_k:\underline{\nabla}\left\langle \underline{v}_k \right\rangle \\ &=\left[\begin{array}{l}\left(a_i\left[\left\langle U_{ki} \right\rangle\underline{\Gamma}_k+\left\langle \underline{q}_i \right\rangle\right]\right) \\ +\left(\left\langle a_i \rho_k\left(U_{ki}'+\frac{v_{ki}'^2}{2}\right)\underline{v}_k' \right\rangle-\left\langle a_i \rho_k\left(U_{ki}'+\frac{v_{ki}'^2}{2}\right)\underline{v}_i' \right\rangle\right)-\left(\left\langle \underline{v}_k \right\rangle\cdot\underline{\underline{S}}\right)\end{array}\right]\cdot\underline{n}_i\end{aligned} \tag{3.40}$$

Equation (3.40) can be further simplified by assuming no phase change or reaction and defining

$$\underline{S}_T=\left\langle a_i \rho_k\left(U_{ki}'+\frac{v_{ki}'^2}{2}\right)\underline{v}_k' \right\rangle-\left\langle a_i \rho_k\left(U_{ki}'+\frac{v_{ki}'^2}{2}\right)\underline{v}_i' \right\rangle \tag{3.41}$$

which is the thermal energy equivalent of the interfluid turbulent interaction term defined for the momentum balance. Equation (3.40) then becomes

$$\begin{aligned}&\frac{\partial}{\partial t}\left(\rho_k\langle U_k\rangle\right)+\underline{\nabla}\cdot\left[\alpha_k\left[\rho_k\langle U_k\rangle\langle\underline{v}_k\rangle+\left\langle\underline{q}_f\right\rangle\right]+\rho_k\left\langle\alpha_k U_k^{'}\underline{v}_k^{'}\right\rangle\right]\\&+\alpha_k\langle q_r\rangle+\alpha_k\underline{\underline{T}}_k:\underline{\nabla}\langle\underline{v}_k\rangle+\underline{\underline{R}}_k:\underline{\nabla}\langle\underline{v}_k\rangle\\&=\left[\left(a_i\left\langle\underline{q}_i\right\rangle\right)+\underline{S}_T-\left(\langle\underline{v}_k\rangle\cdot\underline{\underline{S}}\right)\right]\cdot\underline{n}_i\end{aligned}\tag{3.42}$$

The LHS of eqn (3.42) represents the time-rate of accumulation of internal energy, the convection of internal energy from the surrounding, heat flux to phase k from the surroundings, diffusion of internal energy from turbulent fluctuations within phase k, heat flux from reaction in phase k, and the dissipation of energy from viscous and turbulent fluctuations within phase k. The RHS represents the heat flux across the interface and transfer of internal energy from turbulent fluctuations and turbulent work. Again, the "generalized isotropy" condition applies on the RHS.

3.3.6 Entropy Inequality

Define the following

$$\psi_k=\rho_k s_k \tag{3.43a}$$

$$\phi_k=\frac{\underline{q}_f}{T} \tag{3.43b}$$

$$\phi_i=\frac{\underline{q}_i}{T_i} \tag{3.43c}$$

$$\psi_g\geq 0 \tag{3.43d}$$

These can be inserted into the general balance to give

$$\frac{\partial}{\partial t}\left(\alpha_k\langle\rho_k s_k\rangle\right)+\underline{\nabla}\cdot\left[\alpha_k\left[\langle\rho_k s_k\rangle\langle\underline{v}_k\rangle+\left\langle\frac{\underline{q}_f}{T}\right\rangle\right]+\langle\alpha_k\rho_k^{'}s_k^{'}\underline{v}_k^{'}\rangle\right]$$
$$-\left[\left(a_i\left[\langle\rho_{ki}s_{ki}\rangle\left(\langle\underline{v}_k\rangle-\langle\underline{v}_i\rangle\right)+\left\langle\frac{\underline{q}_i}{T}\right\rangle\right]\right)+\left(\langle a_i\rho_{ki}^{'}s_{ki}^{'}\underline{v}_k^{'}\rangle-\langle a_i\rho_{ki}^{'}s_{ki}^{'}\underline{v}_i^{'}\rangle\right)\right]\cdot\underline{n}_i\geq 0 \tag{3.44}$$

Making the usual simplifications gives

$$\frac{\partial}{\partial t}\left(\alpha_k\rho_k\langle s_k\rangle\right)+\underline{\nabla}\cdot\rho_k\left[\alpha_k\left[\langle s_k\rangle\langle\underline{v}_k\rangle+\left\langle\frac{\underline{q}_f}{T}\right\rangle\right]+\langle\alpha_k s_k^{'}\underline{v}_k^{'}\rangle\right]$$
$$-\left[\left(a_i\left\langle\frac{\underline{q}_i}{T}\right\rangle\right)+\rho_k\left(\langle a_i s_{ki}^{'}\underline{v}_k^{'}\rangle-\langle a_i s_{ki}^{'}\underline{v}_i^{'}\rangle\right)\right]\cdot\underline{n}_i\geq 0 \tag{3.45}$$

which represents the general entropy inequality with turbulent fluctuations for a multi-fluid system. The "generalized isotropy" condition applies to the last term on the LHS of eqn (3.45).

3.4 General Property for a Control Volume with Multiple Fluids

Again, consider a control volume such as the one shown in Figure 3.1. For this case, we are interested in the total balance over the control volume (Kataoka, 1986b, Hestroni, 1982) as opposed to the transfer of a property from phase k to phase j. Therefore, the individual phase k property balance equations can be added

$$\frac{\partial}{\partial t}\left(\sum_{k=1}^{n}\alpha_k\langle\psi_k\rangle+\Psi_i\right)+\underline{\nabla}\cdot\left[\sum_{k=1}^{n}\left[\alpha_k\left[\langle\psi_k\rangle\langle\underline{v}_k\rangle+\langle\phi_k\rangle\right]+\langle\alpha_k\psi_k^{'}\underline{v}_k^{'}\rangle\right]+\Psi_i\langle\underline{v}_i\rangle\right] \tag{3.46}$$
$$+\sum_{k=1}^{n}\alpha_k\langle\psi_g\rangle+\Psi_{ig}=0$$

and the additional terms Ψ_i and Ψ_{ig}, represent properties and the generation of properties specific to the internal interfaces that are present. It is important to note

that these are not transfer terms but are unique to the interface. For example, the interfacial energy that is a result of the surface tension over an area is unique to the interface. In contrast, transfer terms represent the transfer of a property across the interface and have opposite signs in the individual phase k balances. Therefore, when added, these terms cancel out and leave only the interfacial properties. In the above equation, the terms are the time-rate of accumulation, convection and diffusion and generation.

3.4.1 Mass

The following balances are based on a two-fluid system so that n = 2. Given eqns (3.18a-d) and assuming that the interface has no mass and no reaction at the interface allows the following to be defined

$$\Psi_i = 0 \tag{3.47a}$$

$$\Psi_{ig} = 0 \tag{3.47b}$$

therefore eqn (3.46) becomes

$$\frac{\partial}{\partial t}\left(\sum_{k=1}^{2}\alpha_k\rho_k\right)+\underline{\nabla}\cdot\left[\sum_{k=1}^{2}\left\{\alpha_k\rho_k\langle\underline{v}_k\rangle\right\}\right]=0 \tag{3.48}$$

which is the overall material balance for a system of two, non-reacting, incompressible fluids.

3.4.2 Momentum

Given eqns (3.24a-d) and define the following interfacial properties

$$\Psi_i = 0 \tag{3.49a}$$

$$\Psi_{ig} = \left[\frac{\langle \underline{F}_i \rangle}{V}\right] \tag{3.49b}$$

These follow because above we assumed that the interface has no mass, therefore it cannot have any momentum so that Ψ_i is equal to zero. However, because of the relative motion of the two fluids, and the presence of an interface with surface tension there is an apparent 'generation' of momentum due to surface forces which are acting on the interface. This 'generation' is modeled by eqn (3.49b). Therefore, eqn (3.46) becomes

$$\begin{aligned}&\frac{\partial}{\partial t}\left[\sum_{k=1}^{2}\alpha_k\rho_k\langle \underline{v}_k\rangle\right]+\underline{\nabla}\cdot\sum_{k=1}^{2}\left\{\alpha_k\left\{\rho_k\langle \underline{v}_k\rangle\langle \underline{v}_k\rangle+\langle \underline{\underline{T}}_k\rangle\right\}+\rho_k\langle \alpha_k \underline{v}_k' \underline{v}_k'\rangle\right\}\\&-\sum_{k=1}^{2}\alpha_k\rho_k\langle \underline{g}\rangle+\left[\frac{\langle \underline{F}_i\rangle}{V}\right]=0\end{aligned} \tag{3.49}$$

which is the form for a system of two, incompressible fluids. In this equation, the first term is the total time-rate of accumulation of momentum for the mixture, the convection and viscous and turbulent dissipation of momentum in the mixture, and the generation of momentum from gravity and interfacial forces.

3.4.3 Total Energy

Given eqns (3.35a-d) and defining

$$\Psi_i = (\sigma a_i) \tag{3.50a}$$

$$\Psi_{ig} = \left(\langle \underline{v}_i\rangle\cdot\left[\frac{\langle \underline{F}_i\rangle}{V}\right]+\frac{\sigma(\underline{\Gamma}_i\cdot\underline{n}_i)}{\rho_{ki}a_i V}\right) \tag{3.50b}$$

so that Ψ_i is the energy associated with the surface tension over the interface and Ψ_{ig} is the combination of the work on the interface by the motion of the interface and the energy of mass flux at the interface. In writing eqn (3.50b), we are again assuming the "generalized isotropy" condition applies.

Inserting these definitions into eqn (3.46) gives the following

$$\frac{\partial}{\partial t}\sum_{k=1}^{2}\left(\rho_k\left(\langle U_k\rangle+\frac{\langle v_k^2\rangle}{2}\right)+\sigma a_i\right)+$$
$$\underline{\nabla}\cdot\left[\sum_{k=1}^{2}\left[\alpha_k\left[\rho_k\left(\langle U_k\rangle+\frac{\langle v_k^2\rangle}{2}\right)\langle\underline{v}_k\rangle+\langle\underline{\underline{T}}_k\rangle\cdot\langle\underline{v}_k\rangle+\langle\underline{q}_f\rangle\right]+\rho_k\left\langle\alpha_k\left(U_k'+\frac{v_k'^2}{2}\right)\underline{v}_k'\right\rangle\right]+(\sigma a_i)\langle\underline{v}_i\rangle\right] \quad (3.51)$$
$$-\sum_{k=1}^{2}\alpha_k\left(\rho_k\langle\underline{g}\rangle\cdot\langle\underline{v}_k\rangle+\langle q_r\rangle\right)+\left(\langle\underline{v}_i\rangle\cdot\left[\frac{\langle\underline{F}_i\rangle}{V}\right]+\frac{\sigma(\underline{\Gamma}_i\cdot\underline{n}_i)}{\rho_{ki}a_iV}\right)=0$$

which is the total energy balance for a two-phase, incompressible fluid system. Assuming no reaction or phase change, eqn (3.51) can be simplified to

$$\frac{\partial}{\partial t}\sum_{k=1}^{2}\left(\rho_k\left(\langle U_k\rangle+\frac{\langle v_k^2\rangle}{2}\right)+\sigma a_i\right)+$$
$$\underline{\nabla}\cdot\left[\sum_{k=1}^{2}\left[\alpha_k\left[\rho_k\left(\langle U_k\rangle+\frac{\langle v_k^2\rangle}{2}\right)\langle\underline{v}_k\rangle+\langle\underline{\underline{T}}_k\rangle\cdot\langle\underline{v}_k\rangle+\langle\underline{q}_f\rangle\right]+\rho_k\left\langle\alpha_k\left(U_k'+\frac{v_k'^2}{2}\right)\underline{v}_k'\right\rangle\right]+(\sigma a_i)\langle\underline{v}_i\rangle\right] \quad (3.52)$$
$$-\sum_{k=1}^{2}\alpha_k\left(\rho_k\langle\underline{g}\rangle\cdot\langle\underline{v}_k\rangle\right)+\left(\langle\underline{v}_i\rangle\cdot\left[\frac{\langle\underline{F}_i\rangle}{V}\right]\right)=0$$

which is the total energy balance for the fluid mixture. Note that is equivalent to summing eqn (3.42) for each phase and adding the properties unique to the interface as described earlier. In this case, besides the energy properties associated with mixture, it includes the time-rate of accumulation of interfacial energy due to a time-

rate of change of interfacial area concentration, convection of interfacial energy into the volume and the generation of interfacial energy due to work exchanged between the two fluids.

3.5 Transport of Interfacial Area

As shown above and discussed earlier, a knowledge of the interfacial area is critical to properly modeling multi-fluid systems. It is a part of all of the interfacial transfer terms. Therefore, to make progress we are going to draw an analogy to single-phase compressible systems. In a single-fluid compressible system, density is a thermodynamic property which can change with the temperature or pressure of the system. With the appropriate equation of state and the thermal energy balance to calculate the temperature, the momentum balances can be solved. By analogy, we are going to assume that the interfacial area is determined by the mechanical energy and interfacial properties of the system. With the proper 'equation of state' to predict the interfacial tension and the mechanical energy balance, it should be possible to model the transport of interfacial area. First, we need to define a transport equation for the interfacial area.

Assume a system of two, isothermal incompressible fluids with no reaction or phase transitions. Adding the individual phase k total energy equations together to define the energy associated with fluid and not the interface gives

$$\frac{\partial}{\partial t}\sum_{k=1}^{2}\left(\rho_k\left(\langle U_k\rangle+\frac{\langle v_k^2\rangle}{2}\right)\right)$$
$$+\underline{\nabla}\cdot\sum_{k=1}^{2}\left[\alpha_k\left[\rho_k\left(\langle U_k\rangle+\frac{\langle v_k^2\rangle}{2}\right)\langle \underline{v}_k\rangle+\langle \underline{\underline{T}}_k\rangle\cdot\langle \underline{v}_k\rangle+\langle \underline{q}_f\rangle\right]+\rho_k\left\langle\alpha_k\left(U_k^{'}+\frac{v_k^{'2}}{2}\right)\underline{v}_k^{'}\right\rangle\right] \quad (3.53)$$
$$-\sum_{k=1}^{2}\alpha_k\left(\rho_k\langle \underline{g}\rangle\cdot\langle \underline{v}_k\rangle\right)=0$$

This is the internal and kinetic energy associated with the bulk phases in the system. Subtracting eqn (3.53) from the total energy balance, eqn (3.52), one obtains

$$\frac{\partial}{\partial t}(\sigma a_i)+\underline{\nabla}\cdot\left[\sigma a_i\langle \underline{v}_i\rangle\right]=\langle \underline{v}_i\rangle\cdot\left[\frac{\langle \underline{F}_i\rangle}{V}\right] \quad (3.54)$$

The 'equation of state' for most systems with no significant mass or heat transfer can be approximated by

$$\sigma = \text{constant} \quad (3.56)$$

a constant value in the direction normal to the interface. Therefore, eqn (3.54) becomes

$$\frac{\partial}{\partial t}a_i+\underline{\nabla}\cdot\left[a_i\langle \underline{v}_i\rangle\right]=\frac{1}{\sigma}\left(\langle \underline{v}_i\rangle\cdot\left[\frac{\langle \underline{F}_i\rangle}{V}\right]\right) \quad (3.57)$$

which defines the transport of interfacial area.

3.6 Constitutive Equations and Equations of State for Multi-Fluid Systems

3.6.1 Continuum Theory Approach

In order to solve the balance and transport equations for mass, momentum, energy and interfacial area, additional relationships are needed to describe the density, viscous stress, multi-material interaction and turbulence correlations for momentum

and energy transfer and dissipation. Unfortunately, it is difficult to define the appropriate equations for single material systems and often one has to resort to defining relationships for 'ideal' materials such as Newtonian or non-Newtonian materials or assuming incompressibility. Multi-fluid systems are complicated by the fact that under different conditions, various flow regimes exist which defy general description. Empirical correlations are usually used to approximate the system of interest. However, general principles have been determined (Truesdell, 1960) which can be used to guide the selection of appropriate constituitive equations.

Coordinate Invariance

This is a requirement that the relationship cannot depend on the coordinate system. This can usually be achieved by working with the appropriate vector-tensor notation.

Equipresence

This principle requires that all of the dependent variables be functions of the same set of independent and dependent variables. For example, if T is a function of ΔV then all other variables must also be functions of ΔV. It is intended to ensure that all of the dependencies are included. However, this is often a difficult principle to satisfy because of the complicated relationships that must be defined and often functions must be included for which there is no physical evidence (Drew and Lahey, 1979).

Material Frame Indifference (Objectivity)

This is similar to the first principle of coordinate system indifference except that this is referring to coordinate frame, such as, Euclidean or non-Euclidean space. Unfortunately, the materials being modeled do not always know the 'coordinate frame of reference' that we have assigned them. This has been thoroughly studied by various researchers (Ishii, 1975, Drew and Lahey, 1979, Dobran, 1984). A conclusion is that if the constituitive equations are formulated from objective variables then the final expression will be objective (Drew and Wood, 1985). This is the approach generally followed in this work.

Homogeneity

This principle requires that the equations be formulated for the particular material being studied. Therefore, in mixtures, various relationships are needed as functions of time and space to properly predict the system behavior.

Material Isotropy

Some materials behave differently depending on the direction that force is applied. This may be true in some multi-fluid flow situations. If there is no dependence on direction or orientation, then the material is isotropic.

Just Setting

This simple principle requires that the appropriate balance equations, with the proper constituitive equations and correct initial and boundary conditions, have a unique solution.

Dimensional Invariance

All constituitive equations must be dimensionally correct and any arbitrary relationships must be satisfied through dimensionless variables.

Correct Low Concentration Limits

This principle (Drew and Lahey, 1979) ensures that the limiting cases have the appropriate single fluid form. In fact, this principle could be generalized to ensure that the equations predict the proper behavior under all limiting cases, such as zero velocity or zero interfacial area.

3.6.2 Entropy Inequality

The entropy inequality restricts the constituitive equations by forcing the second law of thermodynamics to be satisfied. Essentially, this requires that for 'real' systems, entropy must increase. While exact formulations cannot be predicted, it can give guidance on the values and proper final forms.

3.7 Equations of State

When working with compressible fluids, conditions of extreme pressure or large temperature changes, an equation of state is required to define the thermodynamic variables in a system. In this work, the fluids and system conditions have been restricted so that the fluids can be considered to be incompressible. Also, the systems have been observed at small ambient temperature changes so that they can be assumed to be isothermal. Therefore, the equation of state reduces to

$$\rho_k = K_k \tag{3.58}$$

which is a constant density. Also, the internal energy equation is not required because the system is isothermal.

3.8 Equation Summary of the General Model

The general model for predicting interfacial area transport in an isothermal system of two Newtonian, incompressible fluids with no phase change, reaction or mass transfer is summarized below.

Mass:

$$\frac{\partial \alpha_k}{\partial t} + \underline{\nabla} \cdot \alpha_k \langle \underline{v}_k \rangle = 0 \tag{3.59}$$

Momentum:

Continuous Phase

$$\begin{aligned} &\frac{\partial}{\partial t} \alpha_c \rho_c \langle \underline{v}_c \rangle + \underline{\nabla} \cdot \alpha_c \rho_c \langle \underline{v}_c \rangle \langle \underline{v}_c \rangle + \underline{\nabla} \cdot \underline{\underline{R}}_c + \underline{\nabla} \cdot \alpha_c \underline{\underline{T}}_k - \alpha_k \rho_k \underline{g} \\ &= \left\{ \left[a_i \langle \underline{\underline{T}}_i \rangle \right] + \underline{\underline{S}} \right\} \cdot \underline{n}_i \end{aligned} \tag{3.60}$$

Dispersed Phase

$$\begin{aligned} &\frac{\partial}{\partial t} \alpha_d \rho_d \langle \underline{v}_d \rangle + \underline{\nabla} \cdot \alpha_d \rho_d \langle \underline{v}_d \rangle \langle \underline{v}_d \rangle + \underline{\nabla} \cdot \underline{\underline{R}}_d + \underline{\nabla} \cdot \alpha_d \underline{\underline{T}}_d - \alpha_d \rho_d \underline{g} \\ &= \left\{ \left[a_i \langle \underline{\underline{T}}_i \rangle \right] + \underline{\underline{S}} \right\} \cdot \underline{n}_i \end{aligned} \tag{3.61}$$

Mechanical Energy Continuous Phase:

$$\frac{\partial}{\partial t}\alpha_c\rho_c\frac{\langle \underline{v}_c^2\rangle}{2}+\underline{\nabla}\cdot\alpha_c\rho_c\frac{\langle \underline{v}_c^2\rangle}{2}\langle \underline{v}_c\rangle-\langle \underline{v}_c\rangle\cdot\rho_c\langle \underline{g}\rangle$$
$$+\underline{\nabla}\cdot\left[\underline{\underline{R}}_c\cdot\langle \underline{v}_c\rangle\right]-\underline{\underline{R}}_c:\underline{\nabla}\langle \underline{v}_c\rangle+\underline{\nabla}\cdot\left[\alpha_c\underline{\underline{T}}_c\cdot\langle \underline{v}_c\rangle\right]-\alpha_c\underline{\underline{T}}_c:\underline{\nabla}\langle \underline{v}_c\rangle \tag{3.62}$$
$$=\left[\langle \underline{v}_i\rangle\cdot\left(\left\{\left[a_i\langle \underline{\underline{T}}_i\rangle\right]\right\}+\underline{\underline{S}}\right\}\cdot\underline{n}_i\right)\right]$$

Interfacial Area:

$$\frac{\partial}{\partial t}a_i+\underline{\nabla}\cdot\left(a_i\langle \underline{v}_i\rangle\right)=\frac{1}{\sigma}\left(\langle \underline{v}_i\rangle\cdot\left[\frac{\langle \underline{F}_i\rangle}{V}\right]\right) \tag{3.63}$$

To interpret the equations, it helps to non-dimensionalize them and examine limiting cases. First, define the following dimensionless variables

$$\langle \underline{v}_k^*\rangle=\frac{\langle \underline{v}_k\rangle}{v} \tag{3.64a}$$

$$\langle p_k^*\rangle=\frac{\langle p_k\rangle}{\rho_k v^2} \tag{3.64b}$$

$$t^*=\frac{tv}{D} \tag{3.64c}$$

$$a_i^*=a_iD \tag{3.64d}$$

$$\underline{\nabla}^*=\underline{\nabla}D \tag{3.64e}$$

$$\nabla^{*2}=\nabla^2D^2 \tag{3.64f}$$

$$\underline{\underline{R}}_k^*=\frac{\underline{\underline{R}}_k}{\rho_k v^2} \tag{3.64g}$$

$$T_k^* = \underline{\underline{T}}_k \frac{D}{\mu_k v} \tag{3.64f}$$

$$\underline{\underline{T}}_i^* = \underline{\underline{T}}_i \frac{D}{\rho_k v^2} \tag{3.64g}$$

$$\underline{\underline{S}}^* = \underline{\underline{S}} \frac{D}{\rho_k v^2} \tag{3.64h}$$

where v and D are a characteristic velocity and length for the system. In this case, we will define v as the total final average velocity and D is the outer pipe diameter of the system. If we insert these definitions into the vector-tensor form of the various equations, we get for the mass, momentum, and mechanical energy (Drew and Wood, 1985, Bird, 1960)

Mass :

$$\frac{\partial \alpha_k}{\partial t^*} + \underline{\nabla}^* \cdot \alpha_k \langle \underline{v}_k^* \rangle = 0 \tag{3.65}$$

Momentum:

Continuous

$$\begin{aligned} &\frac{\partial}{\partial t^*} \alpha_c \rho_c \langle \underline{v}_c^* \rangle + \underline{\nabla}^* \cdot \alpha_c \rho_c \langle \underline{v}_c^* \rangle \langle \underline{v}_c^* \rangle + \underline{\nabla}^* \cdot \underline{\underline{R}}_c^* + \frac{1}{\mathrm{Re}} \underline{\nabla}^* \cdot \alpha_c \underline{\underline{T}}_c^* - \frac{\alpha_c}{Fr} \frac{\underline{g}}{g} \\ &= \left\{ \left[a_i^* \langle \underline{\underline{T}}_i^* \rangle \right] + \underline{\underline{S}}^* \right\} \cdot \underline{n}_i \end{aligned} \tag{3.66}$$

Dispersed

$$\frac{\partial}{\partial t^*}\alpha_d\rho_d\langle \underline{v}_d^*\rangle+\underline{\nabla}^*\cdot\alpha_d\rho_d\langle \underline{v}_d^*\rangle\langle \underline{v}_d^*\rangle+\underline{\nabla}^*\cdot\underline{\underline{R}}_d^*+\frac{1}{\mathrm{Re}}\underline{\nabla}^*\cdot\alpha_d\underline{\underline{T}}_d^*-\frac{\alpha_d}{Fr}\frac{\underline{g}}{g}$$
$$=\left\{\left[a_i^*\langle \underline{\underline{T}}_i^*\rangle\right]+\underline{\underline{S}}^*\right\}\cdot\underline{n}_i \qquad (3.67)$$

Mechanical Energy

$$\frac{\partial}{\partial^* t}\alpha_c\rho_c\frac{\langle v_c^{*2}\rangle}{2}+\underline{\nabla}^*\cdot\alpha_c\rho_c\frac{\langle v_c^{*2}\rangle}{2}\langle \underline{v}_c^*\rangle-\langle \underline{v}_c^*\rangle\frac{\alpha_c}{Fr}\cdot\frac{\underline{g}}{g}$$
$$+\underline{\nabla}^*\cdot\left[\underline{\underline{R}}_c^*\cdot\langle \underline{v}_c^*\rangle\right]-\underline{\underline{R}}_c^*:\underline{\nabla}^*\langle \underline{v}_c^*\rangle+\frac{1}{\mathrm{Re}}\left(\underline{\nabla}^*\cdot\left[\alpha_c\underline{\underline{T}}_c^*\cdot\langle \underline{v}_c^*\rangle\right]-\alpha_c\underline{\underline{T}}_c^*:\underline{\nabla}^*\langle \underline{v}_c^*\rangle\right) \qquad (3.68)$$
$$=\left[\langle \underline{v}_i^*\rangle\cdot\left(\left\{a_i^*\langle \underline{\underline{T}}_i^*\rangle+\underline{\underline{S}}^*\right\}\cdot\underline{n}_i\right)\right]$$

For the interfacial area concentration transport equation, we need to scale the "source terms" on the RHS. Observations of the mixing process (Reimus, 1983; Lin, 1985; Jacob, 1995) indicate that most of the drop production process happens very rapidly and appears to be mainly the result of interfacial shear. Therefore, based on these observations, we shall define the following

$$\frac{1}{\sigma}\left(\langle \underline{v}_i\rangle\cdot\left[\frac{\langle \underline{F}_i\rangle}{V}\right]\right)=\frac{1}{\sigma}\left[\langle \underline{v}_i\rangle\cdot\left(\left\{a_i\langle \underline{\underline{T}}_i\rangle+\underline{\underline{S}}\right\}\cdot\underline{n}_i\right)\right]\approx O\left(\frac{\mu v^2}{\sigma D^2}\right) \qquad (3.69)$$

With that definition and inserting into the interfacial area concentration transport equation, eqn (3.63) becomes

$$\left(\frac{v}{D^2}\right)\frac{\partial}{\partial t^*}a_i^*+\left(\frac{v}{D^2}\right)\underline{\nabla}\cdot\left(a_i^*\langle \underline{v}_i^*\rangle\right)=-\left(\frac{\mu v^2}{\sigma D^2}\right)\left[\langle \underline{v}_i^*\rangle\cdot\left(\left\{a_i^*\langle \underline{\underline{T}}_i^*\rangle+\underline{\underline{S}}^*\right\}\cdot\underline{n}_i\right)\right] \qquad (3.70)$$

and multiplying both sides by D^2/v we obtain

$$\frac{\partial}{\partial t^*} a_i^* + \underline{\nabla} \cdot \left(a_i^* \langle \underline{v}_i^* \rangle \right) = -\frac{\mu v}{\sigma} \left[\langle \underline{v}_i^* \rangle \cdot \left(\left\{ a_i^* \langle \underline{\underline{T}}_i^* \rangle + \underline{\underline{S}}^* \right\} \cdot \underline{n}_i \right) \right] \tag{3.71}$$

These dimensionless groups can be re-defined as the well-known Weber and Reynold's numbers as follows

$$\frac{\partial}{\partial t^*} a_i^* + \underline{\nabla} \cdot \left(a_i^* \langle \underline{v}_i^* \rangle \right) = -\frac{We}{\mathrm{Re}} \left[\langle \underline{v}_i^* \rangle \cdot \left(\left\{ a_i^* \langle \underline{\underline{T}}_i^* \rangle + \underline{\underline{S}}^* \right\} \cdot \underline{n}_i \right) \right] \tag{3.72}$$

Therefore, we conclude that the general model meets all of the important requirements to begin formulating a practical model to predict the transport of interfacial area.

Chapter 4

MODELING INTERFACIAL AREA TRANSPORT

4.1 The One-Dimensional Model

A one-dimensional model will be derived to predict the interfacial area transport in selected static mixing devices. Even though earlier attempts to determine the type of turbulence and potentially the mixing phenomena have been inconclusive (Tavarez, 1991), and even though mixing is a multi-dimensional behavior, using a one-dimensional model is justified to begin to explore the basis of interfacial area transport. This allows the focus to be on the main effects in the formulation as opposed to numerical problems that can arise from higher dimensional models (Gresho, 1982). Many researchers have used one-dimensional models (Ishii, 1984; Jones and Prosperetti; 1985, Bannerjee and Chan, 1980; Pauchon and Bannerjee, 1986,1988; Lahey, 1991) to examine various closures relationships for the momentum balances, in particular, for the momentum interaction terms. Because of the effectiveness of this approach, we will adopt it for this work.

4.2 Constitutive Equations

4.2.1 Momentum Diffusion

For a Newtonian fluid, the following linear relationship is valid for the normal and tangential stress within phase k (Bird, 1960)

$$\underline{\underline{T}}_k = p_k \underline{\underline{I}} + \underline{\underline{\tau}}_k \tag{4.1}$$

$$\underline{\underline{\tau}}_k = -\mu_k \left\{ \underline{\nabla v}_k + \left(\underline{\nabla v}_k \right)^T \right\} + \left(\frac{2}{3}\mu_k - \kappa \right) \left(\underline{\nabla} \cdot \underline{v}_k \right) \underline{\underline{I}} \tag{4.2}$$

However, for most systems, κ, the bulk viscosity can be neglected and will be set to zero (Bird, 1960).

Now, the average of eqn (4.2) is

$$\left\langle \underline{\underline{T}}_k \right\rangle = \left(\left\langle p_k \right\rangle + \frac{2}{3}\mu_k \left\langle \underline{\nabla} \cdot \underline{v}_k \right\rangle \right) \underline{\underline{I}} - \left[\mu_k \left\langle \underline{\nabla v}_k + \left(\underline{\nabla v}_k \right)^T \right\rangle \right] \tag{4.3}$$

The question is what is the average of the divergence and dyadic terms? If we recall the definition of the ensemble average and Leibnitz's rule for differentiating an integral (Spiegel, 1992)

$$\left\langle \psi(\underline{x},t) \right\rangle = \int_{\mu} \psi(\underline{x},t;\mu) f(\mu) d\mu \tag{4.4}$$

$$\left(\frac{d}{d\underline{x}} \left\langle \psi(\underline{x},t) \right\rangle \right)_t = \int_a^b \frac{\partial}{\partial \underline{x}} \psi(\underline{x},t;\mu) f(\mu) d\mu + \psi(b,\underline{x}) f(b) \frac{db}{d\underline{x}} - \psi(a,\underline{x}) f(a) \frac{da}{d\underline{x}} \tag{4.5}$$

where the subscript t represents the differential with time held constant and a and b are constants which define the range of μ. We also assume that ψ is a continuous and differentiable function which is true within phase k. If a and b are constants, then their differentials are zero and

$$\left(\frac{d}{d\underline{x}} \left\langle \psi(\underline{x},t) \right\rangle \right)_t = \int_a^b \frac{\partial}{\partial \underline{x}} \psi(\underline{x},t;\mu) f(\mu) d\mu \tag{4.6}$$

which is the result given in Brodkey (1967),

$$\langle \underline{\nabla}\psi_k \rangle = \underline{\nabla}\langle \psi_k \rangle \tag{4.8}$$

and is true for the case

$$\langle \underline{\nabla}\cdot\psi \rangle = \underline{\nabla}\cdot\langle \psi \rangle \tag{4.9}$$

Given these transformations, we can write the total momentum diffusion term as

$$\langle \underline{\underline{T}}_k \rangle = \langle p_k \rangle \underline{\underline{I}} + \frac{2}{3}\mu_k \left(\underline{\nabla}\cdot\langle \underline{v}_k \rangle\right)\underline{\underline{I}} - \mu_k \left\{ \underline{\nabla}\langle \underline{v}_k \rangle + \left(\underline{\nabla}\langle \underline{v}_k \rangle\right)^T \right\} \tag{4.10}$$

We can simplify this for incompressible fluids by setting $\underline{\nabla}\cdot\langle \underline{v}_k \rangle = 0$. However, when two incompressible fluids are rapidly mixed, such as in static mixers, there can be significant acceleration and deceleration. Therefore, there is a question as to whether the divergence is zero in this case. For this work, we will allow a non-zero divergence because each component in the mixture separately behaves like a compressible fluid. Taking the divergence of the expression gives

$$\underline{\nabla}\cdot\alpha_k\langle \underline{\underline{T}}_k \rangle = \underline{\nabla}\cdot\left\{\alpha_k\langle p_k \rangle \underline{\underline{I}}\right\} + \underline{\nabla}\cdot\left\{\frac{2}{3}\alpha_k\mu_k\left(\underline{\nabla}\cdot\langle \underline{v}_k \rangle\right)\underline{\underline{I}}\right\} - \underline{\nabla}\cdot\left\{\alpha_k\mu_k\left\{\underline{\nabla}\langle \underline{v}_k \rangle + \left(\underline{\nabla}\langle \underline{v}_k \rangle\right)^T\right\}\right\} \tag{4.11}$$

With the following identities, assuming a constant viscosity

$$-\underline{\nabla}\cdot\alpha_k\mu_k\left(\underline{\nabla}\langle \underline{v}_k \rangle\right)^T = -\mu_k\left[\underline{\nabla}\langle \underline{v}_k \rangle\cdot\underline{\nabla}\alpha_k + \alpha_k\underline{\nabla}\left(\underline{\nabla}\cdot\langle \underline{v}_k \rangle\right)\right] \tag{4.12a}$$

$$-\underline{\nabla}\cdot\alpha_k\mu_k\left(\underline{\nabla}\langle \underline{v}_k \rangle\right) = -\mu_k\left[\underline{\nabla}\alpha_k\cdot\underline{\nabla}\langle \underline{v}_k \rangle + \alpha_k\nabla^2\langle \underline{v}_k \rangle\right] \tag{4.12b}$$

and carrying out the differentiation for the remaining terms give the following

$$\underline{\nabla}\cdot\left\{\alpha_k\langle p_k \rangle \underline{\underline{I}}\right\} = \alpha_k\underline{\nabla}\langle p_k \rangle + \langle p_k \rangle\underline{\nabla}\alpha_k \tag{4.13a}$$

$$\underline{\nabla}\cdot\left\{\frac{2}{3}\alpha_k\mu_k\left(\underline{\nabla}\cdot\langle \underline{v}_k \rangle\right)\underline{\underline{I}}\right\} = \frac{2}{3}\mu_k\left[\underline{\nabla}\alpha_k\left(\underline{\nabla}\cdot\langle \underline{v}_k \rangle\right) + \alpha_k\underline{\nabla}\left(\underline{\nabla}\cdot\langle \underline{v}_k \rangle\right)\right] \tag{4.13b}$$

Inserting these terms into eqn (4.11) and simplifying give

$$\begin{aligned}\underline{\nabla}\cdot\alpha_k\langle\underline{\underline{T}}_k\rangle &= \alpha_k\left[\underline{\nabla}\langle p_k\rangle-\mu_k\left[\nabla^2\langle\underline{v}_k\rangle+\frac{1}{3}\underline{\nabla}\left(\underline{\nabla}\cdot\langle\underline{v}_k\rangle\right)\right]\right]+\langle p_k\rangle\underline{\nabla}\alpha_k \\ &+\mu_k\left[\frac{2}{3}\underline{\nabla}\alpha_k\left(\underline{\nabla}\cdot\langle\underline{v}_k\rangle\right)-\left[\underline{\nabla}\alpha_k\cdot\underline{\nabla}\langle\underline{v}_k\rangle+\underline{\nabla}\langle\underline{v}_k\rangle\cdot\underline{\nabla}\alpha_k\right]\right]\end{aligned} \tag{4.14}$$

where the first three terms on the right-hand side are the pressure and viscous stress associated with phase k and the last four terms are the multi-material pressure and stress which arise from having two fluids occupying the same control volume.

4.2.2 Interfluid Momentum Transfer

If we take the momentum equation, eqn (3.27),

$$\begin{aligned}&\frac{\partial}{\partial t}\alpha_k\rho_k\langle\underline{v}_k\rangle+\underline{\nabla}\cdot\left\{\alpha_k\left\{\rho_k\langle\underline{v}_k\rangle\langle\underline{v}_k\rangle+\langle\underline{\underline{T}}_k\rangle\right\}+\underline{\underline{R}}_k\right\}-\alpha_k\rho_k\langle\underline{g}\rangle \\ &=\left\{\left[a_i\langle\underline{\underline{T}}_i\rangle\right]+\underline{\underline{S}}\right\}\cdot\underline{n}_i\end{aligned} \tag{4.15}$$

and insert eqn (4.14) then

$$\begin{aligned}&\frac{\partial}{\partial t}\alpha_k\rho_k\langle\underline{v}_k\rangle+\underline{\nabla}\cdot\alpha_k\rho_k\langle\underline{v}_k\rangle\langle\underline{v}_k\rangle \\ &+\alpha_k\left[\nabla\langle p_k\rangle-\rho_k\langle\underline{g}\rangle-\mu_k\left[\nabla^2\langle\underline{v}_k\rangle+\frac{1}{3}\underline{\nabla}\left(\underline{\nabla}\cdot\langle\underline{v}_k\rangle\right)\right]\right]+\underline{\nabla}\cdot\underline{\underline{R}}_k \\ &=-\mu_k\left[\frac{2}{3}\underline{\nabla}\alpha_k\left(\underline{\nabla}\cdot\langle\underline{v}_k\rangle\right)-\left[\underline{\nabla}\alpha_k\cdot\underline{\nabla}\langle\underline{v}_k\rangle+\underline{\nabla}\langle\underline{v}_k\rangle\cdot\underline{\nabla}\alpha_k\right]\right] \\ &-\langle p_k\rangle\underline{\nabla}\alpha_k+\left\{\left[a_i\langle\underline{\underline{T}}_i\rangle\right]+\underline{\underline{S}}\right\}\cdot\underline{n}_i\end{aligned} \tag{4.16}$$

We can compare this equation to others that have been published, such as Drew (1985) and Ishii (1984).

$$\frac{\partial}{\partial t}\alpha_k\rho_k\langle\underline{v}_k\rangle+\underline{\nabla}\cdot\left(\alpha_k\rho_k\langle\underline{v}_k\rangle\langle\underline{v}_k\rangle\right)=-\alpha_k\nabla p_k+\underline{\nabla}\cdot\alpha_k\left(\underline{\underline{\tau}}_k+\underline{\underline{\tau}}_k^{\mathrm{Re}}\right)+\alpha_k\rho_k\underline{g}$$
$$+\langle\underline{v}_{ki}\rangle\Gamma_k+\underline{M}_k-\nabla\alpha_k\cdot\underline{\underline{\tau}}_{ki} \tag{4.17}$$

It has been customary to define $\underline{M}_k$ similiar to Ishii (1984) as

$$\underline{M}_k=-p_{ki}\nabla\alpha_k+\sum\frac{\underline{F}_i}{V} \tag{4.18}$$

where the second term is the sum of forces which are associated with drag, virtual mass, and unsteady state viscous effects. Allowing for differences in averaging approaches, by comparison

$$-\alpha_k\mu_k\left[\nabla^2\langle\underline{v}_k\rangle+\frac{1}{3}\underline{\nabla}\left(\underline{\nabla}\cdot\langle\underline{v}_k\rangle\right)\right]=\alpha_k\underline{\nabla}\cdot\langle\underline{\underline{\tau}}_k\rangle \tag{4.19a}$$

$$\underline{\underline{R}}_k=-\alpha_k\underline{\underline{\tau}}_k^{\mathrm{Re}} \tag{4.19b}$$

$$\mu_k\left[\frac{2}{3}\underline{\nabla}\alpha_k\left(\underline{\nabla}\cdot\langle\underline{v}_k\rangle\right)-\left[\underline{\nabla}\alpha_k\cdot\underline{\nabla}\langle\underline{v}_k\rangle+\underline{\nabla}\langle\underline{v}_k\rangle\cdot\underline{\nabla}\alpha_k\right]\right]=\nabla\alpha_k\cdot\underline{\underline{\tau}}_{ki} \tag{4.19c}$$

$$-\langle p_k\rangle\underline{\nabla}\alpha_k+\left\{\left[a_i\langle\underline{\underline{T}}_i\rangle\right]+\underline{\underline{S}}\right\}\cdot\underline{n}_i=-p_{ki}\nabla\alpha_k+\sum\frac{\underline{\underline{F}}_i}{V} \tag{4.19d}$$

With the above relationships, we can complete the balances for momentum and interfacial area concentration. Given eqn (4.18) above

$$\left\{\left[a_i\langle\underline{\underline{T}}_i\rangle\right]+\underline{\underline{S}}\right\}\cdot\underline{n}_i=\sum\frac{\underline{\underline{F}}_i}{V} \tag{4.20}$$

and this can be inserted into the transport equation for interfacial area concentration to give

$$\frac{\partial}{\partial t}a_i+\underline{\nabla}\cdot\left(a_i\langle\underline{v}_i\rangle\right)=\frac{1}{\sigma}\left(\langle\underline{v}_i\rangle\cdot\left[\left\{a_i\langle\underline{\underline{T}}_i\rangle+\underline{\underline{S}}\right\}\cdot\underline{n}_i\right]\right) \tag{4.21}$$

This allows a_i to be calculated in terms of the momentum and mechanical energy balances.

At this point, because of the complexity of the fluid interactions, general forms can only be formulated for the various pressure and additional force terms after some type of assumption has been made for the flow regime. Flow regimes have been extensively studied and various 'maps' have been measured. An example is the 'Baker' area plot for two-phase gas/liquid horizontal flow, see Figure 4.1.

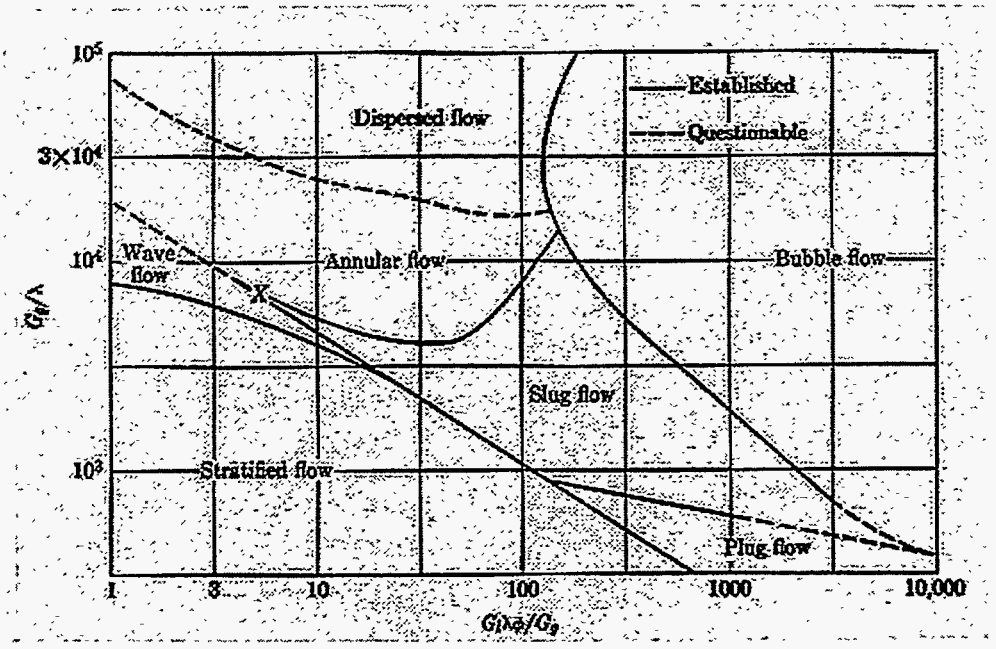

Figure 4.1 Area Plot for Two-Phase Horizontal Flow (Brodkey, 1967)

This is still an area of much research (Kalkach-Navarro, 1994) and for the present empirical equations are used to describe portions of the flow behavior. Unfortunately, since this is still the state-of-the-art, we will use that approach in this work.

Therefore, we will assume bubbly/dispersed flow so that for the pressure terms with constant surface tension and spherical drops or bubbles, we can define

$$\langle p_{di} \rangle = \langle p_d \rangle - 2\sigma a_i \tag{4.22}$$

Also, calculations assuming inviscid flow around a sphere (Stuhmiller, 1977) show that

$$\langle p_{ci} \rangle = \langle p_c \rangle - \xi \rho_c \left| \langle \underline{v}_c \rangle - \langle \underline{v}_d \rangle \right|^2 \tag{4.23}$$

where ξ is equal to 1/4 when the boundary layer remains attached to the bubble or drop.

There is still much active research into the types of forces that influence momentum and energy transfer between fluids. Because we are interested in how the interfacial area transport affects multi-fluid systems, we are going to assume that the forces that dominate the flow situations studied in this work are drag and virtual mass and that a simple linear combination is adequate. Other forces, such as lift, Faxen, Basset and additional surface tension forces, which are known to exist will be neglected, mainly because there is still some controversy over the proper forms (Drew and Lahey, 1979; Ishii and Mishima, 1984).

The drag force can be defined as (Lahey, 1991)

$$F_d = \frac{3}{8} \frac{\alpha_d \rho_c C_d}{r_b} \left| \langle \underline{v}_c \rangle - \langle \underline{v}_d \rangle \right| \left(\langle \underline{v}_c \rangle - \langle \underline{v}_d \rangle \right) \tag{4.24}$$

where r_b is the radius of a bubble or drop. Given eqn (4.24) we are going to re-define the drag force as (Lahey, 1990)

$$F_d = \frac{3}{8}\alpha_d \rho_c C_d a_i \left|\langle \underline{v}_c \rangle - \langle \underline{v}_d \rangle\right| \left(\langle \underline{v}_c \rangle - \langle \underline{v}_d \rangle\right) \tag{4.25}$$

so that the total drag force is proportional to the interfacial area concentration. According to Ishii (1979), C_d is a function of the dispersed phase fraction and the particle Reynold's number. A variety of different drag coefficient correlations are reviewed in Ishii (1979) and Ishii (1980) and will not be repeated here. Typically, the effect of Reynold's number is accounted for explicitly in the correlations for the Stokes and viscous regimes but dispersed phase fraction does not appear. As the Reynold's number increases into Newton's regime and higher, the main correlating factor is the dispersed phase fraction and the effect of Reynold's number is only accounted for by the selection of the correlation. A disconcerting fact is that the drag increases with dispersed phase fraction until the churn-turbulent regime is obtained and then the drag decreases rapidly with dispersed phase fraction (Ishii and Zuber, 1979). Because we are interested in rapid mixing conditions we will assume that the flow is turbulent and in the " Newton's law regime". This is reasonable assumption because in an earlier work (Yarbro and Long, 1995) we used a constant value of C_d = 0.44 in the turbulent limit of the Newton's law regime (Bird, 1960) with good results. Therefore, the drag coefficient will be defined (Ishii and Zuber, 1979) as

$$C_d = 0.45\left(\frac{1+17.67\left[f(\alpha_d)\right]^{6/7}}{18.67 f(\alpha_d)}\right)^2 \tag{4.26}$$

where $f(\alpha_d)$ is defined for drops in liquids as

$$f(\alpha_d) = (1-\alpha_d)^{2.25} \tag{4.27}$$

The virtual mass effect has been defined as (Drew, 1979b, Cook and Harlow, 1984) for the flows of interest in this work

$$F_{vm} = C_{vm}\alpha_d \rho_c \left[\left(\frac{\partial \langle \underline{v}_d \rangle}{\partial t} + \langle \underline{v}_d \rangle \cdot \underline{\nabla} \langle \underline{v}_d \rangle \right) - \left(\frac{\partial \langle \underline{v}_c \rangle}{\partial t} + \langle \underline{v}_c \rangle \cdot \underline{\nabla} \langle \underline{v}_c \rangle \right) \right] \tag{4.28}$$

and the virtual volume coefficient can be defined as a function of the global dispersed phase fraction (Ruggles, 1988)

$$C_{vm} = 0.5\left(1 + 12\left(\overline{\alpha}_d\right)^2\right) \tag{4.29}$$

4.2.3 Turbulence

Turbulence is an extremely complicated phenomena in single-fluid systems and is complicated further in multi-fluid systems with the introduction of an interface. Ishii, (Ishii, 1975), Nigmatulin, (Nigmatulin ,1979), Biesheuvel and van Wijngaarden, (Biesheuvel, 1984), Theofanous and Sullivan, (Theofanous, 1982), Drew and Wood, (Drew, 1985) and VanderHeyden, (VanderHeyden,1995) have studied the problem of multi-fluid turbulence. In many cases, generalizations of a phenomenological mixing length or single-fluid K-ε approach was used. Because we are interested in predicting the transport of interfacial area, we are not going to propose a new turbulence closure, but use the current state-of-the-art. In this work, we have identified an new multi-fluid turbulence term in eqn (3.27)

$$\underline{\underline{S}} = \rho_k \left[\left\langle a_i \underline{v}'_{ki} \underline{v}'_k \right\rangle - \left\langle a_i \underline{v}'_{ki} \underline{v}'_i \right\rangle \right] \tag{4.30}$$

which represents the interaction between turbulent fluctuations in the different fluids.

For the case of incompressible fluids and assuming that the interface has no thickness so that

$$\underline{v}_k' \cong \underline{v}_{ki}' \tag{4.31a}$$

$$v_{k+1}' \cong \underline{v}_i' \tag{4.31b}$$

then $\underline{\underline{S}}$ becomes

$$\underline{\underline{S}} = \left[\left\langle a_i \rho_k \underline{v}_k' \underline{v}_k' \right\rangle - \left\langle a_i \rho_k \underline{v}_k' \underline{v}_{k+1}' \right\rangle\right] = \left[\left\langle a_i \underline{\underline{R}}_{kk} \right\rangle - \left\langle a_i \underline{\underline{R}}_{kk+1} \right\rangle\right] \tag{4.32}$$

If we compare the above equation to similar relationships in single-phase turbulence, then $\underline{\underline{R}}_{kk}$ is the same as the conventional Reynold's stress tensor and represents the inertial transfer of energy by turbulent fluctuations within a phase k. However, the second 'Reynold's' stress term, $\underline{\underline{R}}_{kk+1}$, resembles a spatial statistical correlation.

Consider a statistical property of a random variable at two points separated by a distance vector $\underline{r}$. An Eulerian correlation tensor can be defined (Brodkey, 1967), in cartesian coordinates as follows

$$\underline{\underline{Q}}_{lm}(\underline{r}) = \left\langle \underline{v}_l'(\underline{x}) \underline{v}_m'(\underline{x}+\underline{r}) \right\rangle \tag{4.33}$$

Physically, this can be depicted as shown in Figure 4.2

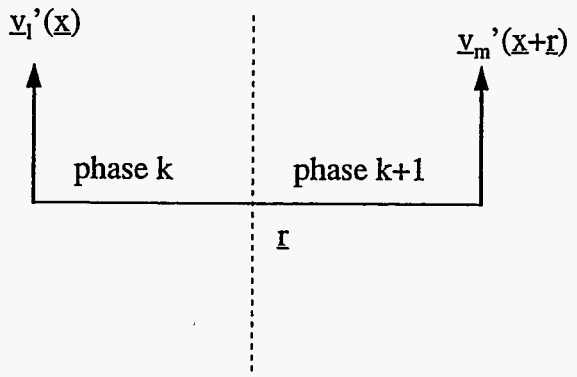

Figure 4.2 Spatial Velocity Fluctuation Correlations across Phase Boundary

If the distance becomes zero, then $\underline{\underline{R}}_{kk+1}$ is the same as the conventional Reynold's stress tensor, however, as the separation increases and the value is non-zero, then there is a large turbulent interaction between the two phases. However, this is a new term and more research is required to begin to positively identify the proper closure form.

Therefore, to proceed, we will define the phase k bubble-induced turbulence as (Drew and Wood, 1985, Lahey, 1991).

$$\underline{\underline{R}}_c = -\frac{3}{20}\alpha_d\rho_c\left|\langle\underline{v}_c\rangle-\langle\underline{v}_d\rangle\right|^2\underline{\underline{I}}-\frac{1}{20}\alpha_d\rho_c\left\{\left(\langle\underline{v}_c\rangle-\langle\underline{v}_d\rangle\right)\left(\langle\underline{v}_c\rangle-\langle\underline{v}_d\rangle\right)\right\}+\mu_l\left\{\underline{\nabla}\langle\underline{v}_c\rangle+\left(\underline{\nabla}\langle\underline{v}_c\rangle\right)^T\right\} \quad (4.34)$$

for the continuous phase and

$$\underline{\underline{R}}_d = \frac{\rho_d}{\rho_c}\underline{\underline{R}}_c \quad (4.35)$$

for the dispersed phase. Because the derivation of this turbulence closure was based on the interaction of a bubble with the continuous phase, we will assume for this work that it includes, to some order of approximation, the interfluid turbulence, $\underline{\underline{S}}$.

In this particular turbulence closure, the only unknown is the turbulent eddy viscosity, μ_t. Since the goal of this work is to define a one-dimensional model for interfacial area concentration transport, only the diagonal terms would be modeled by the eddy viscosity. For one-dimensional models, the non-diagonal terms of the Reynold's stress tensor are neglected and therefore, only the diagonal terms will be retained. Most models for the eddy viscosity mainly define the non-diagonal terms so for this work the eddy viscosity will be neglected. Hence, the final form of the continuous phase turbulence closure is

$$\underline{\underline{R}}_c = -\frac{3}{20}\alpha_d \rho_c \left|\langle \underline{v}_c \rangle - \langle \underline{v}_d \rangle\right|^2 \underline{\underline{I}} - \frac{1}{20}\alpha_d \rho_c \left\{\left(\langle \underline{v}_c \rangle - \langle \underline{v}_d \rangle\right)\left(\langle \underline{v}_c \rangle - \langle \underline{v}_d \rangle\right)\right\} \quad (4.36)$$

4.3 Constitutive Equations Summary

4.3.1 Review

The constitutive equations in the general model were formulated in vector-tensor notation to ensure that the principle of dimensional invariance was satisfied. The principle of material frame indifference (objectivity) has been carefully studied (Drew and Lahey, 1979; Dobran, 1985; Drew and Wood, 1985). Specifically, if a constitutive equation is formulated from objective variables, then the total is objective. From the previously cited work, velocity differences, opposing acceleration differences such as those in the virtual mass term and the linear form of the material stress used in this work are objective and therefore admissible. The scalars for phase fraction and interfacial area are also objective. Therefore, we conclude that the proposed model satisfies the principle of objectivity. The principle

of equipresence has been followed when possible, except in the drag and virtual mass coefficients. Given the empirical nature of these correlations, all of the postulated field variables have not been included. However, it was impractical to try to include all of the dependencies without a better understanding of the basic physics. Incorporating the material phase indicator, X, satisfies the principle of homogeneity by identifying the appropriate phases prior to the averaging process. The principle of material isotropy is nominally satisfied for the systems selected in this work with the exception that the drag correlation was selected based on the assumption of a certain flow regime. All of the equations are dimensionally correct and have been demonstrated to reduce to the proper single-phase models.

4.3.2 Entropy Constraint

The entropy inequality and its application to developing constitutive equations has been thoroughly discussed by Arnold (1988). Based on Arnold's evaluation, the following constitutive equations are consistent with the entropy inequality.

$$\langle p_{ci} \rangle = \langle p_c \rangle - \frac{1}{4} \rho_c \left| \langle \underline{v}_c \rangle - \langle \underline{v}_d \rangle \right|^2 \tag{4.37a}$$

$$\underline{\underline{R}}_c = -\frac{3}{20} \alpha_d \rho_c \left| \langle \underline{v}_c \rangle - \langle \underline{v}_d \rangle \right|^2 \underline{\underline{I}} - \frac{1}{20} \alpha_d \rho_c \left(\langle \underline{v}_c \rangle - \langle \underline{v}_d \rangle \right) \left(\langle \underline{v}_c \rangle - \langle \underline{v}_d \rangle \right) \tag{4.37b}$$

$$\underline{F}_{vm} = C_{vm} \alpha_d \rho_c \left[\left(\frac{\partial \langle \underline{v}_d \rangle}{\partial t} + \langle \underline{v}_d \rangle \cdot \underline{\nabla} \langle \underline{v}_d \rangle \right) - \left(\frac{\partial \langle \underline{v}_c \rangle}{\partial t} + \langle \underline{v}_c \rangle \cdot \underline{\nabla} \langle \underline{v}_c \rangle \right) \right] \tag{4.37c}$$

$$\underline{F}_d = \frac{3}{8} \alpha_d \rho_c C_d \underline{a}_i \left| \langle \underline{v}_c \rangle - \langle \underline{v}_d \rangle \right| \left(\langle \underline{v}_c \rangle - \langle \underline{v}_d \rangle \right) \cdot \underline{n}_i \tag{4.37d}$$

4.4 The Specific One-Dimensional Model

To begin, we will use the ensemble/volume averaged equations summarized in Eqn (3.59-3.63). To approximate an area average, we will re-define the volume average

$$\langle \psi \rangle_V = \frac{1}{Az} \int_{Az} \langle \psi \rangle A dz \tag{4.38}$$

and assume that the area, A, is a unit cross-sectional area that is constant for the equipment studied. Therefore, we can take the z-component of the equations written in cylindrical coordinates for a system of Newtonian, incompressible fluids

Mass:

$$\frac{\partial}{\partial t}\alpha_k + \frac{\partial}{\partial z}\alpha_k \langle v_{kz} \rangle = 0 \tag{4.39}$$

Momentum:

Continuous

$$\begin{aligned} &\rho_c \frac{\partial}{\partial t}\left(\alpha_c \langle v_{cz} \rangle\right) + \rho_c \alpha_c \frac{\partial}{\partial z}\langle v_{cz} \rangle - \alpha_c \left(\frac{\partial}{\partial z}\langle p_c \rangle - \frac{2}{3}\frac{\partial^2}{\partial z^2}\langle v_c \rangle + \rho_c g \cos\theta - \tau_{cw} \right) \\ &+ \frac{\partial}{\partial z}\left(-\frac{1}{5}\alpha_d \rho_c \left(\langle v_{cz} \rangle - \langle v_{dz} \rangle \right)^2 \right) \\ &= -\left(\langle p_{ci} \rangle - \frac{1}{4}\rho_c \left(\langle v_{cz} \rangle - \langle v_{dz} \rangle \right)^2 + \frac{4}{3}\mu_c \frac{\partial}{\partial z}\langle v_{cz} \rangle \right) \frac{\partial}{\partial z}\alpha_c \pm F_d \pm F_{vm} \end{aligned} \tag{4.40}$$

Dispersed

$$\rho_d \frac{\partial}{\partial t}\left(\alpha_d \langle v_{dz}\rangle\right) + \rho_d \alpha_d \frac{\partial}{\partial z}\langle v_{dz}\rangle - \alpha_d\left(\frac{\partial}{\partial z}\langle p_d\rangle - \frac{2}{3}\frac{\partial^2}{\partial z^2}\langle v_{dz}\rangle + \rho_d g\cos\theta - \tau_{dw}\right)$$
$$-\frac{\rho_d}{\rho_c}\frac{\partial}{\partial z}\left(-\frac{1}{5}\alpha_d \rho_c\left(\langle v_{cz}\rangle - \langle v_{dz}\rangle\right)^2\right) \qquad (4.41)$$
$$= -\left(\langle p_{di}\rangle - \frac{1}{4}\rho_c\left(\langle v_{cz}\rangle - \langle v_{dz}\rangle\right)^2 + \frac{4}{3}\mu_d \frac{\partial}{\partial z}\langle v_{cz}\rangle\right)\frac{\partial}{\partial z}\alpha_d \pm F_d \pm F_{vm}$$

Mechanical Energy Continuous Phase:

$$\rho_c \frac{\partial}{\partial t}\left(\alpha_c \frac{\langle v_{cz}^2\rangle}{2}\right) + \rho_c \frac{\partial}{\partial z}\left(\alpha_c \frac{\langle v_{cz}^3\rangle}{2}\right) - \langle v_{cz}\rangle\left(\alpha_c \frac{\partial}{\partial z}\langle p_c\rangle + \rho_c g\cos\theta\right)$$
$$+\frac{\partial}{\partial z}\left[\left(-\frac{1}{5}\alpha_d \rho_c\left(\langle v_{cz}\rangle - \langle v_{dz}\rangle\right)^2\right)\langle v_{cz}\rangle\right] \qquad (4.42)$$
$$-\left(-\frac{1}{5}\alpha_d \rho_c\left(\langle v_{cz}\rangle - \langle v_{dz}\rangle\right)^2\right)\frac{\partial}{\partial z}\langle v_{cz}\rangle + \frac{\partial}{\partial z}\left[\left(2\mu_c \frac{\partial}{\partial z}\langle v_{cz}\rangle\right)\langle v\rangle_{cz}\right] - \left(2\mu_c \frac{\partial}{\partial z}\langle v_{cz}\rangle\right)\frac{\partial}{\partial z}\langle v_{cz}\rangle$$
$$+\langle v_{cz}\rangle\left(\langle p_{ci}\rangle + \frac{1}{4}\rho_c\left(\langle v_{cz}\rangle - \langle v_{dz}\rangle\right)^2\right)\frac{\partial}{\partial z}\alpha_c = \langle T_{iz}\rangle a_i \langle v_{cz}\rangle$$

Interfacial Area:

$$\frac{\partial}{\partial t}a_i + \frac{\partial}{\partial z}a_i\langle v_{cz}\rangle = \frac{1}{\sigma}\left(\langle T_{iz}\rangle a_i \langle v_{cz}\rangle\right) \qquad (4.43)$$

Several simplifications can be made. First, if we examine the non-dimensional momentum and mechanical energy equations, eqn (3.66-3.68), the viscous terms are proportional to the inverse of the Reynold's number. Because we are interested in Reynold's numbers above 1000, the z-components of these terms will be neglected and the viscous shear will be approximated by a simple friction factor model with a friction multiplier similar to the Lockhart-Martinelli method (Hestroni, 1982

$$\tau_{kw} = \frac{\Delta p}{L} = 2\frac{\rho_k}{D_h} v_{kz}^2 f_{kt} \tag{4.43}$$

$$f_{kt} = f_m f_k \tag{4.44a}$$

$$f_m = datafit \tag{4.44b}$$

where f_k is defined by

$$\text{(Turbulent Re} \geq 3100) \quad f_k = \frac{0.0791}{\text{Re}^{1/4}} \tag{4.45}$$

$$\text{(Laminar/Transitional Re<3100)} \quad f_k = \frac{16}{\text{Re}} \tag{4.46}$$

For this work, a simple pressure model will be used. For incompressible fluids, it will be assumed that the individual phase pressures will only differ by the surface tension across the contact area. Therefore, the "interfacial pressure", which can be defined as (Lahey, 1991)

$$(p_k - p_i)\frac{\partial}{\partial z}\alpha_k \propto p_{ki}\frac{\partial}{\partial z}\alpha_k \tag{4.47}$$

can be approximated as (Stuhmiller, 1977)

$$p_{ki} = 2\sigma a_i - \frac{1}{4}\rho_c (v_{cz} - v_{dz})^2 \tag{4.48}$$

For horizontal systems ($\theta = 90^0$), so $\cos(\theta)$ will be equal to zero. Also, $\underline{v}_i$ in eqn (3.63) will be set equal to $\underline{v}_c$ as an approximation because the continuous phase provides the mechanical energy that generates interfacial area.

With these simplifications, the mechanical energy equation (4.42) can be arranged to equal the surface work term, $\left(\langle T_{iz}\rangle a_i \langle v_{cz}\rangle\right)$ and then set equal to the RHS

of the interfacial area concentration transport equation. They can be combined as shown

$$\frac{\partial}{\partial t}a_i+\frac{\partial}{\partial z}a_i\langle v_{\alpha z}\rangle=\frac{1}{\sigma}\left(\langle T_{iz}\rangle a_i\langle v_{\alpha z}\rangle\right)=\frac{1}{\sigma}\begin{pmatrix}\rho_c\frac{\partial}{\partial t}\left(\alpha_t\frac{\langle v_{\alpha z}^2\rangle}{2}\right)-\rho_c\frac{\partial}{\partial z}\left(\alpha_t\frac{\langle v_{\alpha z}^3\rangle}{2}\right)\\-\langle v_{\alpha z}\rangle\left(\alpha_t\frac{\partial}{\partial z}\langle p_c\rangle\right)-\frac{\partial}{\partial z}\left[\left(-\frac{1}{5}\alpha_d\rho_c\left(\langle v_{\alpha z}\rangle-\langle v_{dz}\rangle\right)^2\right)\langle v_{\alpha z}\rangle\right]\\-\left(-\frac{1}{5}\alpha_d\rho_c\left(\langle v_{\alpha z}\rangle-\langle v_{dz}\rangle\right)^2\right)\frac{\partial}{\partial z}\langle v_{\alpha z}\rangle+\frac{\partial}{\partial z}\left[\left(2\mu_t\frac{\partial}{\partial z}\langle v_{\alpha z}\rangle\right)\langle v\rangle_{\alpha z}\right]\\-\left(2\mu_t\frac{\partial}{\partial z}\langle v_{\alpha z}\rangle\right)\frac{\partial}{\partial z}\langle v_{\alpha z}\rangle+\langle v_{\alpha z}\rangle\left(\langle p_{di}\rangle+\frac{1}{4}\rho_c\left(\langle v_{\alpha z}\rangle-\langle v_{dz}\rangle\right)^2\right)\frac{\partial}{\partial z}\alpha_t\end{pmatrix} \quad (4.49)$$

After some re-arrangement, eqn (4.49) becomes

$$\frac{\partial}{\partial t}\left(a_i+\rho_c\alpha_c\frac{\langle v_{cz}^2\rangle}{2}\right)+\frac{\partial}{\partial z}a_i\langle v_{cz}\rangle=\frac{1}{\sigma}\begin{pmatrix}-\rho_c\frac{\partial}{\partial z}\left(\alpha_c\frac{\langle v_{cz}^3\rangle}{2}\right)\\-\langle v_{cz}\rangle\left(\alpha_c\frac{\partial}{\partial z}\langle p_c\rangle+\rho_c g\cos\theta\right)\\-\frac{\partial}{\partial z}\left[\left(-\frac{1}{5}\alpha_d\rho_c\left(\langle v_{cz}\rangle-\langle v_{dz}\rangle\right)^2\right)\langle v_{cz}\rangle\right]\\-\left(-\frac{1}{5}\alpha_d\rho_c\left(\langle v_{cz}\rangle-\langle v_{dz}\rangle\right)^2\right)\frac{\partial}{\partial z}\langle v_{cz}\rangle\\+\frac{\partial}{\partial z}\left[\left(2\mu_c\frac{\partial}{\partial z}\langle v_{cz}\rangle\right)\langle v\rangle_{cz}\right]\\-\left(2\mu_c\frac{\partial}{\partial z}\langle v_{cz}\rangle\right)\frac{\partial}{\partial z}\langle v_{cz}\rangle\\+\langle v_{cz}\rangle\left(\langle p_{ci}\rangle+\frac{1}{4}\rho_c\left(\langle v_{cz}\rangle-\langle v_{dz}\rangle\right)^2\right)\frac{\partial}{\partial z}\alpha_c\end{pmatrix} \quad (4.50)$$

Now, eqns (4.41-4.45) can be re-written substituting the above relationships to obtain a final set of model equations shown below.

Mass:

Continuous

$$\frac{\partial}{\partial t}\alpha_c + \frac{\partial}{\partial z}\alpha_c \langle v_{cz} \rangle = 0 \tag{4.51}$$

Dispersed

$$\frac{\partial}{\partial t}\alpha_d + \frac{\partial}{\partial z}\alpha_d \langle v_{dz} \rangle = 0 \tag{4.52}$$

Momentum:

Continuous

$$\begin{aligned}
&\rho_c \frac{\partial}{\partial t}\alpha_c \langle v_{cz} \rangle + \rho_c \alpha_c \frac{\partial}{\partial z}\langle v_{cz} \rangle - \alpha_c \left(\frac{\partial}{\partial z} p - 2\frac{\rho_c}{D}\langle v_{kz} \rangle^2 f_t \right) + \frac{\partial}{\partial z}\left(-\frac{1}{5}\alpha_d \rho_c \left(\langle v_{cz} \rangle - \langle v_{dz} \rangle \right)^2 \right) \\
&= -\left(2\sigma a_i - \frac{1}{4}\rho_c \left(\langle v_{cz} \rangle - \langle v_{dz} \rangle \right)^2 \right) \frac{\partial}{\partial z}\alpha_c \pm \frac{3}{8}\alpha_d \rho_c C_d a_i \left(\langle v_{cz} \rangle - \langle v_{dz} \rangle \right)^2 \\
&\pm C_{vm}\alpha_d \rho_c \left[\left(\frac{\partial \langle v_{dz} \rangle}{\partial t} + \langle v_{dz} \rangle \frac{\partial}{\partial z}\langle v_{dz} \rangle \right) - \left(\frac{\partial \langle v_{cz} \rangle}{\partial t} + \langle v_{cz} \rangle \frac{\partial}{\partial z}\langle v_{cz} \rangle \right) \right]
\end{aligned} \tag{4.53}$$

Dispersed

$$\begin{aligned}
&\rho_d \frac{\partial}{\partial t}\alpha_d \langle v_{dz} \rangle + \rho_d \alpha_d \frac{\partial}{\partial z}\langle v_{dz} \rangle - \alpha_d \left(\frac{\partial}{\partial z}\langle p \rangle - 2\frac{\rho_d}{D}\langle v_{dz} \rangle^2 f_t \right) - \frac{\rho_d}{\rho_c}\frac{\partial}{\partial z}\left(-\frac{1}{5}\alpha_d \rho_c \left(\langle v_{cz} \rangle - \langle v_{dz} \rangle \right)^2 \right) \\
&= -\left(2\sigma a_i - \frac{1}{4}\rho_c \left(\langle v_{cz} \rangle - \langle v_{dz} \rangle \right)^2 \right) \frac{\partial}{\partial z}\alpha_d \pm \frac{3}{8}\alpha_d \rho_c C_d a_i \left(\langle v_{cz} \rangle - \langle v_{dz} \rangle \right)^2 \\
&\pm C_{vm}\alpha_d \rho_c \left[\left(\frac{\partial \langle v_{dz} \rangle}{\partial t} + \langle v_{dz} \rangle \frac{\partial}{\partial z}\langle v_{dz} \rangle \right) - \left(\frac{\partial \langle v_{cz} \rangle}{\partial t} + \langle v_{cz} \rangle \frac{\partial}{\partial z}\langle v_{cz} \rangle \right) \right]
\end{aligned} \tag{4.54}$$

Interfacial Area:

$$\frac{\partial}{\partial t}\left(a_i+\alpha_c\frac{\langle v_{cz}\rangle^2}{2}\right)+\frac{\partial}{\partial z}\left(a_i\langle v_{cz}\rangle\right)=-\rho_c\frac{\partial}{\partial z}\left(\alpha_c\frac{\langle v_{cz}\rangle^3}{2}\right)$$
$$-\langle v_{cz}\rangle\left(\alpha_c\frac{\partial}{\partial z}\langle p\rangle-2\frac{\rho_c}{D}\langle v_{cz}\rangle^2 f_t\right)$$
$$-\frac{\partial}{\partial z}\left[\left(-\frac{1}{5}\alpha_d\rho_c\left(\langle v_{cz}\rangle-\langle v_{dz}\rangle\right)^2\right)\langle v_{cz}\rangle\right] \qquad (4.55)$$
$$-\left(-\frac{1}{5}\alpha_d\rho_c\left(\langle v_{cz}\rangle-\langle v_{dz}\rangle\right)^2\right)\frac{\partial}{\partial z}\langle v_{cz}\rangle+\langle v_{cz}\rangle\left(2\sigma a_i+\frac{1}{4}\rho_c\left(\langle v_{cz}\rangle-\langle v_{dz}\rangle\right)^2\right)\frac{\partial}{\partial z}\alpha_c$$

These equations define a one-dimensional transient model for interfacial area transport. For the purpose of this initial study, steady-state was assumed and therefore all of the time derivatives may be set to zero.

Furthermore, it should be noted that the "bubble-induced" turbulence is a production term. The viscous interaction terms were neglected so that there is little dissipation in the model except for "wall friction". Also, phase distribution constants have been defined by some authors (Drew and Wood, 1985, Ishii, 1984) to account for the averaging process on the velocity and phase distribution profiles within the conduit. However, we shall adopt the assumption by Pauchon and Bannerjee (1988), that the distribution coefficients are accounted for in the friction factor and other "constant" terms. This is the same as assuming the distribution parameters are equal to one as is the custom.

4.5 Numerical Solution

The NDSolve numerical package in Mathematica 2.2 was used to solve the ordinary differential equations (ODE). Since it is an initial value type solver based on Gear's method (Wolfram Research, 1993), it is very important to define the initial conditions correctly. This is because the ODE's in this work are boundary value problems (BVP) which are usually solved by different methods. However, it is possible to treat z as t and use an initial value technique to solve the equations using a "shooting" method (Finlayson, 1980; Wolfram Research, 1993). The disadvantage is that the final solution is very sensitive to the initial boundary conditions, which for multi-dimensional problems can be difficult to define properly.

4.6 Results and Discussion

4.6.1 Berkman and Calabrese, 1988, Kenics Mixer Data

4.6.1.1 Background

It is well-known that drops are stabilized in agitated liquid-liquid systems by a combination of surface tension and internal viscous forces. Prior work (Middleman, 1978) studied the dispersion of a low-viscosity liquid into a turbulent continuous phase in a static mixer. Middleman used Kolmogoroff theory to obtain a semi-empirical relationship

$$\frac{D_{32}}{D_o} = 0.49We^{-3/5} \tag{4.56}$$

to describe the equilibrium sauter mean drop diameter. Because this approach assumes that the drop is acted upon only by inertial subrange eddies opposed by surface tension, Berkman (1988) extended the correlation to regions where the disruptive force was balanced by both viscous and surface tension forces by examining fluids with a range of viscosities and surface tensions in a Kenics static mixer.

4.6.1.2 Experimental Method

A 24 element, 1.91 cm diameter stainless steel Kenics Mixer with a pitch of 1.5 was used in all of the experimental runs. A diagram of the experimental facility is shown in Figure 4.3.

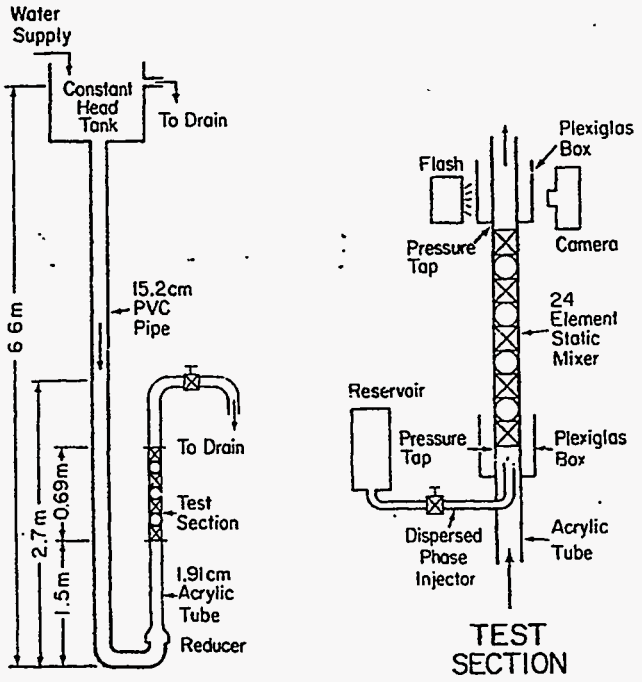

Figure 4.3 Berkman's Experimental Test Facility

The dispersed phase was introduced through a 0.25 cm ID, 0.32 cm OD capillary tube into the body of the mixer much like the co-current jet described later. Drops were photographed and the resulting pictures analyzed for drop size distributions. For each dispersed phase, experiments were conducted at Reynold's numbers from 12,000 to 21,000 based on the velocity of the continuous phase. The phase fraction was to be held constant at 0.001; however, this was difficult to control and varied between 0.00057 and 0.001.

4.6.1.3 Boundary Conditions

The initial velocities were calculated from the Reynold's number and the equilibrium phase fraction.

$$V_{co} = \frac{\mu_c \, \mathrm{Re}}{D_T \rho_c} \tag{4.54}$$

$$V_{do} = V_{co} \frac{\alpha_{do}}{\alpha_{co}} \frac{A_c}{A_d} \tag{4.56}$$

The initial phase fractions and interfacial area concentration were estimated from geometrical considerations. Phase fractions were based on the ratio of the areas of the capillary tube and the pipe body of the mixer.

$$\alpha_{di} = \frac{D_d^2}{D_T^2} \tag{4.57}$$

$$\alpha_{ci} = 1 - \alpha_{di} \tag{4.58}$$

The initial interfacial area concentration was estimated by

$$a_{ii} = \frac{\pi D_d dz}{\frac{\pi D_T^2 dz}{4}} = \frac{4D_d}{D_T^2} \tag{4.59}$$

From Berkman's work, the friction multiplier was estimated to be about 50 as shown below in Figure 4.4.

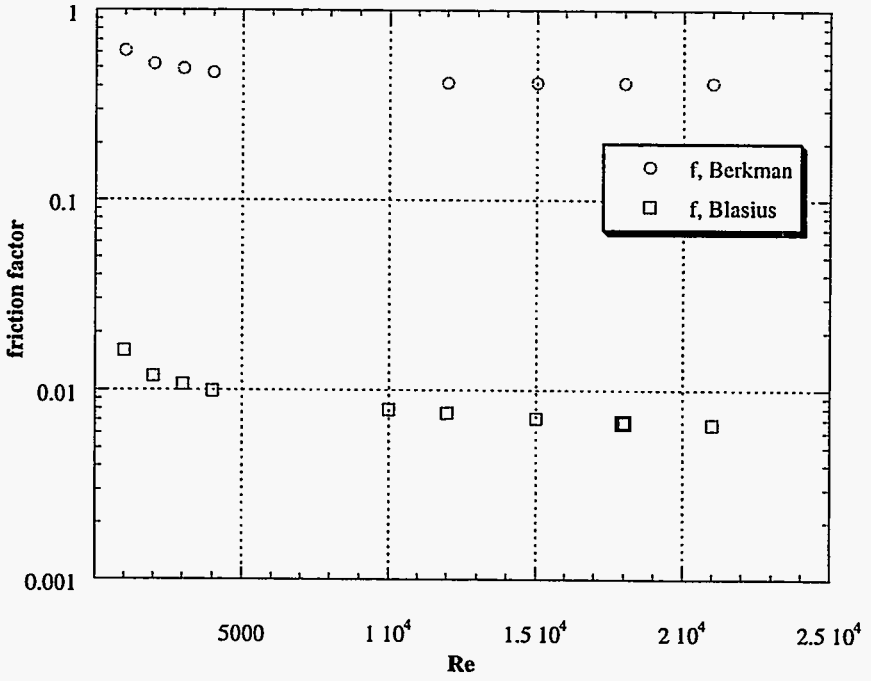

Figure 4.4 Friction Factor for Kenics Static Mixer

After a Reynold's number of 10,000, the friction factor, f_k, is approximately 50 times the Blasius friction factor, f. Therefore, for this case, the friction multiplier was approximated at 50 as was done in Berkman's work.

4.6.1.4 Results

Only the data for the low viscosity fluids (μ_k< 1.0 cp) were used because the effects of viscous shear were neglected for this study except for the wall shear

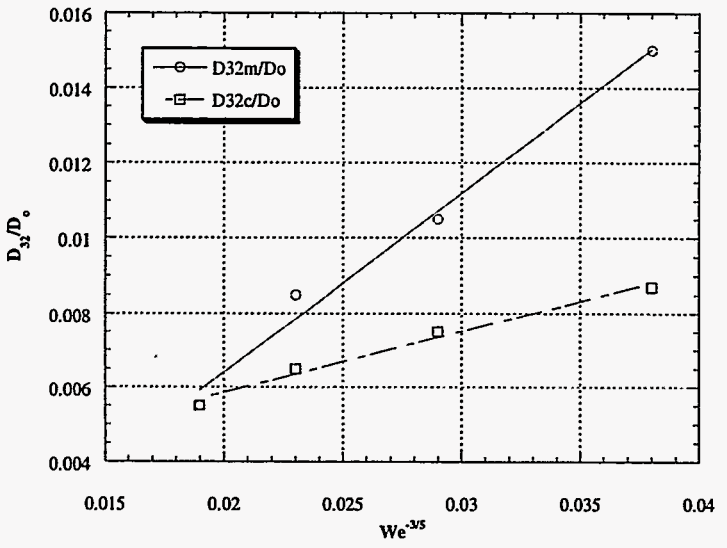

Figure 4.5 Comparison of Experimental and Calculated Values for the 1.91 cm Diameter Kenics Mixer Data (12,000 < Re < 21,000 and α_d = 0.001) (D32m/Do = measured Sauter Mean Diameter/Pipe Diameter, D32c/Do = calculated Sauter Mean Diameter/Pipe Diameter)

. The sauter mean diameters were calculated from the relationship, $D_{32} = (6\ \alpha_d)/a_i$, where the interfacial area concentration was calculated with the model. The results are plotted according to $We^{-3/5}$ shown below. The model overpredicts the interfacial area concentration at lower We numbers, but begins to converge at higher We numbers. In this case, an average friction factor was used based on the published values in Figure 4.4 because this was similar to the approach Berkman and Calabrese used in their empirical correlation work. The friction factor was not fit to the data as

was done for the following cases. If several values are chosen from Figure 4.4, over a Reynold's range of 10,000 to 21,000, the friction multiplier varies from 53 to 63. In addition, the equilibrium phase fraction for the experimental data varied from 0.001 to 0.00057 (Berkman, 1988) and this could potentially cause some variance. However, because both the experimental and model lines are straight, it is more likely due to the neglect of viscous effects in the model.

Also, it was discovered that the final velocity of the dispersed phase fraction was more accurate if the dispersed phase friction factor was approximately 20% higher than the continuous phase. This is because the overall pressure drop was calculated with the continuous phase density, therefore the dispersed phase friction factor was adjusted to compensate.

4.6.2 Yarbro and Long, 1995, Kenics Mixer Data

4.6.2.1 Background

Several groups have successfully studied the problem of empirically predicting interfacial area in systems of immiscible fluids. We are interested in systems where the contactor is a "tubular reactor" such as columns, packed beds or in-line mixers. In-line mixers, such as Kenics or Sulzer mixers, are attractive because they are simple, have low residence times, and are easy to operate and maintain. In this work, a simple multi-fluid model based on the work by Lahey (Lahey, 1991) was used with a variety of simplifying assumptions to estimate the energy dissipation in a liquid-liquid system in a Kenics mixer. The energy dissipation with a residence time correction was equated to

the surface energy of the drop to estimate an average interfacial area concentration. The model results were compared to experimental measurements with fair agreement.

4.6.2.2 Experimental Method

In this study, a 12-element, 0.635 cm diameter, 31.75 cm long Kenics mixer with a pitch ratio of 0.8 was used. Micropump gear metering pumps (2500 ml/min capacity) were used with stainless steel pump heads. All hardware was Teflon tube with compression fittings. Five-liter glass carboys were used to hold the phases. Flowrates and phase fractions were measured by timing the flow into a graduated cylinder and measuring the resultant volumes. The drop size distributions were measured using a Kodak COHU electronic camera with a CCD speed of 30 frames-per-second, a electronic shutter speed of 1/10,000 of a sec and a drop resolution of approximately 30 microns. The light source was a 100 W incandescent bulb. The bulb was placed behind a shield with a slit width of 20 mm and a light diffuser of either frosted glass or paper. The light source was then oriented to produce some contrast in the image to enhance the drops. The data was recorded on VCR tape and processed on a Gateway 2000 PC installed with a Raptor frame capture board and Image Pro software for image manipulation. Drop sizes were counted manually by taking individual pictures from the video tape and counting the drops in the picture. The Image Pro software allowed a calibration for length on the picture. This was done by placing an object in the picture with a known size. The number of pixels per length was calculated. Circles drawn around each identified drop were then measured by the

software and placed in a data file. Reagent grade dodecane and distilled water were the fluids used in this study. The equipment is shown below in Figure 4.6.

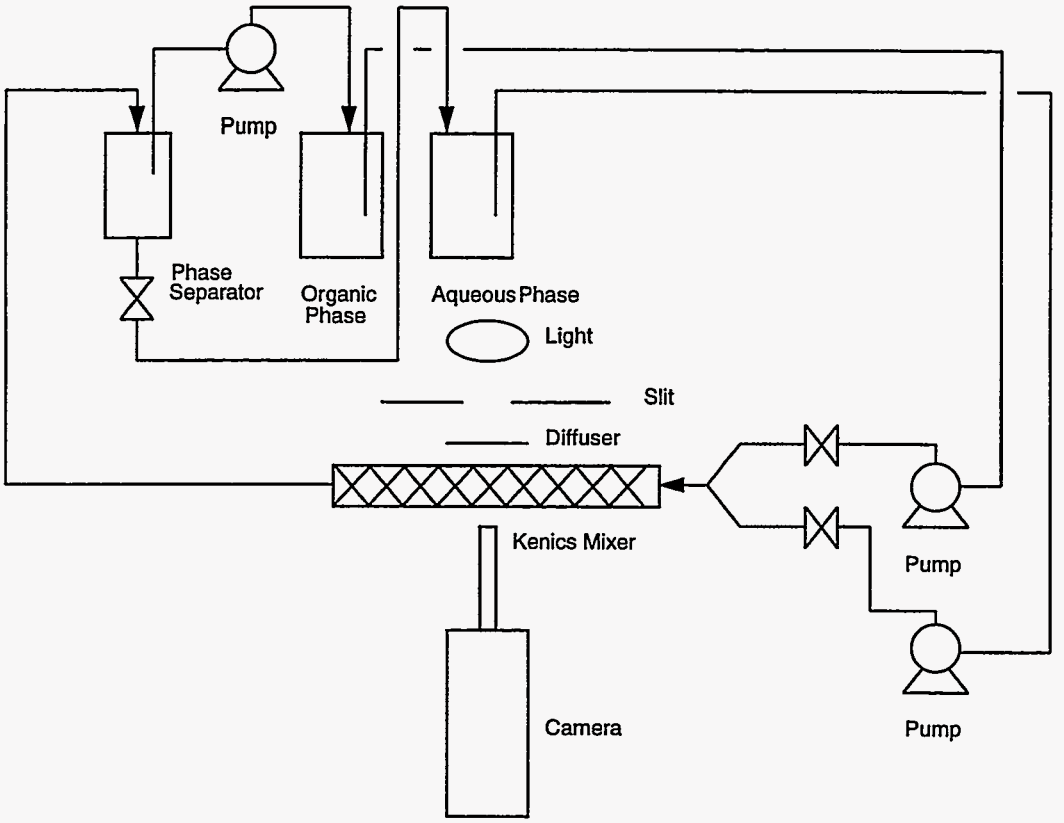

Figure 4.6 Kenics Mixer Test Equipment

4.6.2.3 Boundary Conditions

Because the liquids were introduced through a "Y" teflon fitting where the two inlet areas were equal to the outlet area, setting the initial velocities and interfacial area was a challenge. The initial volumetric flowrates were calculated as follows

$$Q_{do} = V_f \left(1 - \alpha_{do}\right) A \tag{4.60}$$

$$Q_{co} = V_f \alpha_{do} A \tag{4.61}$$

and the final linear velocity measured according to a calibrated pump setting was based on the Reynold's number to make it easier to run the model.

$$V_f = \frac{\mu \mathrm{Re}}{D\rho} \tag{4.62}$$

Because the phase fractions were high for this portion of the study ($0.11 < \alpha < 0.28$), the viscosity and density were estimated according to a simple mixing rule

$$\mu = \alpha_{do}\mu_d + (1-\alpha_{do})\mu_c \tag{4.63}$$

$$\rho = \alpha_{do}\rho_d + (1-\alpha_{do})\rho_c \tag{4.64}$$

and then these values were used to estimate a Reynold's number so that the proper friction factor model was used.

The initial linear velocities were calculated by assuming that each fluid occupied a portion of the common inlet area at the point of the "Y" proportional to the volumetric phase fraction. Therefore, each was estimated

$$V_{co} = \frac{Q_{co}}{A - A_f} \tag{4.65}$$

$$V_{do} = \frac{Q_{do}}{A_f} \tag{4.66}$$

$$A_f = \frac{1}{2} A \frac{\alpha_{do}}{\alpha_{co}} \tag{4.67}$$

As shown, if the phase fractions are equal at 0.5, then each phase occupies exactly one-half of the inlet area and their linear velocities would be equal. In the same manner, the initial phase fractions were estimated by

$$\alpha_{di} = \frac{1}{2}\frac{\alpha_{do}}{\alpha_{co}} \tag{4.68}$$

$$\alpha_{ci} = 1 - \alpha_{di} \tag{4.69}$$

The initial interfacial area concentration was estimated by using the geometry of the initial contact plane of the two phases as they contact at the common inlet. This was calculated as the intersection plane divided by the inlet area

$$a_{ii} = \frac{Ddz}{\frac{\pi D^2}{4}}\frac{\alpha_{do}}{\alpha_{co}} = \frac{4}{\pi D}\frac{\alpha_{do}}{\alpha_{co}} \tag{4.70}$$

This is also proportional to the phase fraction because the intersection will shift depending on the proportion of the inlet volumetric flows.

In the following cases, the friction factor multiplier was found by adjusting the value to get the correct interfacial area concentration for a single data point from each phase fraction set. This differs from the Berkman case because he only used low phase fractions, 0.001 or less so that the pressure drop was due mainly to the static mixer elements. In addition, he had measured the pressure drop and had experimental values for the total friction factor.

After a value was set, it was used for each data point within the same phase fraction. Then, the value would be adjusted for the next data set at a different phase fraction. Typically, the friction factor multiplier followed a power law curve and

could easily be fitted after only three points. For this case, the laminar friction factor model that was chosen was used for both the laminar and transitional flows.

$$f = \frac{16}{\mathrm{Re}} \tag{4.71}$$

4.6.2.4 Results

The experimental and calculated results are shown below in Figures 4.7 and 4.8.

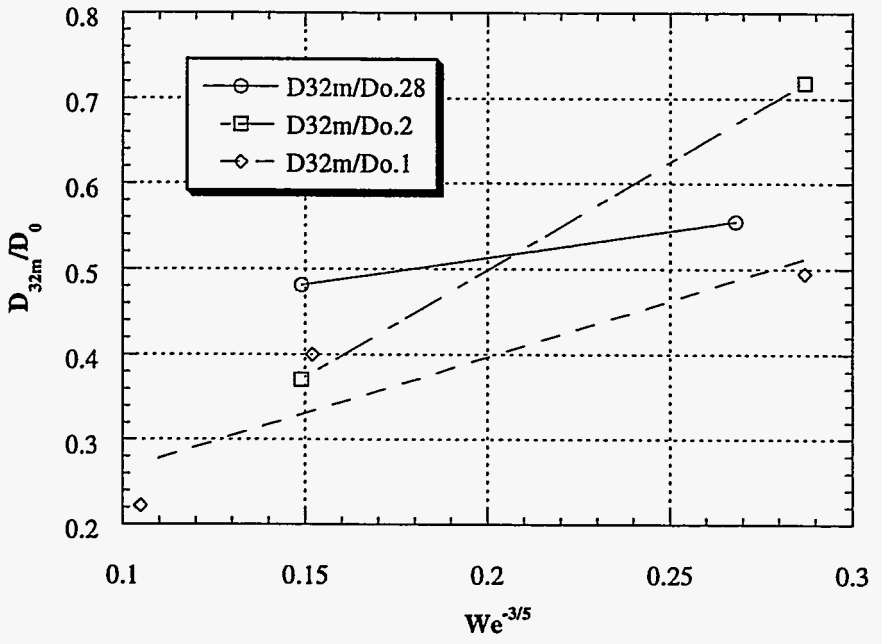

Figure 4.7 Experimental Data for the 0.635 cm Diameter Kenics Mixer ($1300 < Re < 3100$ and $0.1 < \alpha_d < 0.28$)

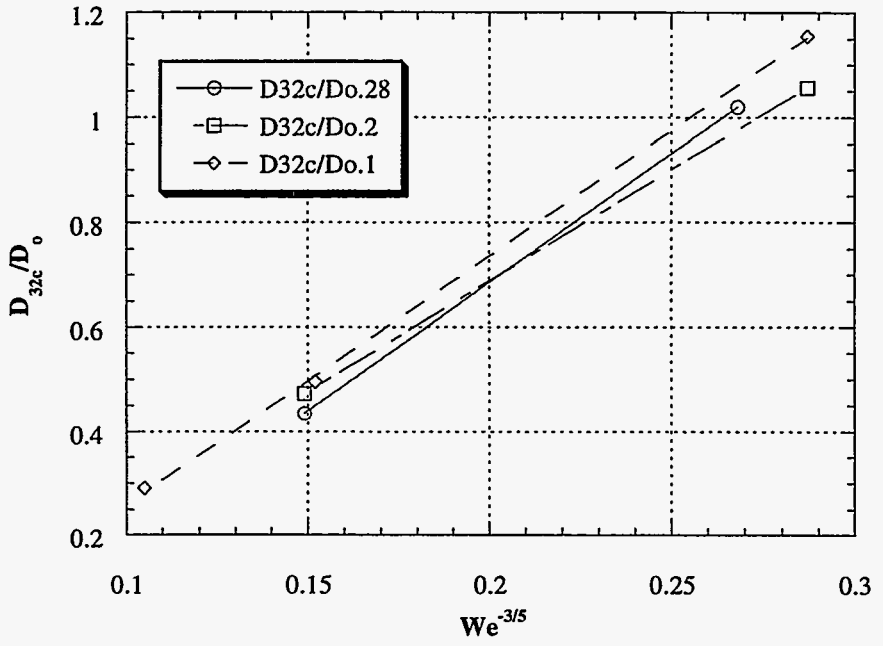

Figure 4.8 Calculated Values for the 0.635 cm Diameter Kenics Mixer

With the exception of scatter because of experimental error (estimated at ~ +/- 25%), the data shows a reasonable qualitative fit at low Reynold's numbers. The error estimate is based on Azzopardi's (Azzopardi, 1979) paper. Some drop coalescence was occurring at the lowest Weber numbers which made it difficult to get extremely accurate drop size estimates. In addition, even though the pumps were carefully calibrated to ensure consistent flows and the phase fractions and average flowrates were checked by timing the volumes captured in a graduated cylinder, the actual photos of the drops were difficult to use. In order to get pictures that caught rapid drop movements without overlap, the shutter speed of the camera was adjusted to between 1/6000th and 1/10,000th of a second. At this high-shutter speed mode,

only every other 'horizontal' line was captured on the video tape and the image had to be 'blended' to overcome this semi-checker effect. This 'filtering' operation caused the fine detail to be lost in the image. At high phase fractions ($\alpha_d > 0.1$) some of the drop boundaries were estimated and it is most likely that some of the smaller drops were lost to view.

This case is also similar to the Tee mixer discussed later because the phases were brought together in a "Y". With a "Y", it was difficult to assign exact geometric factors for the inlet boundary values for phase fraction and interfacial area concentration. This may account for some of the variance between the model and the experimental data. Also, as with Berkman's data, the velocity profile for the dispersed phase was better if the wall drag friction factor was set approximately 20% higher than the continuous phase.

4.6.3 Lin, 1985, Co-Current Jet Mixer Data

4.6.3.1 Background

Most interfacial area concentration predictions are based on an assumption of isotropic turbulence and relate the drop breakage to a total energy dissipation calculated from macroscopic system variables, such as pressure drop. In this work, a dimensional analysis approach was used to relate the final drop size distribution to phase velocities and system geometry. A low viscosity oil (kerosene) was dispersed into water in a co-current jet mixer. Data were obtained for two mixer sizes, 0.027" and 0.041", over a Reynold's number range of 3,100 to 29,960 and were correlated by the following equation

$$D_{32} = 8.8x10^{6}\left(\frac{D_I}{D_O}\right)^{0.89}\left(\frac{V_{do}}{V_{co}}\right)^{-0.711}(V_m)^{-1.549} + 535\left(\frac{D_I}{D_O}\right)^{1.458} \quad (4.72)$$

4.6.3.2 Experimental Method

The co-current jet apparatus and the supporting equipment are shown in Figure 4.9.

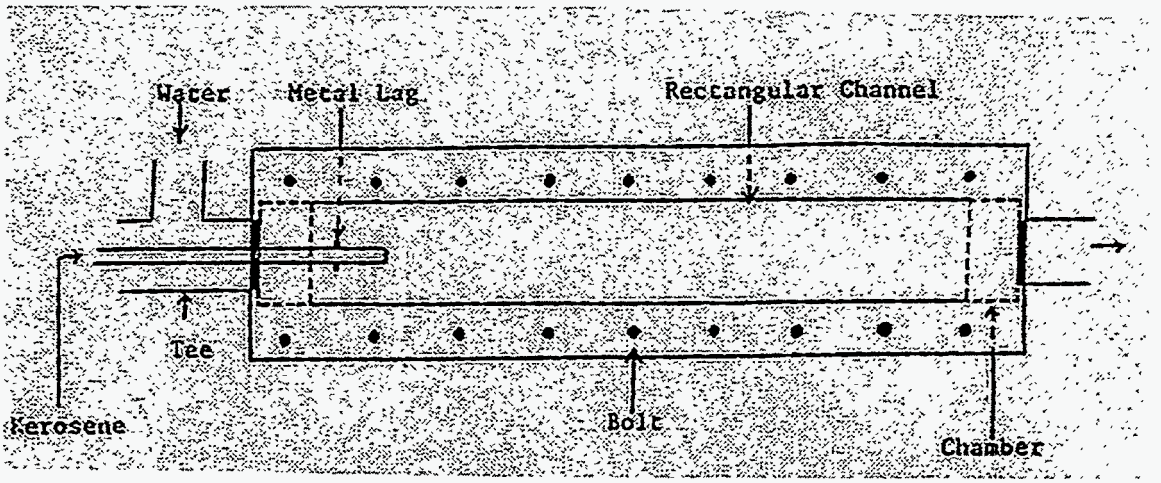

Figure 4.9 Lin's Co-Current Jet

Two immiscible phases were mixed over ranges of phase fractions and Reynold's numbers. Drop sizes were measured using a light attenuation techniques (Azzopardi, 1979). The light attenuation apparatus was calibrated with photographs of the flowing dispersion. The data was then correlated to the proposed equation. A detailed description of the equipment is given by Lin, 1985.

4.6.3.3 Boundary Conditions

The initial volumetric flowrates were available with the geometry of the equipment so that initial velocities were calculated as follows

$$V_{co} = \frac{Q_c}{A_T - A_d} \tag{4.73}$$

$$V_{do} = \frac{Q_d}{A_d} \tag{4.74}$$

Again, like Berkman's work, the initial phase fractions and interfacial area concentration were based on the system geometry

$$\alpha_{di} = \frac{\pi D_d^2}{4A_T} \tag{4.75}$$

$$a_{ii} = \frac{\pi D_d dz}{A_T dz} = \frac{\pi D_d}{A_T} \tag{4.76}$$

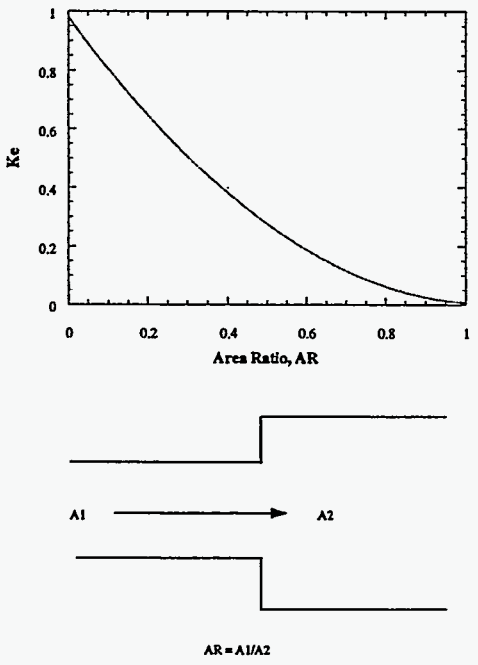

Figure 4.10 Loss Coefficients for Flow through Sudden Area Changes (Fox and Macdonald, 1973)

As mentioned earlier, the friction factor relationship was found by adjusting the value of the friction multiplier to get the correct interfacial area concentration for a single data point from each phase fraction set. It appears to follow the expansion loss coefficient trend shown above in Figure 4.10.

In all cases, the friction multiplier was fit to a power law expression similar to the Blasius friction factor correlation as shown in Figure 4.11.

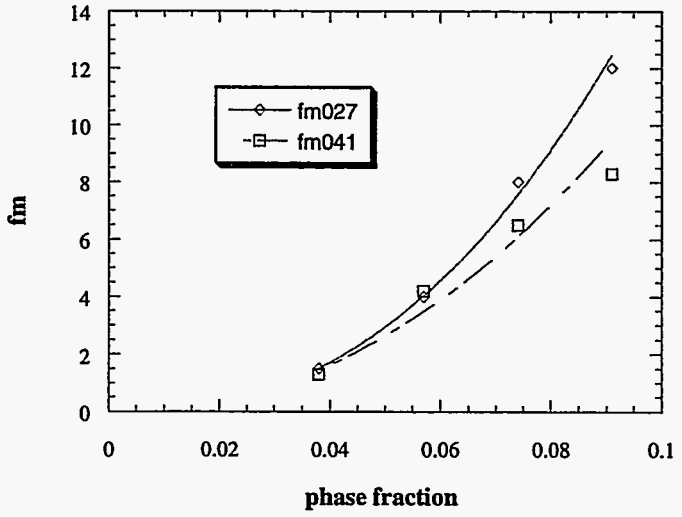

Figure 4.11 Friction Multiplier for 0.027" and 0.041" Co-Current Jet

4.6.3.4 Results

The experimental and calculated values for phase fractions from 0.091 to 0.038 are shown in Figures 4.12 and 4.13.

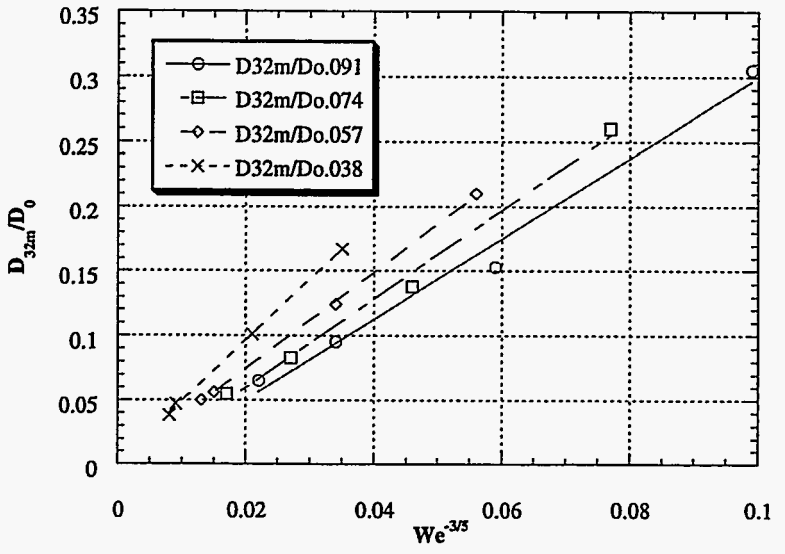

Figure 4.12 Experimental Data for the 0.027" Co-Current Jet

($2300 < Re < 16{,}300$ and $0.038 < a_d < 0.091$)

As shown in the Figures, there is an excellent agreement between the measured values and the ones calculated by the model. The data for the 0.041" injector is shown in Figures 4.14 and 4.15.

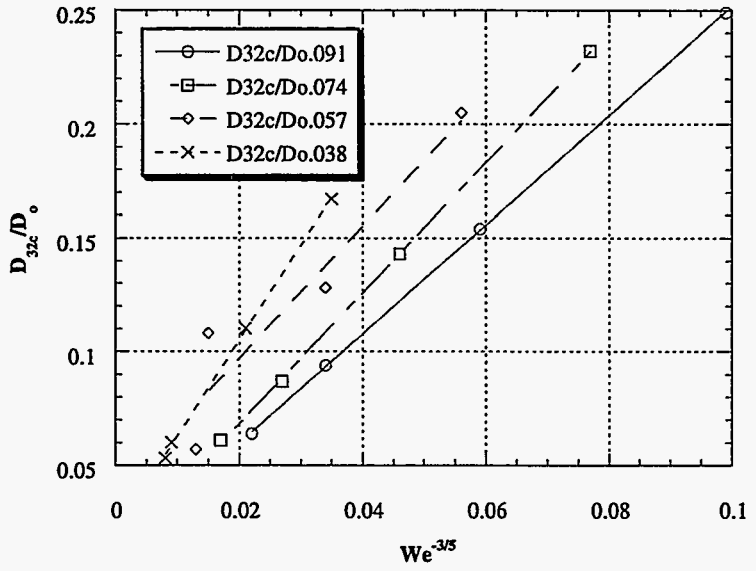

Figure 4.13 Calculated Values for the 0.027" Co-Current Jet

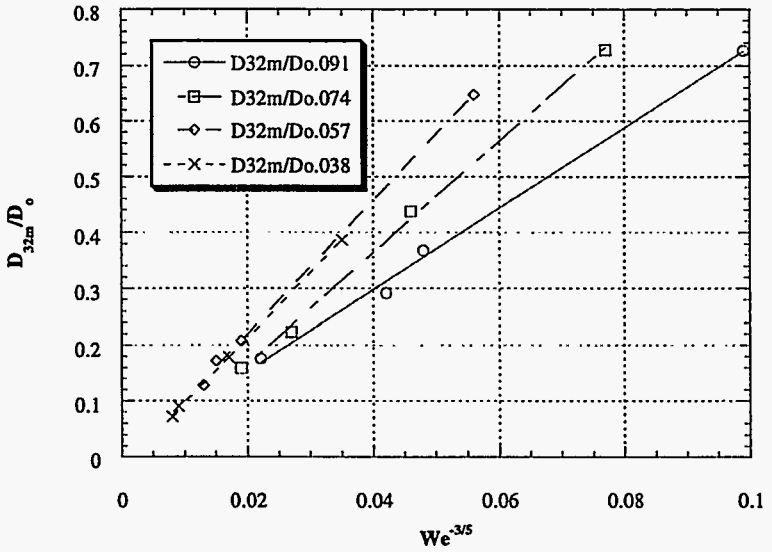

Figure 4.14 Experimental Data for the 0.041" Co-Current Jet

($2300 < Re < 16{,}300$ and $0.038 < a_d < 0.091$)

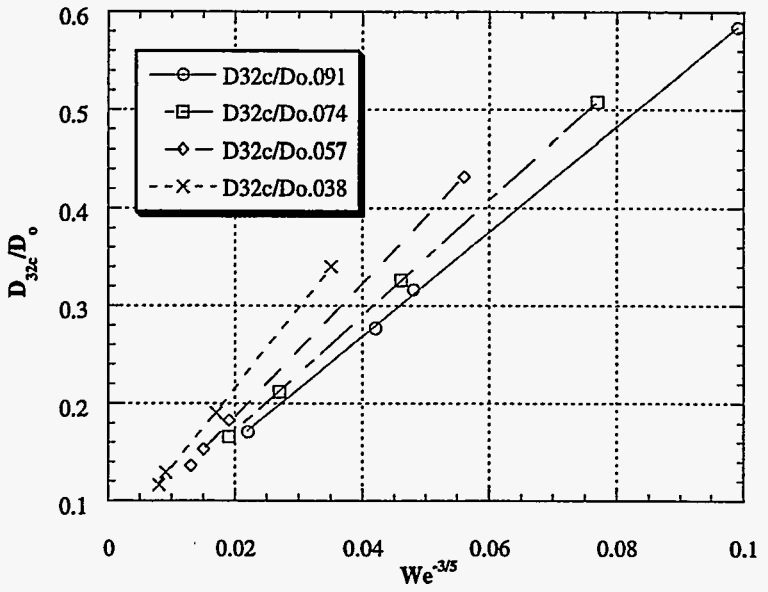

Figure 4.15 Calculated Values for the 0.041" Co-Current Jet

The agreement is extremely good for Weber numbers up to approximately 1000 and begins to diverge at the higher Weber Numbers. This is most likely due to the fact that the interphase viscosity and turbulence effects were neglected and there is not enough dissipation calculated in the model. If we examine eqn (4.14)

$$\underline{\nabla}\cdot\alpha_k\langle\underline{\underline{T}}_k\rangle=\alpha_k\left[-\underline{\nabla}\langle p_k\rangle+\mu_k\left[\nabla^2\langle\underline{v}_k\rangle-\frac{1}{3}\underline{\nabla}(\underline{\nabla}\cdot\langle\underline{v}_k\rangle)\right]\right]-\langle p_k\rangle\underline{\nabla}\alpha_k$$
$$+\mu_k\left[\frac{2}{3}\underline{\nabla}\alpha_k(\underline{\nabla}\cdot\langle\underline{v}_k\rangle)-\left[\underline{\nabla}\alpha_k\cdot\underline{\nabla}\langle\underline{v}_k\rangle+\underline{\nabla}\langle\underline{v}_k\rangle\cdot\underline{\nabla}\alpha_k\right]\right]$$

note that there are several 'multi-fluid viscous stress' terms in the last bracket on the RHS. When the fluid velocities are equal, these terms are zero and the standard engineering assumption of neglecting the viscous terms is probably valid for the momentum and mechanical energy balances. However, most of the drop production

occurs when the two fluids are mixed and there are large gradients of velocity and phase fraction. From the numerical results, these terms should be included in a complete model.

In this case and in the 1.91 cm diameter Kenics mixer case, the experimental configuration enabled exact geometric factors to be defined for the inlet boundary conditions for phase fraction, velocities and interfacial area concentration. The turbulence in jets can be locally isotropic for Reynold's number > 780 (Brodkey, 1967). Because the model assumed a "generalized isotropy", this enabled the model to give good predictions for these cases. Again, it was discovered that the dispersed phase velocity profile was more accurate if its wall drag friction factor was approximately 20% higher than the continuous phase value.

4.6.4 Reimus, 1983, Tee Mixer Data

4.6.4.1 Background

Because static mixers offer many advantages over conventional mixers in certain applications, there is a strong interest in how the flow parameters relate to mixing characteristics. As mentioned above, a common approach is to use Kolmogoroff theory to correlate drop size data. However, this assumes an equilibrium has been achieved and in the case of the Tee mixer, a non-equilibrium situation exists. Reimus and Long discovered that Kolmogoroff theory only approximately applies due to strong non-isotropic wall and non-equilibrium effects. They were able characterize the mixing and the droplet breakup process with the

energy dissipated in the tee and the residence time. The final equation form for prediction of Sauter Mean drop diameter is

$$D_{32} = C\left(1+k_2(\alpha_d)^a\right)\left(\frac{\mu_d}{\mu_c}\right)^b (\Delta p)^c + k_1\alpha_d + D_{p_{min}} \qquad (4.77)$$

which includes the dissipation energy through the pressure drop, the effect of viscosity and phase fraction and a minimum drop diameter.

4.6.4.2 Experimental Method

The tee mixer used is shown in Figure 4.16 below.

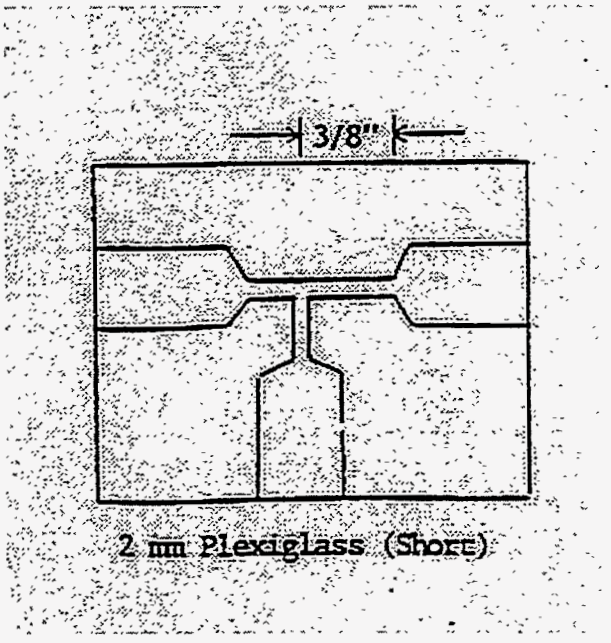

Figure 4.16 Tee Mixer Schematic

The supporting equipment is exactly like that used by Lin. A light attenuation technique was used as described above and was calibrated with a photographic method. The runs varied over a phase fraction of 0.01 to 0.2 and Reynold's numbers

of 25,000 to 80,000. A detailed description of the equipment and data is in Reimus, 1983.

4.6.4.3 Boundary Conditions

The boundary conditions for this case are considerably more complex than for co-current jets, which is essentially what the first two cases were. This system has already been demonstrated to be non-isotropic and multi-dimensional. The question arises as to what is the initial dispersed phase velocity, phase fraction and interfacial area concentration? This is difficult for a one-dimensional model. Therefore the following approach was used. If we examine a simple diagram of what is happening in the Tee mixer (See Figure 4.17 below)

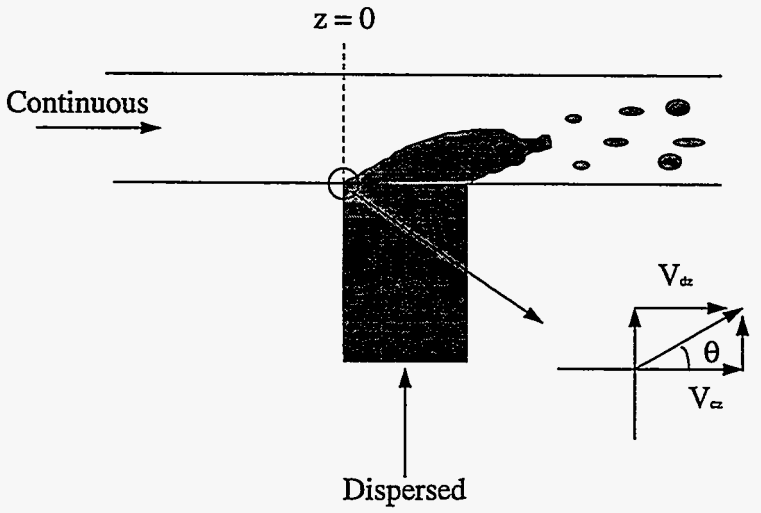

Figure 4.17 Boundary Condition for Velocity in the Tee Mixer

we see that the initial velocities are actually functions of the angle formed when the two fluids collide in the junction. Therefore, given the volumetric flowrates and inlet pipe cross-sectional areas, the initial velocities can be defined

$$V_{doz} = \frac{Q_d}{A_d}\cot(\theta) \tag{4.78}$$

$$V_{coz} = \frac{Q_c}{A_c}\cos(90^\circ - \theta) \tag{4.79}$$

Hence, the method was to assign various values of theta to a single data point until the final interfacial area concentration agreed, then it was assumed that that angle would be constant within a set of data for a single phase fraction. A plot of the angle vs phase fraction is shown in Figure 4.18 below.

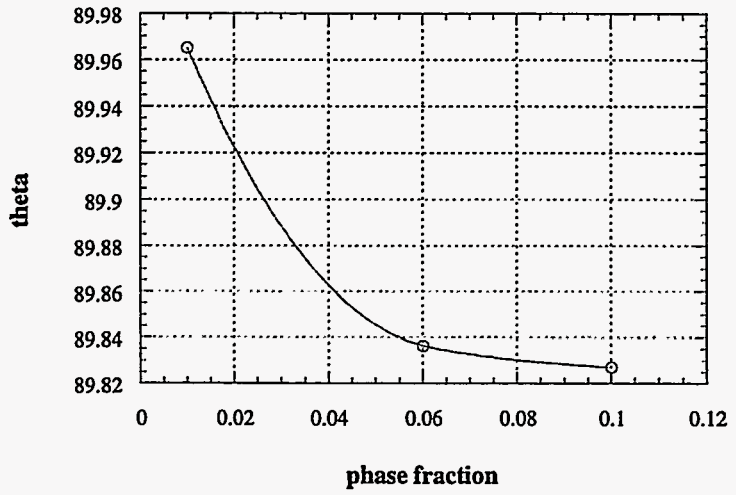

Figure 4.18 Estimates of Phase Contact Angle from Calculations

Unfortunately, there is no 'a priori' method to predict the initial phase fraction and interfacial area concentration. It is evident from Figure 4.17 that the initial dispersed phase fraction is close to zero, but most likely not zero, therefore, it was estimated as

$$\alpha_{di} = \cos(\theta) \tag{4.80}$$

which allows it to be scaled to the volumetric flow ratio of the two fluids. Following that same reasoning, the initial interfacial area concentration was estimated as

$$a_{ii} = 100\alpha_d \tag{4.81}$$

so that it would be scaled to the final phase fraction in the device. The value of 100 was chosen because that gave the best results. A similar approach was used for the friction multiplier.

4.6.4.4 Results

The results from the 0.2 cm plexiglas Tee mixer at 0.01,0.06 and 0.1 phase fractions are shown in Figures 4.19 and 4.20 below.

The quantitative agreement between the model is not as good with the Tee data as with the other cases, but the qualitative agreement is reasonable.

Most of the discrepancy is likely due to the 'scaled' estimates of the inlet boundary conditions. As shown in Figure 4.17, it is difficult to calculate 'a priori' the inlet phase fractions and interfacial area concentrations for a one-dimensional model. For inlet phase fraction and interfacial area concentration, the values were not based

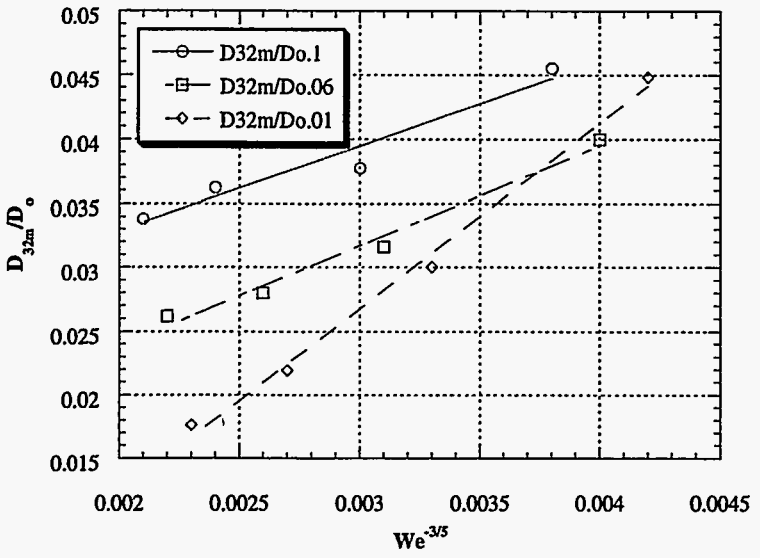

Figure 4.19 Experimental Data for the 0.2 cm Plexiglas Tee Mixer

($27{,}000 < Re < 51{,}000$ and $0.01 < a_d < 0.1$)

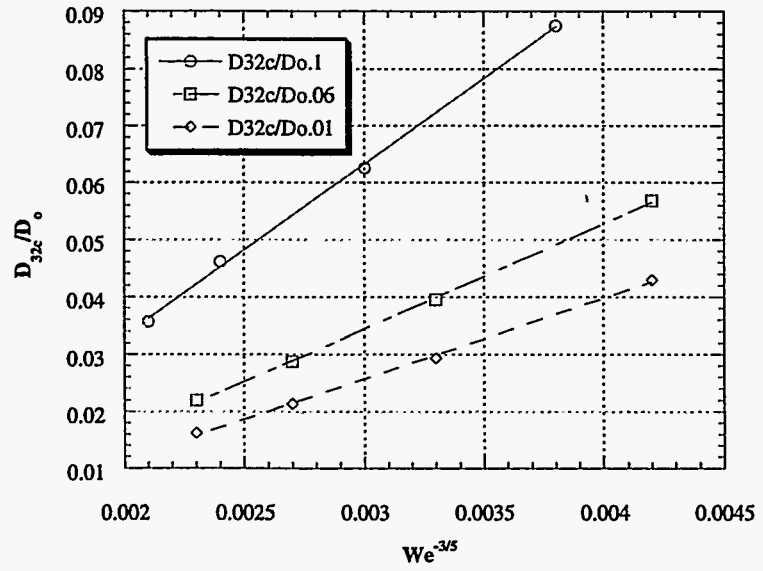

Figure 4.20 Calculated Values for the 0.2 cm Tee Mixer

on geometric factors as in the other cases, but only on empirical scaling factors. From the numerical work, it would help to go to a higher dimensional model to better define the boundary conditions.

The mixing in the Tee is the most vigorous of all the applications and therefore has the highest gradients of phase fraction and velocity and therefore, the additional viscous terms are most important. Also, the conditions are most likely the least isotropic of all of the experimental cases. Again, the dispersed phase wall drag friction factor was set 20% higher than the continuous phase value.

4.7 Discussion

It appears that the model without viscous effects qualitatively models the interfacial area, especially when the turbulence conditions are reasonably isotropic like the co-current jet. Also, when the inlet boundary conditions can be based on known geometric factors, as in the 1.91 cm Kenics mixer and the co-current jet, the model results are in reasonable quantitative agreement with the experimental values, allowing for experimental error.

To help interpret the results in terms of the balance equations, we will derive the non-dimensional form of the final model equation for interfacial area transport. Using the dimensionless variables defined earlier and inserting them into the vector-tensor form of eqn (4.55) including viscous shear and gravity effects to obtain

$$
\begin{aligned}
&\left(\frac{\nu}{D^2}\right)\frac{\partial}{\partial t^*}a_i^* + \left(\frac{\nu}{D^2}\right)\underline{\nabla}\cdot\left(a_i^*\langle\underline{v}_c^*\rangle\right) \\
&= \left(\frac{\rho\nu^3}{D\sigma}\right)\frac{\partial}{\partial t^*}\alpha_c\frac{\langle v_c^{*2}\rangle}{2} + \left(\frac{\rho\nu^3}{D\sigma}\right)\underline{\nabla}^*\cdot\alpha_c\frac{\langle v_c^{*2}\rangle}{2}\langle\underline{v}_c^*\rangle \\
&+ \langle\underline{v}_c^*\rangle\cdot\left(\left(\frac{\rho\nu^3}{D\sigma}\right)\alpha_c\nabla p^* + \rho\nu\frac{\underline{g}}{g}\right) \\
&+ \left(\frac{\rho\nu^3}{D\sigma}\right)\langle\underline{v}_c^*\rangle\cdot\left[\langle p^*\rangle\nabla^*\alpha_c\right] + \left(\frac{\rho\nu^3}{D\sigma}\right)\underline{\nabla}^*\cdot\left[\underline{\underline{R}}_c^*\cdot\langle\underline{v}_c^*\rangle\right] - \left(\frac{\rho\nu^3}{D\sigma}\right)\underline{\underline{R}}_c^*:\underline{\nabla}^*\langle\underline{v}_c^*\rangle \\
&- \left(\frac{\mu\nu^2}{\sigma D^2}\right)\left(\underline{\nabla}^*\cdot\left[\alpha_c\underline{\underline{\tau}}_c^*\cdot\langle\underline{v}_c^*\rangle\right] - \alpha_c\underline{\underline{\tau}}_c^*:\underline{\nabla}^*\langle\underline{v}_c^*\rangle\right)
\end{aligned}
\tag{4.82}
$$

Multiply both sides by D^2/ν gives

$$
\begin{aligned}
&\frac{\partial}{\partial t^*}a_i^* + \underline{\nabla}\cdot\left(a_i^*\langle\underline{v}_c^*\rangle\right) \\
&= \left(\frac{\rho\nu^2 D}{\sigma}\right)\left(\begin{aligned}&\frac{\partial}{\partial t^*}\alpha_c\frac{\langle v_c^{*2}\rangle}{2} + \underline{\nabla}^*\cdot\alpha_c\frac{\langle v_c^{*2}\rangle}{2}\langle\underline{v}_c^*\rangle + \langle\underline{v}_c^*\rangle\cdot\left(\alpha_c\nabla p^* + \frac{\underline{g}D}{g\nu^2}\right) \\ &+\langle\underline{v}_c^*\rangle\cdot\left[\langle p^*\rangle\nabla^*\alpha_c\right] + \underline{\nabla}^*\cdot\left[\underline{\underline{R}}_c^*\cdot\langle\underline{v}_c^*\rangle\right] - \underline{\underline{R}}_c^*:\underline{\nabla}^*\langle\underline{v}_c^*\rangle\end{aligned}\right) \\
&- \frac{\mu\nu}{\sigma}\left(\underline{\nabla}^*\cdot\left[\alpha_c\underline{\underline{\tau}}_c^*\cdot\langle\underline{v}_c^*\rangle\right] - \alpha_c\underline{\underline{\tau}}_c^*:\underline{\nabla}^*\langle\underline{v}_c^*\rangle\right)
\end{aligned}
\tag{4.83}
$$

These dimensionless groups can be re-defined as the well-known Weber, Froude and Reynold's numbers as follows

$$
\begin{aligned}
&\frac{\partial}{\partial t^*}a_i^* + \underline{\nabla}\cdot\left(a_i^*\langle\underline{v}_c^*\rangle\right) = We\left(\begin{aligned}&\frac{\partial}{\partial t^*}\alpha_c\frac{\langle v_c^{*2}\rangle}{2} + \underline{\nabla}^*\cdot\alpha_c\frac{\langle v_c^{*2}\rangle}{2}\langle\underline{v}_c^*\rangle + \langle\underline{v}_c^*\rangle\cdot\left(\alpha_c\nabla p^* + \frac{1}{Fr}\frac{\underline{g}}{g}\right) \\ &+\langle\underline{v}_c^*\rangle\cdot\left[\langle p^*\rangle\nabla^*\alpha_c\right] + \underline{\nabla}^*\cdot\left[\underline{\underline{R}}_c^*\cdot\langle\underline{v}_c^*\rangle\right] - \underline{\underline{R}}_c^*:\underline{\nabla}^*\langle\underline{v}_c^*\rangle\end{aligned}\right) \\
&- \frac{We}{\mathrm{Re}}\left(\underline{\nabla}^*\cdot\left[\alpha_c\underline{\underline{\tau}}_c^*\cdot\langle\underline{v}_c^*\rangle\right] - \alpha_c\underline{\underline{\tau}}_c^*:\underline{\nabla}^*\langle\underline{v}_c^*\rangle\right)
\end{aligned}
\tag{4.84}
$$

Assuming steady-state and rearranging the equation we obtain

$$\frac{1}{We}\underline{\nabla}^*\left(\underline{a}_i^*\cdot\left\langle\underline{v}_c^*\right\rangle\right)=\underline{\nabla}^*\cdot\alpha_c\frac{\left\langle v_c^{*2}\right\rangle}{2}\left\langle\underline{v}_c^*\right\rangle+\left\langle\underline{v}_c^*\right\rangle\cdot\left(\alpha_c\nabla p^*+\frac{1}{Fr}\frac{\underline{g}}{g}\right)$$
$$+\left\langle\underline{v}_c^*\right\rangle\cdot\left[\left\langle p^*\right\rangle\nabla^*\alpha_c\right]+\underline{\nabla}^*\cdot\left[\underline{\underline{R}}_c^*\cdot\left\langle\underline{v}_c^*\right\rangle\right]-\underline{\underline{R}}_c^*:\underline{\nabla}^*\left\langle\underline{v}_c^*\right\rangle \tag{4.85}$$
$$-\frac{1}{\mathrm{Re}}\left(\underline{\nabla}^*\cdot\left[\alpha_c\underline{\underline{\tau}}_c^*\cdot\left\langle\underline{v}_c^*\right\rangle\right]-\alpha_c\underline{\underline{\tau}}_c^*:\underline{\nabla}^*\left\langle\underline{v}_c^*\right\rangle\right)$$

The Weber number has been moved to the LHS of the equation because originally the surface tension was associated with the interfacial area concentration in the total mixture energy balance. We restricted the system to those with reasonably constant surface tensions so that σ could be brought outside the gradient operator.

Allowing the velocity to increase without bound, we find that eqn (4.85) becomes

$$0=\underline{\nabla}^*\cdot\alpha_c\frac{\left\langle v_c^{*2}\right\rangle}{2}\left\langle\underline{v}_c^*\right\rangle+\left\langle\underline{v}_c^*\right\rangle\cdot\left(\alpha_c\nabla p^*\right)$$
$$+\left\langle\underline{v}_c^*\right\rangle\cdot\left[\left\langle p^*\right\rangle\nabla^*\alpha_c\right]+\underline{\nabla}^*\cdot\left[\underline{\underline{R}}_c^*\cdot\left\langle\underline{v}_c^*\right\rangle\right]-\underline{\underline{R}}_c^*:\underline{\nabla}^*\left\langle\underline{v}_c^*\right\rangle \tag{4.86}$$

which resembles the mechanical energy balance for a single phase. Therefore, it implies a minimum drop size. This supports results found experimentally (Long and Reimus, 1992a) where they correlated their data by adding a constant for the minimum drop size so that as the velocity increased, the drop size asymptotically reached the minimum drop size.

For systems with 'constant' surface tension, eqn (4.84) has an interesting relationship. The ratio of the Weber and Reynold's numbers appears with the viscous stress and dissipation terms. This implies that that

$$\frac{We}{\mathrm{Re}} = \frac{\mu v}{\sigma} = \frac{viscous\ forces}{surface\ forces} \tag{4.87}$$

so that as the viscosity increases, these forces are important even though the Reynold's number is high. Therefore, the viscous forces should be included in a complete model. This is supported by the comparison of the calculated and experimental data. In support of this observation, data on a variety of systems have been plotted in Figure 4.21 for a Kenics static mixer as a function of Weber number and viscosity ratio

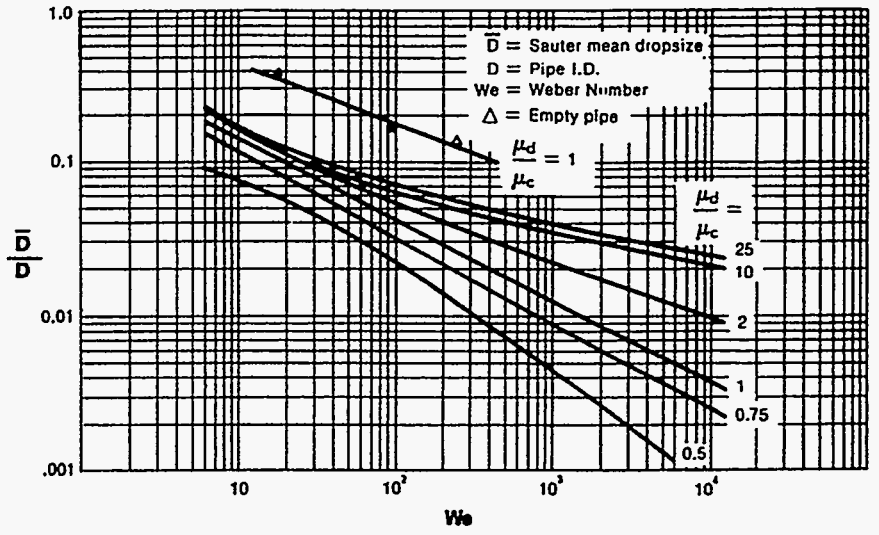

Figure 4.21 Drop Size Data for Kenics Static Mixer (Chemineer, 1988)

Chapter 5

CONCLUSIONS AND FUTURE WORK

5.1 Summary

A multi-fluid model was derived using a combination of ensemble- and volume-averaging techniques. The model contained five equations for

- Mass (each fluid)
- Momentum (each fluid)
- Interfacial area concentration/Mechanical energy Balance (continuous phase)

A key concept in the derivation was the assumption that the property exchange rate on the interface is the same everywhere on the interface at a particular location in the fluid, relative to the interface, regardless of the interface orientation. This was defined as the "generalized isotropy" condition for the interface. With this definition, the property exchange could be separated from the interface and a separate term, a_i, the interfacial area averaged over the volume could be defined. Once the interfacial area concentration was defined, then it appeared in all of the property exchange terms for the interface. In particular, a new turbulence term for the interaction of two fluids across an interface appeared as a result from the momentum balance equation.

Treating the interfacial area concentration as a separate variable enabled an equation to be defined for its transport. This was accomplished by looking at a total energy balance for the fluid mixture in a control volume and treating the energy of the

interface as a combination of the surface tension and interfacial area concentration. Subtracting the energy carried by the individual fluids that did not contribute specifically to the transport of area, it appeared that the transport of interfacial area concentration was mainly due to convection and surface work. In the various experiments, there were definite continuous and dispersed phases. In these cases, particularly for rapid mixing, the continuous phase acts as an 'impeller' and disperses the second phase through convection and surface work. Therefore, a mechanical energy balance on the continuous phase completed the model and provided the source term for the generation of interfacial area.

5.2 Conclusion

Based on the comparison of experimental and calculated data for four different static mixer systems over a large range of Weber and Reynold's numbers, the proposed model is correctly predicting the transport of interfacial area up to Weber numbers of 1000. The accuracy of the model is shown below.

From Figure 5.1, the data points are reasonably distributed about a straight line fitted through all of the points. The effect of Weber number is illustrated in Figures 5.2 and 5.3 below

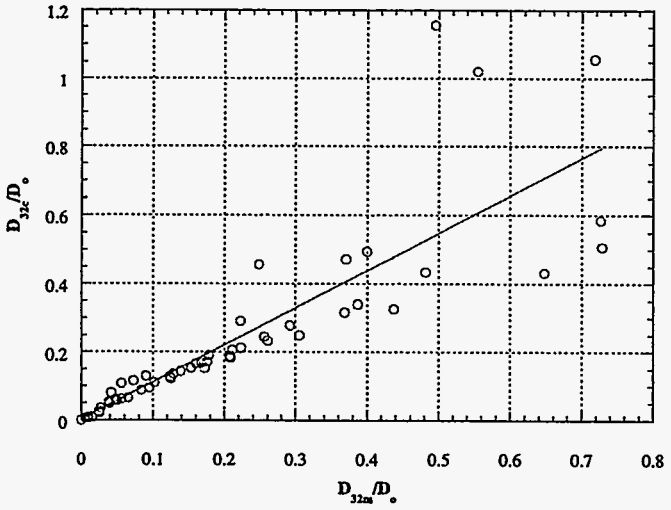

Figure 5.1 Overall Comparison of Experimental and Calculated Sauter Mean Drop Diameter/Diameter Ratios

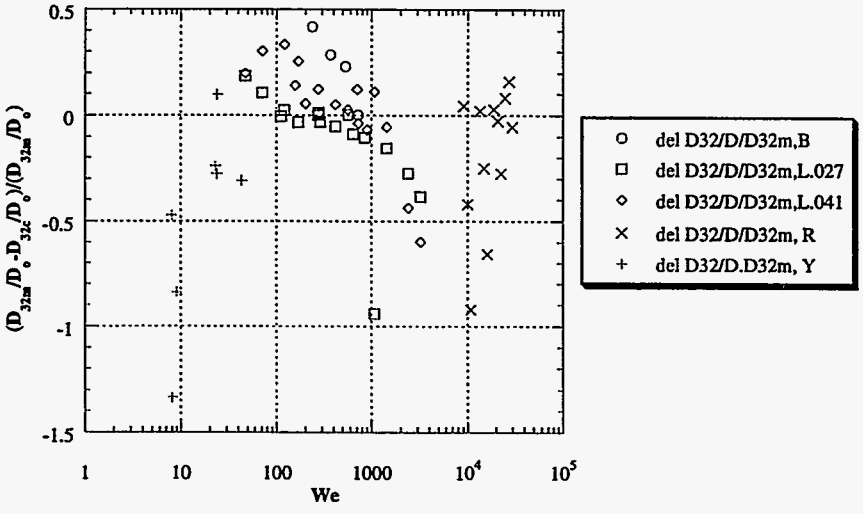

Figure 5.2 Variation of the Normalized Error Magnitude for the Sauter Mean Drop Diameter with Weber Number

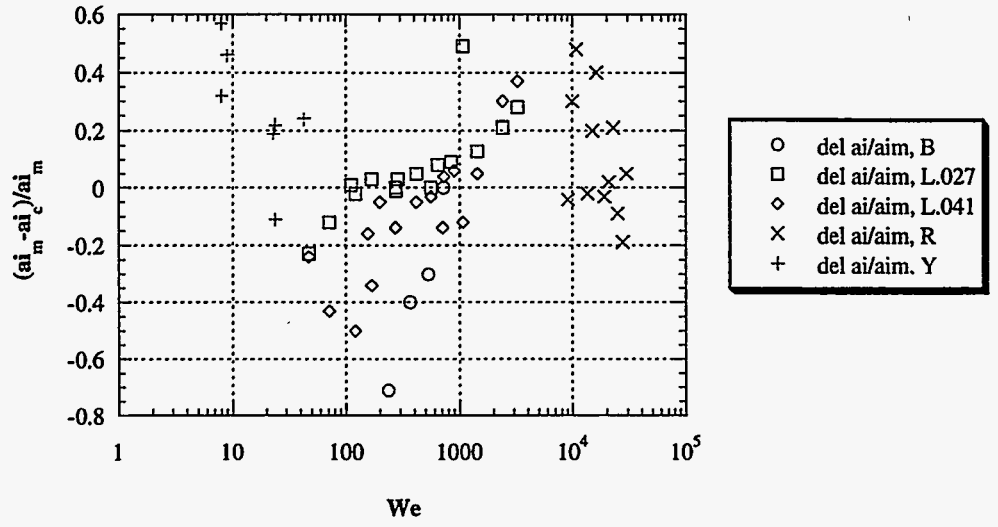

Figure 5.3 Variation of Measured and Calculated Interfacial Area Concentration with Weber Number

As discussed earlier, viscosity effects were neglected. However, examining the non-dimensionlized interfacial area transport equation showed that this is not a good assumption for a complete model and viscosity effects are important at the higher velocities in contrast with conventional wisdom for single-fluid systems. This possibly explains the slope of the line in Figure 5.2. In addition, accurate inlet conditions are important for this type of numerical approach. The trends in the data seem to indicate that the largest scatter was in the Kenics mixer with the "Y" and the Tee. As mentioned earlier, these cases did not have an exact geometric basis for the inlet boundary conditions. All of the other cases were essentially co-current jets and a

geometric basis was applied to the inlet conditions. However, the general conclusion is that the model is accurate and portrays a significant step towards solving a difficult problem.

5.3 Future Work

The current model should be extended to include the viscosity effects and compared to experimental data. This will be difficult because of the numerical difficulties in solving the equations with higher-order differential terms. Therefore, a more robust numerical procedure, such as a finite-volume or finite-element procedure, should be used to enable better definition of the boundary conditions. Also, progress should be made in defining better turbulence terms and in particular, defining a correlation for the inter-fluid turbulence.

Some possibilities for better multi-phase turbulence models include using the drop-size in a mixing-length model or in defining a multi-fluid K-epsilon such as in Kashiwa and Gore, 1992.

REFERENCES

Al Khani, S., C. Gourdon and G. Casamatta. 1989. "Dynamic and Steady-State Simulation of Hydrodynamics and Mass Transfer in Liquid-Liquid Extraction Column." Chem.Eng.Sci., Vol. 44, pp. 1295.

Al Taweel, A.M. and D.L. Walker. 1983. "Liquid Dispersion in Static In-Line Mixers." Can. J. of Chem. Eng., Vol. 61, pp. 527.

Arnold, G.S., D.A. Drew and R.T. Lahey. 1988. "An Assessment of Multiphase Flow Models using the Second Law of Thermodynamics." Int. J. of Multiphase Flow, Vol. 16, No. 3, pp. 481.

Azzopardi, B.J. 1979. "Measurement of Drop Sizes." Int. J. of Heat and Mass Trans., Vol. 22, pp. 1245.

Banerjee, S. and A.M.C. Chan. 1980. "Separated Flow Models-I: Analysis of the Averaged and Local Instantaneous Formulations." Int. J. of Multiphase Flow, Vol. 6, pp. 1.

Barnea, Dvora, Micheal Hoffer and William Resnick. 1978. "Dynamic Behavior of an Agitated Two-Phase Reactor with Dynamic Variations in Drop Diameter-I." Chem. Eng. Sci. Vol. 33, pp.205.

Bayens, C.A. and R.L. Laurence. 1969. "A Model for Mass Transfer in a Coalescesing Dispersion." Ind.Eng.Chem.Fund., Vol.8, pp.71.

Benedict, M., T.H. Pigford and H.W. Levi. 1981. Nuclear Chemical Engineering. New York: McGraw-Hill.

Berkman, P.D. and R.V. Calabrese. 1988. "Dispersion of Viscous Liquids by Turbulent Flow in a Static Mixer." AIChE J., Vol. 34, pp. 602.

Biesheuvel, A. and L. van Wijngaarden. 1984. "Two-Phase Flow Equations for a Dilute Dispersion of Gas Bubbles in Liquid." J. Fluid Mech., Vol. 148, pp. 301.

Bird, R.B., W.E. Stewart and E.N. Lightfoot. 1960. Transport Phenomena. New York: John Wiley & Sons.

Brodkey, R. 1967. The Phenomena of Fluid Motion. New York: Dover Publications, Inc.

Calabrese, R.V., T.P.K. Chang and P.T. Dang. 1986a. "Drop Breakup in Turbulent Stirred-Tank Reactors Part I: Effect of Dispersed Phase Viscosity." AIChE J., Vol. 32, pp. 657.

Calabrese, R.V., C.Y. Wang and N.P. Bryner. 1986b. "Drop Breakup in Turbulent Stirred-Tank Reactors Part III: Correlations for Mean Size and Drop Size Distribution." AIChE J., Vol. 32, pp. 677.

Chemineer. 1988. Kenics Static Mixers: KTEK Series.

Chen, H.T. and S. Middleman. 1967. "Drop Size Distribution in Agitated Liquid-Liquid Systems." AIChE J., Vol. 13, pp. 989.

Curl, R.L. 1963. "Dispersed Phase Mixing: I. Theory and Effects in Simple Reactors." AIChE J., Vol.9, pp.175.

Cook, T.L. and F.H. Harlow. 1984. "Virtual Mass in Multiphase Flow." Int. J. of Multiphase Flow, Vol. 10. No. 6, pp. 691.

Coulaloglou, C.A. and L.L. Tavlarides. 1976. "Drop Size Distributions and Coalescence Frequencies of Liquid-Liquid Dispersions in Flow Vessels." AIChE J. Vol.22, pp.289.

Coulaloglou, C.A. and L.L. Tavlarides. 1977. "Description of Interaction Processes in Agitated Liquid-Liquid Dispersions." Chem.Eng.Sci., Vol. 32, pp. 1289.

Cruz-Pinto, J.J.C. and W.J. Korchinsky. 1981. "Drop Breakage in Counter-Current Flow Liquid-Liquid Extraction Columns." Chem.Eng.Sci., Vol. 36, pp. 687.

Das, P.K., R. Kumar and D. Ramkrishna. 1987. "Coalescence of Drops in Stirred Dispersion. A White Noise Model for Coalescence." Chem.Eng.Sci., Vol. 42, pp. 213.

Davies, J.T.1985. "Drop Sizes of Emulsions Related to Turbulent Energy Dissipation Rates." Chem.Eng.Sci., Vol. 40, pp. 839.

Delhaye, J.M. 1974. "Jump Conditions and Entropy Sources in Two-Phase Systems. Local Instant Formulation." Int. J. of Multiphase Flow, Vol. 1, pp. 395.

Delhaye, J.M. and P. Bricard. 1994. "Interfacial Area in Bubbly Flow: Experimental Data and Correlations." Nuclear Engineering and Design, Vol.151, pp. 65.

Delichatsios, M.A. and R.F. Probstein. 1976. "The Effect of Coalescence on the Average Drop Size in Liquid-Liquid Dispersions." Ind.Eng.Chem.Fund., Vol.15, pp.134.

Dobran, F. 1984. "Constitutive Equations for Multiphase Mixtures of Fluids." Int. J. of Multiphase Flow, Vol. 10, No. 3, pp. 273.

Dobran, F. 1985. "Theory of Multiphase Mixtures: A Thermomechanical Formulation." Int. J. of Multiphase Flow, Vol. 11, No. 1, pp. 1.

Drew, D.A. and L.A. Segal. 1971. "Averaged Equations for Two-Phase Flows." Studies in App. Math., Vol. L, No. 3, pp. 205.

Drew, D.A. and R.T. Lahey, 1979a. "Application of General Constitutive Principles to the Derivation of Multidimensional Two-Phase Flow Equations." Int. J. of Multiphase Flow, Vol. 5, pp. 243.

Drew, D.A., L. Cheng and R.T. Lahey. 1979b. "The Analysis of Virtual Mass Effects in Two-Phase Flow." Int. J. of Multiphase Flow, Vol. 5, pp. 233.

Drew, D.A. and R.T. Wood. 1985. "Overview and Taxonomy of Models and Methods for Workshop on Two-Phase Flow Fundamentals." Proceedings of the First International Workshop on Two-Phase Flow Fundamentals.

Eakman, J.M., A.G. Fredrickson and H.M. Tsuchiya. 1966. AIChE Symp.Ser. No. 69, pp. 37.

Finlayson, B.A. 1980. Nonlinear Analysis in Chemical Engineering. New York: McGraw-Hill.

Fox, R.W. and A.T. McDonald. 1973. Introduction to Fluid Mechanics. New York: John Wiley & Sons.

Gal-Or, B. and H.E. Hoelsher. 1966. "A Mathematical Treatment of the Effect of Particle Size Distribution on Mass Transfer." AIChE J. Vol.12, pp. 499.

Grau, R.J. and H.J. Cantero. 1994. "A Systematic Time-, Space-, and Time-Space-Averaging Procedure for Bulk Phase Equations in Systems with Multiphase Flow." Chem.Eng.Sci., Vol. 49, No. 4, pp. 449.

Gresho, P.M. and R.L. Lee. 1981. "Don't Suppress the Wiggles - They're Telling You Something!" Computers and Fluids, Vol. 9, pp. 223.

Guimaraes, M.M.L.and J.J.C. Cruz-Pinto. 1988. "Mass Transfer and Dispersed Phase Mixing in Liquid-Liquid Systems-I." Comp.Chem.Eng., Vol. 12, pp. 1075.

Harlow, F.H. and A.A. Amsden. 1975. "Numerical Calculation of Multiphase Fluid Flow." J. of Comp. Physics, Vol. 17, pp. 19.

Hassanizadeh, M. and W.G. Gray. 1979. "General Conservation Equations for Multi-Phase Systems: 1. Averaging Procedure." Adv. in Water Res., Vol. 2, pp. 131.

Hestroni, G. 1982. Handbook of Multiphase Systems. New York: McGraw-Hill.

Hinze, J.O., 1955. "Fundamentals of the Hydrodynamic Mechanism of Splitting in Dispersion Process." AIChE J., Vol. 1, pp. 289.

Howarth, W.J. 1964. "Coalescence of Drops in a Turbulent Flow Field." Chem.Eng.Sci., Vol.19, pp.33.

Howarth, W.J. 1967. "Measurement of Coalescence Frequency in an Agitated Tank." AIChE J., Vol.13, pp. 1007.

Hulbert, H.M. and S. Katz. 1964. "Some Problems in Particle Technology." Chem.Eng.Sci., Vol. 19, pp. 555.

Ishii, M. 1975. Thermo-Fluid Dynamic Theory of Two-Phase Flow. Commissariat a' l'Energie Atomique, Paris, France:Eyrolles.

Ishii, M. and N. Zuber. 1979. "Drag-Coefficient and Relative Velocity in Bubbly, Droplet or Particulate Flows." AIChE J., Vol. 25, No. 5, pp. 843.

Ishii, M. and K. Mishima. 1980. "Study of Two-Fluid Model and Interfacial Area." Argonne National Laboratory Report, ANL-80-111. December.

Ishii, M. and K. Mishima. 1984. "Two-Fluid Model and Hydrodynamic Constitutive Relations." Nuclear Engineering and Design. Vol. 82, pp. 107.

Ishii, M. and G. Kocamustafaogullari. 1995. "Foundation of the Interfacial Area Transport Equation and its Closure Relations." Int. J. Heat and Mass Transfer, Vol. 38, No. 3, pp. 481.

Jacob, J. 1995. "Models for Prediction of Mean Drop Diameters in Tee Joints and Co-Current Jets." M.S. Thesis, New Mexico State University, Las Cruces.

Jeon, Y.M. and W.K. Lee. 1986. "A Drop Population Balance Model for Mass Transfer in Liquid-Liquid Dispersion. 1. Simulation and Its Results.", Ind.Eng.Chem.Fundam. Vol. 25, pp. 293.

Jones, A.V. and A. Prosperetti. 1985. "On the Suitability of First-Order Differential Models for Two-Phase Flow Prediction." Int. J. of Multiphase Flow, Vol. 11, No. 2, pp. 133.

Kalkach-Navarro, S., R.T. Lahey, D.A. Drew and R. Meyder. 1993. "Interfacial Area Density, Mean Radius and Number Density Measurements in Bubbly Two-Phase Flow." Nuclear Engineering and Design, Vol. 42, pp. 341.

Kalkach-Navarro, S., R.T. Lahey and D.A. Drew. 1994. "Analysis of the Bubbly/Slug Flow Regime Transition." Nuclear Engineering and Design, Vol. 151, pp. 15.

Kashiwa, B. 1987. "Statistical Theory of Turbulent Incompressible Multimaterial Flow." Los Alamos National Laboratory Report, LA-11088-T, October.

Kashiwa, B and R.A. Gore. 1990. "A Four Equation Model for Multiphase Turbulent Flow." Los Alamos National Laboratory Report, LA-UR-90-2273, June.

Kashiwa, B. and R.M. Rauenzahn. 1994. "A Multimaterial Formalism." Los Alamos National Laboratory Report, LA-UR-94-771, June.

Kataoka, I., M. Ishii and A. Serizawa. 1986a. "Local Formulation and Measurements of Interfacial Area Concentration in Two-Phase Flow." Int. J. Multiphase Flow, Vol. 12, No. 4, pp. 505.

Kataoka, I. 1986b. "Local Instant Formulation of Two-Phase Flow." Int. J. of Multiphase Flow, Vol.12, No. 5, pp. 745.

Kataoka, I. and A. Serizawa. 1990. "Interfacial Area Concentration in Bubbly Flow." Nuclear Engineering and Design, Vol. 120, pp. 163.

Kataoka, I., D.C. Besnard and A. Serizawa. 1992. "Basic Equation of Turbulence and Modeling of the Interfacial Transfer Terms in Gas-Liquid Two-Phase Flow." Chem. Eng. Comm., Vol. 118, pp. 221.

Kocamustafaogullari, G. and M. Ishii, 1995. "Foundation of the Interfacial Area Transport Equation and its Closure Relations." Int.J.Heat Mass Trans., Vol. 38, No. 3, pp. 481.

Koch Engineering Co. 1991. Static Mixing Technology. Bulletin KSM-6.

Lahey, R.T. and D.A. Drew. 1989. "The Three-Dimensional Time and Volume-Averaged Conservation Equations of Two-Phase Flow." Adv.Nucl.Sci.Technol., Vol.20, pp. 1.

Lahey, R.T. 1990. "The Analysis of Phase Separation and Phase Distribution Phenomena using Two-Fluid Models." Nuclear Engineering and Design, Vol. 122, pp. 17.

Lahey, R.T. 1991. "Void Wave Propagation Phenomena in Two-Phase Flow." AIChE J., Vol. 37, No. 1, pp. 123.

Lahey, R.T., J.W. Park and D.A. Drew. 1993. "The Analysis of Void Waves in Two-Phase Flow." Nuclear Engineering and Design, Vol. 141, pp. 203.

Lam, A., A.N. Sathyagal, S. Kumar and D. Ramkrishna. 1996. "Maximum Stable Drop Diameter in Stirred Dispersions." AIChE J., Vol. 42, No. 6, pp. 1547.

Laso, M., L. Steiner and S. Hartland. 1987. "Dynamic Simulation of Liquid-Liquid Agitated Dispersions-I. Derivation of a Simplified Model." Chem.Eng.Sci., Vol. 42, pp. 2429.

Leacock, J. and Stuart Churchill. 1961. "Mass Transfer Between Isobutanol and Water in Concurrent Flow Through a Packed Column." AIChE J., Vol.7, pp. 196.

Levenspiel, O. 1972. Chemical Reaction Engineering. New York: John Wiley & Sons.

Li, Y. and C. Wang. 1983. "Performance of Kenics In-Line Mixer in Solvent Extraction.", AIChE Symp.Ser. 283, Vol. 80, pp. 148.

Lin, W. 1985. "Prediction of the Sauter Mean Droplet Size from a Co-Current Jet Mixer." M.S. Thesis, New Mexico State University, Las Cruces.

Long, R.L.1983. "Application of Interfacial Mechanics in Liquid-Liquid Mixing.", Fourth International Conference on Physicochemical Hydrodynamics, Annals of the New York Academy of Sciences, Vol. 404, pp. 428.

Long, R.L. and P. Reimus. 1988a. "Interfacial Area Production at a 'T' Junction." Paper 36, Second International Symposium on Two-Phase Annular and Dispersed Flows, Abstracts, p. 139.

Long, R.L. and P. Reimus. 1988b. "Interfacial Area Production at a Tee Junction.", Session 134, AIChE Annual Meeting, Washington, D.C., December, 1988.

Long, R.L. and P. Reimus. 1992a. "Interfacial Area Production at a Tee Junction.", Chem.Eng.Comm., Vol.3, pp.1.

Long, R.L., I. Tavarez, W. Lin and P. Reimus. 1992b. "Interfacial Area Production in Tees and Jets.", Process Mixing: Chemical and Biochemical Applications., AIChE Symp.Ser. 286, Vol. 88, pp. 65.

Long, R.L., I. Tavarez, W. Lin and P. Reimus. 1993. "Interfacial Area Production in Tees and Jets.", Chem. Eng. Comm., Vol. 134, pp. 68.

Long, R.L. 1994. Personal Communication.

Madden, A.J. and G.L. Damerell. 1962. "Coalescence Frequencies in Agitated Liquid-Liquid Systems." AIChE J., Vol. 8, pp. 233.

Merchuk, J., R. Shai and D. Wolf. 1980a. "Experimental Study of Copper Extraction with LIX-64N by Means of Motionless Mixers." Ind.Eng.Chem.Proc.Des.Dev., Vol.19, pp.91.

Merchuk, J.C., D. Wolf, R. Shai and D.H. White, 1980b. "Experimental Study of Dispersion and Separation of Phases in Liquid-Liquid Extraction of Copper by LIX-64N in Various Types of Mixers." Ind.Eng.Chem.Proc.Dev., Vol. 19, pp. 522.

Middleman, S. 1974. "Drop Size Distributions Produced by Trubulent Pipe Flow of Immiscible Fluids through a Static Mixer." Ind.Eng.Chem. Process Des.Dev., Vol.13, pp.78.

Min, K.W. and W.H. Ray. 1978. "The Computer Simulation of Batch Emulsion Polymerization Reactors Through a Detailed Mathematical Model." J.Appl.Poly.Sci., Vol. 22, pp. 89.

Muralidhar, R. and D. Ramkrishna. 1986. "Analysis of Droplet Coalescence in Turbulent Liquid-Liquid Dispersions." Ind.Eng.Chem.Fundam., Vol. 25, pp. 554.

Muralidhar, R., D. Ramkrishna and P. Das. 1988. "Coalescence of Rigid Droplets in a Stirred Dispersion-II. Band-Limited Force Fluctuations." Chem.Eng.Sci., Vol. 43, pp. 1559.

Narsimhan, G., G. Nejfelt and D. Ramkrishna. 1984. "Breakage Functions for Droplets in Agitated Liquid-Liquid Dispersions." AIChE J., Vol. 30, pp. 457.

Nigmatulin, R.I. 1979. "Spatial Averaging in the Mechanics of Heterogeneous and Dispersed Systems." Int. J. of Multiphase Flow, Vol. 5, pp. 353.

Park, J.Y. and L.M. Blair. 1975. "The Effect of Coalescence on Drop Size Distributions in an Agitated Liquid-Liquid Dispersion." Chem.Eng.Sci., Vol.30, pp.1057.

Pavlica, R.T. and J.H. Olson. 1970. "Unified Design Method for Continuous-Contact Mass Transfer Operations." Ind.Eng.Chem., Vol. 62, pp. 45.

Pauchon, C. and S. Banerjee. 1986. "Interphase Momentum Interaction Effects in the Averaged Multifield Model. Part 1: Void Propagation in Bubbly Flows." Int. J. of Multiphase Flow, Vol. 12, No. 4, pp. 559.

Pauchon, C. and S. Banerjee. 1988. "Interphase Momentum Interaction Effects in the Averaged Multifield Model. Part 2: Kinematic Waves and Interfacial Drag in Bubbly Flows." Int. J. of Multiphase Flow, Vol. 14, No. 3, pp. 253.

Pillay, K.K.S. 1993. Personal Communication. Los Alamos National Laboratory.

Prince, M.J. and H.W. Blanch. 1990. "Bubble Coalescence and Break-up in Air-Sparged Bubble Columns." AIChE J., Vol. 36, No. 10, pp. 1485.

Ramkrishna, D. and J.D. Borwanker. 1973. "A Puristic Analysis of Population Balance-I." Chem.Eng.Sci., Vol. 28, pp. 1423.

Ramkrishna, D. and J.D. Borwanker. 1974a. "A Puristic Analysis of Population Balance-II." Chem.Eng.Sci., Vol. 29, pp. 1711.

Ramkrishna, D. 1974b. "Drop-Breakage in Agitated Liquid-Liquid Dispersions." Chem.Eng.Sci., Vol.29, pp.987.

Ramkrishna, D. 1980. "Analysis of Population Balance-IV: The Precise Connection Between Monte Carlo Simulation and Population Balances." Chem.Eng.Sci., Vol.36, pp. 1203.

Ramkrishna, D., A. Sathyagal and G. Narsimhan. 1995. "Analysis of Dispersed Phase Systems: A Fresh Perspective." AIChE J., Vol. 41, No. 1, pp. 35.

Reimus, P. 1983. "A Model for Predicting the Sauter Mean Droplet Diameter of Kerosene in Water Dispersions Generated by Tee Mixers." M.S. Thesis, New Mexico State University, Las Cruces.

Ruggles, A.E., R.T. Lahey and D.A. Drew. 1988. "An Analysis of Void Wave Propagation in Bubbly Flows." Proc. 15th Annual Miami Intl. Symp. Multiphase Transport and Particulate Phenomena.

Shah, B.H. and D. Ramkrishna. 1973. "A Population Balance Model for Mass Transfer in Lean Liquid-Liquid Dispersions." Chem.Eng.Sci., Vol.28, pp.389.

Shinnar, Reuel and James Church. 1960. "Predicting Particle Size in Agitated Dispersions." Ind.Eng.Chem., Vol.52, pp. 253.

Spiegel, M.R. 1992. Advanced Mathematics for Engineers and Scientists. Schaum's Outline Series, New York:McGraw-Hill.

Standart, G. 1964. "The Mass, Momentum and Energy Equations for Heterogeneous Flow Systems." Chem.Eng.Sci., Vol. 19, pp. 227.

Stewart, H.B. and B. Wendroff. 1984. "Two-Phase Flow: Models and Methods." J. of Comp. Physics, Vol. 56, pp. 363.

Stuhmiller, J.H. 1977. "The Influence of Interfacial Pressure Forces on the Character of Two-Phase Flow Model Equations." Int. J. of Multiphase Flow, Vol. 3, pp. 551.

Tavarez, I. 1991. "Models for Interfacial Area Production in Static Mixers." M.S. Thesis, New Mexico State University, Las Cruces.

Tavlarides, L.L. and Benjamin Gal-Or. 1969. "A General Analysis of Multicomponent Mass Transfer with Simultaneous Reversible Chemical Reactions in Multiphase Systems." Chem.Eng.Sci., Vol.24, pp. 553.

Tavlarides, L.L. and M. Stamatoudis. 1981. "The Analysis of Interphase Reactions and Mass Transfer in Liquid-Liquid Dispersions." Adv.Chem.Eng., Vol. 11, pp. 199.

Tavlarides, L.L. and P.M. Bapat. 1983. "Models for Scale-up of Dispersed Phase Liquid-Liquid Reactors." AIChE Symp.Ser. No. 238. Vol.80, pp. 12.

Theofanous, T.G. and J.P. Sullivan. 1982. "Turbulence in Two-Phase Dispersed Flows." J. Fluid Mech., Vol. 116., pp. 343.

Thornton, J.D. 1956a. "Mechanical Contactors for Liquid-Liquid Extraction-Part 1." Nucl.Eng. July. pp. 156.

Thornton, J.D. 1956b. "Mechanical Contactors for Liquid-Liquid Extraction-Part 2." Nucl.Eng. August. pp. 204.

Tobin, R., R. Muralidhar, H. Wright and D. Ramkrishna. 1990. "Determination of Coalescence Frequencies in Liquid-Liquid Dispersions: Effect of Drop Size Dependence." Chem.Eng.Sci., Vol. 45, pp. 3491.

Travis, J.R., F.H. Harlow and A.A. Amsden. 1976. "Numerical Calculation of Two-Phase Flows." Nuclear Science and Engineering, Vol. 61, pp. 1.

Treybal, R.E. 1963. Liquid Extraction. New York: McGraw-Hill.

Truesdell, C. and R. Toupin. 1960. Handbuch der Physik. Vol. III/1, Berlin:Springer-Verlag.

Tse, S.E.S. 1978. "Mass Transfer Rates in the Solvent Extraction of Metal Chlorides by Tri-isooctylamine." M.S. Thesis. University of Wisconsin. Madison.

Tsouris, C. and L.L. Tavlarides. 1994. "Breakage and Coalescence Models for Drops in Turbulent Dispersions." AIChE J., Vol. 40, pp. 395.

Tunison, M.E. 1976. "Characterization of Plug-Flow, Two-Phase Reactors with Applications to the Solvent Extraction of Metals." Ph.D. Dissertation. University of Wisconsin. Madison.

Tunison, M.E. and Thomas Chapman. 1978. "Characterization of the Kenics Mixer as a Liquid-Liquid Extractor." AIChE Symp.Ser. No.173, Vol.74, pp.112.

Valentas, K.J. and N.R. Amundson. 1966a. "Breakage and Coalescence in Dispersed Phase Systems." Ind.Eng.Chem.Fund., Vol.5, pp.533.

Valentas, K.J., O. Bilous and N.R. Amundson. 1966b. "Analysis of Breakage in Dispersed Phase System." Ind.Eng.Chem.Fund., Vol.5, pp.271.

VanderHeyden, W.B. and B.A. Kashiwa. 1995. "Explicit Multiphase Reynolds Stress Tensor from Homogeneous Tensor Transport Equation using Tensor Algebra Integrity Basis Method." Los Alamos National Laboratory Report, LA-UR-95-1719, November.

Verhoff, F.H., S.L. Ross and R.L. Curl. 1977. "Breakage and Coalescence Processes in an Agitated Dispersion. Experimental System and Data Reduction." Ind.Eng.Chem.Fundam., Vol. 16, pp. 371.

Versteeg, H.K. and W. Malalasekera. 1995. An Introduction to Computational Fluid Dynamics: The Finite Volume Method. Essex, England: Longman Group Limited.

Wang, C.Y. and R.V. Calabrese. 1986. "Drop Breakup in Turbulent Stirred-Tank Reactors Part II: Relative Influence of Viscosity and Interfacial Tension." AIChE J., Vol. 32, pp. 667.

Wish, E.R., 1959. USAEC Report HW-60116, April 30.

Wolfram Research, Inc. 1993. Mathematica: Selected Tutorial Notes, Wolfram Research, Inc.

Yarbro, S.L. 1987. "Using Solvent Extraction to Process Nitrate Anion Exchange Column Effluents." M.S. Thesis. University of New Mexico. Albuquerque.

Yarbro, S.L. and R.L. Long. 1995. "Hydrodynamic Analysis of a Two-Phase Tubular Reactor", Industrial Mixing Fundamentals with Applications, AIChE Sym. Ser. No. 305.

APPENDIX A

Berkman and Calabrese

1.91 cm Kenics Mixer

A.1 Equation Summary

A.1.1 Model Equations (Steady-State)

Mass:

Continuous

$$\frac{\partial}{\partial z}\alpha_c v_{cz} = 0 \tag{A.1}$$

Dispersed

$$\frac{\partial}{\partial z}\alpha_d v_{dz} = 0 \tag{A.2}$$

Momentum:

Continuous

$$\begin{aligned}
&\rho_c \alpha_c \frac{\partial}{\partial z} v_{cz} - \alpha_c \left(\frac{\partial}{\partial z} p - 2\frac{\rho_c}{D} v_{kz}^2 f_t \right) + \frac{\partial}{\partial z}\left(-\frac{1}{5}\alpha_d \rho_c \left(v_{cz} - v_{dz} \right)^2 \right) \\
&= -\left(2\sigma a_i - \frac{1}{4}\rho_c \left(v_{cz} - v_{dz} \right)^2 \right) \frac{\partial}{\partial z}\alpha_c - \frac{3}{8}\alpha_d \rho_c C_d a_i \left(v_{cz} - v_{dz} \right)^2 \\
&- C_{vm}\alpha_d \rho_c \left[\left(v_{dz} \frac{\partial}{\partial z} v_{dz} \right) - \left(v_{cz} \frac{\partial}{\partial z} v_{cz} \right) \right]
\end{aligned} \tag{A.3}$$

Dispersed

$$\rho_d\alpha_d\frac{\partial}{\partial z}v_{dz}-\alpha_d\left(\frac{\partial}{\partial z}p-2\frac{\rho_d}{D}v_{dz}^2f_t\right)-\frac{\rho_d}{\rho_c}\frac{\partial}{\partial z}\left(-\frac{1}{5}\alpha_d\rho_c\left(v_{cz}-v_{dz}\right)^2\right)$$
$$=-\left(2\sigma a_i-\frac{1}{4}\rho_c\left(v_{cz}-v_{dz}\right)^2\right)\frac{\partial}{\partial z}\alpha_d+\frac{3}{8}\alpha_d\rho_cC_da_i\left(v_{cz}-v_{dz}\right)^2 \qquad \text{(A.4)}$$
$$+C_{vm}\alpha_d\rho_c\left[\left(v_{dz}\frac{\partial}{\partial z}v_{dz}\right)-\left(v_{cz}\frac{\partial}{\partial z}v_{cz}\right)\right]$$

Interfacial Area:

$$\frac{\partial}{\partial z}\left(a_iv_{cz}\right)=-\rho_c\frac{\partial}{\partial z}\left(\alpha_c\frac{v_{cz}^3}{2}\right)-v_{cz}\left(\alpha_c\frac{\partial}{\partial z}p-2\frac{\rho_c}{D}v_{cz}^2f_t\right)$$
$$-\frac{\partial}{\partial z}\left[\left(-\frac{1}{5}\alpha_d\rho_c\left(v_{cz}-v_{dz}\right)^2\right)v_{cz}\right] \qquad \text{(A.5)}$$
$$+\left(-\frac{1}{5}\alpha_d\rho_c\left(v_{cz}-v_{dz}\right)^2\right)\frac{\partial}{\partial z}v_{cz}+v_{cz}\left(2\sigma a_i+\frac{1}{4}\rho_c\left(v_{cz}-v_{dz}\right)^2\right)\frac{\partial}{\partial z}\alpha_c$$

A.1.2 Equation Coefficients

Drag Coefficient (Lahey, 1990)

$$F_d=\frac{3}{8}\alpha_d\rho_cC_da_i\left|v_c-v_d\right|^2 \qquad \text{(A.6a)}$$

$$C_d=0.45\left(\frac{1+17.67\left[f\left(\alpha_d\right)\right]^{6/7}}{18.67f\left(\alpha_d\right)}\right)^2 \qquad \text{(A.6b)}$$

where $f(\alpha_d)$ is defined for drops in liquids as (Ishii, 1979)

$$f\left(\alpha_d\right)=\left(1-\alpha_d\right)^{2.25} \qquad \text{(A.6c)}$$

Virtual Mass (Lahey, 1991)

$$F_{vm}=C_{vm}\alpha_d\rho_c\left[\left(v_{dz}\frac{\partial}{\partial z}v_{dz}\right)-\left(v_{cz}\frac{\partial}{\partial z}v_{cz}\right)\right] \qquad \text{(A.7a)}$$

and the virtual volume coefficient can be defined as a function of the global dispersed phase fraction (Ruggles, et.al., 1988)

$$C_{vm} = 0.5\left(1+12\left(\bar{\alpha}_d\right)^2\right) \tag{A.7b}$$

A.1.3 Turbulence (Drew and Wood, 1985)

$$\underline{\underline{R}}_c = -\frac{1}{5}\alpha_d \rho_c \left|v_{cz} - v_{dz}\right|^2 \tag{A.8a}$$

$$\underline{\underline{R}}_d = \frac{\rho_d}{\rho_c}\underline{\underline{R}}_c \tag{A.8b}$$

A.1.4 Interfacial Pressure and Friction Factor

Friction Factor (Re > 3000) (Bird, 1960, Hestroni, 1982)

$$\tau_{kw} = \frac{\Delta p}{L} = 2\frac{\rho_k}{D_h} v_{kz}^2 f_{kt} \tag{A.9a}$$

$$f_{kt} = f_m f_k \tag{A.9b}$$

$$f_d \approx 1.2 f_c \tag{A.9d}$$

where f is defined by

$$\text{(Turbulent Re} > 3000) \quad f_k = \frac{0.0791}{\text{Re}^{1/4}} \tag{A.9c}$$

Interfacial Pressure (Stuhmiller, 1977, Drew and Wood, 1985)

$$p_{ki} = 2\sigma a_i - \frac{1}{4}\rho_c \left(v_{cz} - v_{dz}\right)^2 \tag{A.10a}$$

(horizontal systems) $\rho g \cos(\theta) = 0$ (A.10b)

A.2 Boundary Conditions

A.2.1 Initial Velocities

$$V_{co} = \frac{\mu_c \mathrm{Re}}{D_T \rho_c} \tag{A.11a}$$

$$V_{do} = V_{co} \frac{\alpha_{do}}{\alpha_{co}} \frac{A_c}{A_d} \tag{A.11b}$$

A.2.2 Initial Phase Fractions

$$\alpha_{di} = \frac{D_d^2}{D_T^2} \tag{A.12a}$$

$$\alpha_{ci} = 1 - \alpha_{di} \tag{A.12b}$$

A.2.3 Initial interfacial area concentration

$$a_{ii} = \frac{\frac{\pi D_d dz}{4}}{\frac{\pi D_T^2 dz}{4}} = \frac{4D_d}{D_T^2} \tag{A.13}$$

A.2.4 Friction multiplier

$$f_m = 50 \tag{A.14}$$

A.3 Results

Table A.1 Results of Modeling the 1.91 cm Diameter Kenics Mixer Data

Kenics Mixer: Diameter 1.91 cm, 24 elements, pitch 1.5

Fluids: Continuous phase - water, Dispersed Phase - p-xylene

ad	Re	D32m/Do	D32c/Do	del D32/Do	We	We(-3/5)
0.001	12000	0.0150	0.0087	0.0062	235.6	0.0377
0.001	15000	0.0105	0.0075	0.0030	368.1	0.0289
0.001	18000	0.0085	0.0065	0.0019	530.1	0.0232
0.001	21000	0.0055	0.0055	0.0000	721.5	0.0193

D_{32m}/D_o = measured values, D_{32c}/D_o = calculated values

A.4 Mathematica 2.2 Program

Hydrodynamic Model of Drop Formation in a Kenics Mixer

Test of interfacial area data on Berkman's data for Kenics Mixer

Define System Constants:

Density of the continuous and dispersed phases (g/cm3)

rhoc = 1.0

rhod = 0.857

Viscosity of the continuous and dispersed phases (poise)

muc = 0.01

mud = 0.01

Surface Tension of the system water/p-xylene (g/s2)

ST = 32

Diameter of the outer pipe, continuous and dispersed phase inlets (cm)

Dia = 1.91

Diac = 1.91

Diad = 0.25

Radius, Length and Volume (cm,cm3)

R = Dia/2

L = 345 Dia

Vol = 3.14159 Dia^2/4 L

Area of the outer pipe, continuous and dispersed phase inlets (cm2)

area = 3.14159 R^2

areac = area - 3.14159 (Diad/2)^2

aread = 3.14159 (Diad/2)^2

Calculate initial phase fraction and average phase fraction (c-continuous, d-dispersed)

phidi = Diad^2/Diac^2

phido = 0.001

phico = 1-phido

Calculate final velocity and initial velocities

re = 12000

Vf = ((muc re)/(Dia rhoc))/phico

Vco = ((muc re)/(Dia rhoc))

Vdo = Vco (phido/phico) (areac/aread)

Calculate initial interfacial area, We No., Hydraulic Diameter and check Re No.

we = rhoc Vco^2 Dia/ST

nre = rhoc Dia Vf/muc

Dh = 0.25 Dia/L

aio = 4 Diad/Diac^2

Calculate Friction Factors:

f = 50 (0.0791/nre^0.25)

fd = 50 (0.0791/nre^0.25) 1.17

delp = 2 rhoc/Dia Vf^2 f

Calculate Wall Drag, Interfacial Drag, Interfacial Pressure, Virtual Mass,

Bubble-Induced Turbulence and Interfacial Work:

Fw = 2 rhoc/Dia Vc[z]^2 f

Fdw = 2 rhod/Dia Vd[z]^2 fd

fphid = (1 - phid[z])^2.25

Cd = 0.45 ((1 + 17.67 fphid^(6/7)) /(18.67 fphid))^2

Cvm = 0.5 (1+12 (phido^2))

DynP = 0.25 rhoc (Vc[z] - Vd[z])^2

Fd = 3/8 phid[z] rhoc Cd ai[z] (Vc[z] - Vd[z])^2

Tzz = -0.2 phid[z] rhoc (Vc[z]-Vd[z])^2

Fvm = phid[z] rhoc Cvm (Vd[z] Vd'[z]-Vc[z] Vc'[z])

```
Wi = -(D[phic[z] rhoc 1/2 Vc[z]^3,z] + D[phic[z] Tzz Vc[z],z]
    - phic[z] Tzz Vc'[z] - Vc[z] phic[z] (delp - Fw)
    + Vc[z] (2 ST ai[z] - DynP) phic'[z])
```

Define Balance Equations:

Continuity Equations:

```
eqn1 = phid'[z] == (-phid[z]/Vd[z]) Vd'[z]
eqn2 = phic'[z] == (-phic[z]/Vc[z]) Vc'[z]
```

Momentum Equations:

```
eqn3 = Vd'[z] == (phid[z] (delp - Fdw) - (2 ST ai[z] - DynP) phid'[z]
        + (rhod/rhoc) D[phid[z] Tzz,z] + Fvm
        + Fd)/(rhod phid[z] Vd[z])
eqn4 = Vc'[z] == (phic[z] (delp - Fw) - (2 ST ai[z] - DynP) phic'[z]
      - D[phic[z] Tzz,z] - Fvm
      - Fd)/(rhoc phic[z] Vc[z])
eqn5 = ai'[z] == (1/ST Wi - ai[z] Vc'[z])/Vc[z]
```

Input Boundary Conditions and Solve:

```
sol = NDSolve[{eqn1,eqn2,eqn3,eqn4,eqn5,
 phid[0] == phidi, phic[0] == 1-phidi,Vd[0] == Vdo,
 Vc[0] == Vco, ai[0] == aio},
 {phid[z],phic[z],Vd[z],Vc[z],ai[z]}, {z,0,L}, MaxSteps->5000]
```

Output Plot of Dispersed Phase Velocity:

Plot[Evaluate[Vd[z]/.sol],{z,0,5}, PlotRange->All,

AxesLabel->{"Length, cm","Vd[z], cm/s"}]

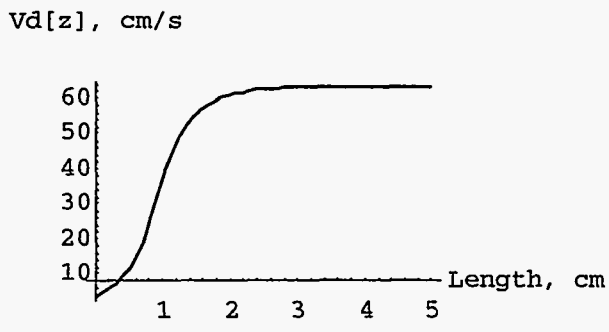

Output Plot for Continuous Phase Velocity:

Plot[Evaluate[Vc[z]/.sol],{z,0,5}, PlotRange->All,

AxesLabel->{"Length, cm","Vc[z], cm/s"}]

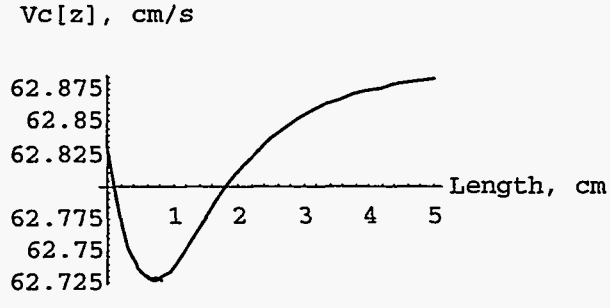

Output Plot for Interfacial Area Concentration:

Plot[Evaluate[ai[z]/.sol],{z,0,5}, PlotRange->All,

AxesLabel->{"Length, cm","ai[z], 1/cm"}]

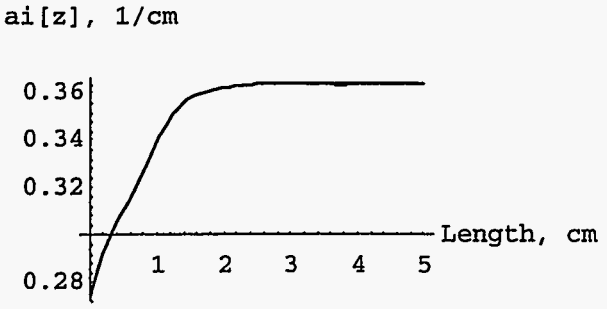
ai[z], 1/cm
0.36
0.34
0.32
0.28
1
2
3
4
5
Length, cm

APPENDIX B
Yarbro

0.635 cm Diameter Kenics Mixer

B.1 Equation Summary

B.1.1 Model Equations (Steady-State)

Mass:

Continuous

$$\frac{\partial}{\partial z}\alpha_c v_{cz} = 0 \tag{B.1}$$

Dispersed

$$\frac{\partial}{\partial z}\alpha_d v_{dz} = 0 \tag{B.2}$$

Momentum:

Continuous

$$\begin{aligned}
&\rho_c \alpha_c \frac{\partial}{\partial z} v_{cz} - \alpha_c \left(\frac{\partial}{\partial z} p - 2\frac{\rho_c}{D} v_{kz}^2 f_t \right) + \frac{\partial}{\partial z}\left(-\frac{1}{5}\alpha_d \rho_c \left(v_{cz} - v_{dz} \right)^2 \right) \\
&= -\left(2\sigma a_i - \frac{1}{4}\rho_c \left(v_{cz} - v_{dz} \right)^2 \right) \frac{\partial}{\partial z}\alpha_c + \frac{3}{8}\alpha_d \rho_c C_d a_i \left(v_{cz} - v_{dz} \right)^2 \\
&+ C_{vm}\alpha_d \rho_c \left[\left(v_{dz} \frac{\partial}{\partial z} v_{dz} \right) - \left(v_{cz} \frac{\partial}{\partial z} v_{cz} \right) \right]
\end{aligned} \tag{B.3}$$

Dispersed

$$\rho_d\alpha_d\frac{\partial}{\partial z}v_{dz}-\alpha_d\left(\frac{\partial}{\partial z}p-2\frac{\rho_d}{D}v_{dz}^2f_t\right)-\frac{\rho_d}{\rho_c}\frac{\partial}{\partial z}\left(-\frac{1}{5}\alpha_d\rho_c\left(v_{cz}-v_{dz}\right)^2\right)$$
$$=-\left(2\sigma a_i-\frac{1}{4}\rho_c\left(v_{cz}-v_{dz}\right)^2\right)\frac{\partial}{\partial z}\alpha_d-\frac{3}{8}\alpha_d\rho_cC_da_i\left(v_{cz}-v_{dz}\right)^2 \qquad \text{(B.4)}$$
$$-C_{vm}\alpha_d\rho_c\left[\left(v_{dz}\frac{\partial}{\partial z}v_{dz}\right)-\left(v_{cz}\frac{\partial}{\partial z}v_{cz}\right)\right]$$

Interfacial Area:

$$\frac{\partial}{\partial z}\left(a_iv_{cz}\right)=-\rho_c\frac{\partial}{\partial z}\left(\alpha_c\frac{v_{cz}^3}{2}\right)-v_{cz}\left(\alpha_c\frac{\partial}{\partial z}p-2\frac{\rho_c}{D}v_{cz}^2f_t\right)$$
$$-\frac{\partial}{\partial z}\left[\left(-\frac{1}{5}\alpha_d\rho_c\left(v_{cz}-v_{dz}\right)^2\right)v_{cz}\right] \qquad \text{(B.5)}$$
$$+\left(-\frac{1}{5}\alpha_d\rho_c\left(v_{cz}-v_{dz}\right)^2\right)\frac{\partial}{\partial z}v_{cz}+v_{cz}\left(2\sigma a_i+\frac{1}{4}\rho_c\left(v_{cz}-v_{dz}\right)^2\right)\frac{\partial}{\partial z}\alpha_c$$

B.1.2 Equation Coefficients

Drag Coefficient (Lahey, 1990)

$$F_d=\frac{3}{8}\alpha_d\rho_cC_da_i\left|v_c-v_d\right|^2 \qquad \text{(B.6a)}$$

$$C_d=0.45\left(\frac{1+17.67\left[f\left(\alpha_d\right)\right]^{6/7}}{18.67f\left(\alpha_d\right)}\right)^2 \qquad \text{(B.6b)}$$

where $f(\alpha_d)$ is defined for drops in liquids as (Ishii, 1979)

$$f\left(\alpha_d\right)=\left(1-\alpha_d\right)^{2.25} \qquad \text{(B.6c)}$$

Virtual Mass (Lahey, 1991)

$$F_{vm}=C_{vm}\alpha_d\rho_c\left[\left(v_{dz}\frac{\partial}{\partial z}v_{dz}\right)-\left(v_{cz}\frac{\partial}{\partial z}v_{cz}\right)\right] \qquad \text{(B.7a)}$$

and the virtual volume coefficient can be defined as a function of the global dispersed phase fraction (Ruggles, et.al., 1988)

$$C_{vm} = 0.5\left(1+12\left(\overline{\alpha}_d\right)^2\right) \tag{B.7b}$$

B.1.3 Turbulence (Drew and Wood, 1985)

$$\underline{\underline{R}}_c = -\frac{1}{5}\alpha_d \rho_c \left|v_{cz} - v_{dz}\right|^2 \tag{B.8a}$$

$$\underline{\underline{R}}_d = \frac{\rho_d}{\rho_c}\underline{\underline{R}}_c \tag{B.8b}$$

B.1.4 Interfacial Pressure and Friction Factor

Friction Factor (Re > 3000) (Bird, 1960, Hestroni, 1982)

$$\tau_{kw} = \frac{\Delta p}{L} = 2\frac{\rho_k}{D_h} v_{kz}^2 f_{kt} \tag{B.9a}$$

$$f_{kt} = f_m f_k \tag{B.9b}$$

$$f_d \approx 1.2 f_c \tag{B.9d}$$

where f is defined by

$$\text{(Turbulent Re} > 3000) \quad f_k = \frac{16}{\text{Re}} \tag{B.9c}$$

Interfacial Pressure (Stuhmiller, 1977, Drew and Wood, 1985)

$$p_{ki} = 2\sigma a_i - \frac{1}{4}\rho_c \left(v_{cz} - v_{dz}\right)^2 \tag{B.10a}$$

$$\text{(horizontal systems)} \qquad \rho g \cos(\theta) = 0 \tag{B.10b}$$

B.2 Boundary Conditions

B.2.1 Initial Volumetric Flowrates and Final Average Velocity

$$Q_{do} = V_f (1 - \alpha_{do}) A \tag{B.11a}$$

$$Q_{co} = V_f \alpha_{do} A \tag{B.11b}$$

$$V_f = \frac{\mu \mathrm{Re}}{D\rho} \tag{B.11c}$$

B.2.2 Average Viscosity and Density

$$\mu = \alpha_{do}\mu_d + (1 - \alpha_{do})\mu_c \tag{B.12a}$$

$$\rho = \alpha_{do}\rho_d + (1 - \alpha_{do})\rho_c \tag{B.12b}$$

B.2.3 Initial Linear Velocities and Flow Area

$$V_{co} = \frac{Q_{co}}{A - A_f} \tag{B.13a}$$

$$V_{do} = \frac{Q_{do}}{A_f} \tag{B.13b}$$

$$A_f = \frac{1}{2} A \frac{\alpha_{do}}{\alpha_{co}} \tag{B.13c}$$

B.2.4 Initial Phase Fractions and Interfacial Area Concentration

$$\alpha_{di} = \frac{1}{2} \frac{\alpha_{do}}{\alpha_{co}} \tag{B.14a}$$

$$\alpha_{ci} = 1 - \alpha_{di} \tag{B.14b}$$

$$aii = \frac{Ddz}{\frac{\pi D^2}{4}} \frac{\alpha_{do}}{\alpha_{co}} = \frac{4}{\pi D} \frac{\alpha_{do}}{\alpha_{co}} \qquad \text{(B.14c)}$$

B.2.5 Friction multiplier

$$f_m = datafit \qquad \text{(B.15)}$$

B.3 Results

Table B.1 Results of Modeling the 0.635 cm Diameter Kenics Mixer Data

Kenics Mixer: Diameter 0.635 cm, 12 elements, pitch 1.5

Fluids: Continuous phase - water, Dispersed Phase - dodecane

ad	Re	D32m/Do	D32c/Do	del D32/Do	We	We(-3/5)
0.28	2320	0.481	0.434	0.047	24	0.149
0.27	1383	0.555	1.020	-0.466	9	0.268
0.20	2299	0.371	0.472	-0.102	24	0.149
0.19	1363	0.718	1.056	-0.338	8	0.287
0.12	3081	0.222	0.291	-0.068	43	0.105
0.11	2271	0.400	0.495	-0.095	23	0.152
0.11	1363	0.495	1.155	-0.660	8	0.287

B.4 Mathematica 2.2 Program

Hydrodynamic Model of Drop Formation in a Kenics Mixer

Test of interfacial area data on Yarbro's data for Kenics Mixer

Define System Constants:

Densities of the continuous and dispersed phases (g/cm3)

rhoc = 1.0

rhod = 0.857

Viscosities of the continuous and dispersed phases (poise)

muc = 0.01

mud = 0.01

Surface Tension of the system water/dodecane (g/s2)

ST = 35

Diameter, radius, length and volume of the system (cm, cm3)

Dia = 0.635

R = Dia/2

L = 50 Dia

Vol = 3.14159 Dia^2/4 L

Area and average phase fractions (cm2, dimensionless)

area = 3.14159 R^2

phido = 0.12

phico = 1-phido

Set Re No. and calculate average viscosities and densities

re = 3081

mu = muc phico + mud phido

rho = rhoc phico + rhod phido

Calculate final linear and volumetric flowrates

Vf = ((mu re)/(Dia rho))

Qco = Vf phico area

Qdo = Vf phido area

Calculate initial flow area and initial velocities

areaf = 0.5 area (phido/phico)

Vco = Qco/(area - areaf)

Vdo = Qdo/areaf

we = rhoc Vf^2 Dia/ST

Dh = 0.25 Dia/L

Calculate initial phase fraction and interfacial area concentration

phidi = 0.5 (phido/phico)

aio = (4/(3.14159 Dia)) phido/phico

Estimate friction multiplier and calculate friction factors and pressure drop

fm = 150

f = N[fm (16/re)]

fd = f 1.2

delp = 2 rhoc/Dia Vf^2 f

Calculate wall drag, interfacial drag, interfacial pressure and virtual mass,

bubble-induced turbulence and interfacial work:

Fw = 2 rhoc/Dia Vc[z]^2 f

Fdw = 2 rhod/Dia Vd[z]^2 fd

fphid = (1 - phid[z])^2.25

Cd = 0.45 ((1 + 17.67 fphid^(6/7))/(18.67 fphid))^2

```
Cvm = 0.5 (1+12 (phido^2))

DynP = 0.25 rhoc (Vc[z] - Vd[z])^2

Fd =  3/8 phid[z] rhoc Cd ai[z] (Vc[z] - Vd[z])^2

Tzz = -0.2 phid[z] rhoc (Vc[z]-Vd[z])^2

Fvm = phid[z] rhoc Cvm (Vd[z] Vd'[z]-Vc[z] Vc'[z])

Wi = -(D[phic[z] rhoc 1/2 Vc[z]^3,z] + D[phic[z] Tzz Vc[z],z]
   - phic[z] Tzz Vc'[z] - Vc[z] phic[z] (delp - Fw)
   + Vc[z] (2 ST ai[z] - DynP) phic'[z])
```

Define Balance Equations:

Continuity Equations:

```
eqn1 = phid'[z] == (-phid[z]/Vd[z]) Vd'[z]

eqn2 = phic'[z] == (-phic[z]/Vc[z]) Vc'[z]
```

Momentum Equations:

```
eqn3 = Vd'[z] == (phid[z] (delp - Fdw)
      - (2 ST ai[z] - DynP) phid'[z]
      + (rhod/rhoc) D[phid[z] Tzz,z] - Fvm
      - Fd)/(rhod phid[z] Vd[z])

eqn4 = Vc'[z] == (phic[z] (delp - Fw) - (2 ST ai[z] - DynP) phic'[z]
      - D[phic[z] Tzz,z] + Fvm
      + Fd)/(rhoc phic[z] Vc[z])

eqn5 = ai'[z] == (1/ST Wi - ai[z] Vc'[z])/Vc[z]
```

Input Boundary Conditions and Solve:

```
sol = NDSolve[{eqn1,eqn2,eqn3,eqn4,eqn5,
 phid[0] == phidi,
 phic[0] == 1 - phidi,Vd[0] == Vdo,
 Vc[0] == Vco, ai[0] == aio},
 {phid[z],phic[z],Vd[z],Vc[z],ai[z]},
 {z,0,L}, MaxSteps->5000]
```

Output Plot for the Dispersed Phase Velocity:

```
Plot[Evaluate[Vd[z]/.sol],{z,0,5}, PlotRange->All,
AxesLabel->{"Length, cm", "Vd[z], cm/s"}]
```

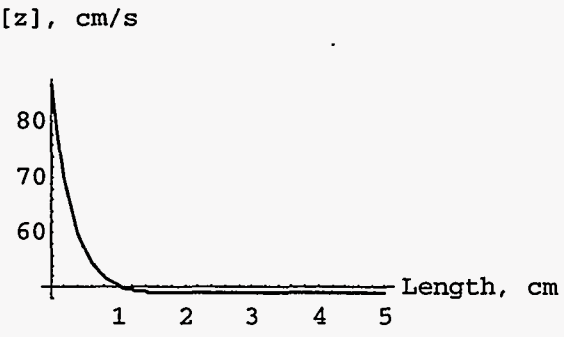

Output Plot for Continuous Phase Velocity:

```
Plot[Evaluate[Vc[z]/.sol],{z,0,5}, PlotRange->All,
AxesLabel->{"Length, cm", "Vc[z], cm/s"}]
```

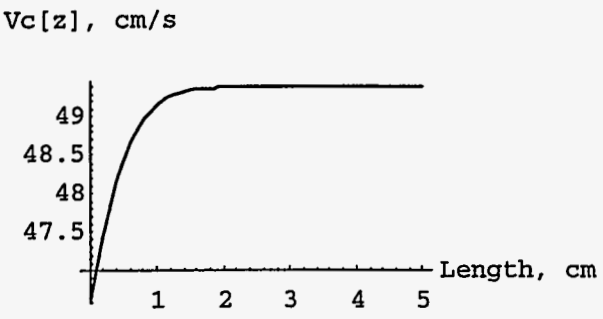

Output Plot for the Interfacial Area Concentration

Plot[Evaluate[ai[z]/.sol],{z,0,5}, PlotRange->All,

AxesLabel->{"Length, cm", "ai[z], 1/cm"}]

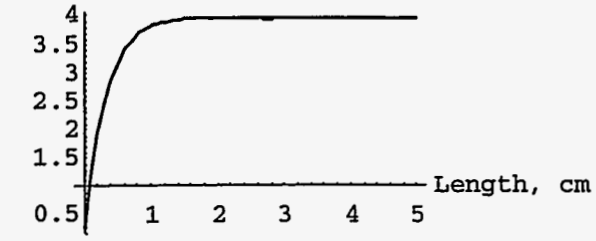

APPENDIX C
Lin

Co-Current Jet

C.1 Equation Summary

C.1.1 Model Equations

Mass:

Continuous

$$\frac{\partial}{\partial z}\alpha_c v_{cz} = 0 \tag{C.1}$$

Dispersed

$$\frac{\partial}{\partial z}\alpha_d v_{dz} = 0 \tag{C.2}$$

Momentum:

Continuous

$$\begin{aligned}
&\rho_c \alpha_c \frac{\partial}{\partial z} v_{cz} - \alpha_c \left(\frac{\partial}{\partial z} p - 2\frac{\rho_c}{D} v_{kz}^2 f_t \right) + \frac{\partial}{\partial z}\left(-\frac{1}{5}\alpha_d \rho_c \left(v_{cz} - v_{dz} \right)^2 \right) \\
&= -\left(2\sigma a_i - \frac{1}{4}\rho_c \left(v_{cz} - v_{dz} \right)^2 \right) \frac{\partial}{\partial z}\alpha_c + \frac{3}{8}\alpha_d \rho_c C_d a_i \left(v_{cz} - v_{dz} \right)^2 \\
&+ C_{vm}\alpha_d \rho_c \left[\left(v_{dz} \frac{\partial}{\partial z} v_{dz} \right) - \left(v_{cz} \frac{\partial}{\partial z} v_{cz} \right) \right]
\end{aligned} \tag{C.3}$$

Dispersed

$$\rho_d\alpha_d\frac{\partial}{\partial z}v_{dz}-\alpha_d\left(\frac{\partial}{\partial z}p-2\frac{\rho_d}{D}v_{dz}^2f_t\right)-\frac{\rho_d}{\rho_c}\frac{\partial}{\partial z}\left(-\frac{1}{5}\alpha_d\rho_c\left(v_{cz}-v_{dz}\right)^2\right)$$
$$=-\left(2\sigma a_i-\frac{1}{4}\rho_c\left(v_{cz}-v_{dz}\right)^2\right)\frac{\partial}{\partial z}\alpha_d-\frac{3}{8}\alpha_d\rho_cC_da_i\left(v_{cz}-v_{dz}\right)^2 \qquad \text{(C.4)}$$
$$-C_{vm}\alpha_d\rho_c\left[\left(v_{dz}\frac{\partial}{\partial z}v_{dz}\right)-\left(v_{cz}\frac{\partial}{\partial z}v_{cz}\right)\right]$$

Interfacial Area:

$$\frac{\partial}{\partial z}\left(a_iv_{cz}\right)=-\rho_c\frac{\partial}{\partial z}\left(\alpha_c\frac{v_{cz}^3}{2}\right)-v_{cz}\left(\alpha_c\frac{\partial}{\partial z}p-2\frac{\rho_c}{D}v_{cz}^2f_t\right)$$
$$-\frac{\partial}{\partial z}\left[\left(-\frac{1}{5}\alpha_d\rho_c\left(v_{cz}-v_{dz}\right)^2\right)v_{cz}\right] \qquad \text{(C.5)}$$
$$+\left(-\frac{1}{5}\alpha_d\rho_c\left(v_{cz}-v_{dz}\right)^2\right)\frac{\partial}{\partial z}v_{cz}+v_{cz}\left(2\sigma a_i+\frac{1}{4}\rho_c\left(v_{cz}-v_{dz}\right)^2\right)\frac{\partial}{\partial z}\alpha_c$$

C.1.2 Equation Coefficients

Drag Coefficient (Lahey, 1990)

$$F_d=\frac{3}{8}\alpha_d\rho_cC_da_i\left|v_c-v_d\right|^2 \qquad \text{(C.6a)}$$

$$C_d=0.45\left(\frac{1+17.67\left[f\left(\alpha_d\right)\right]^{6/7}}{18.67f\left(\alpha_d\right)}\right)^2 \qquad \text{(C.6b)}$$

where $f(\alpha_d)$ is defined for drops in liquids as (Ishii, 1979)

$$f\left(\alpha_d\right)=\left(1-\alpha_d\right)^{2.25} \qquad \text{(C.6c)}$$

Virtual Mass (Lahey, 1991)

$$F_{vm}=C_{vm}\alpha_d\rho_c\left[\left(v_{dz}\frac{\partial}{\partial z}v_{dz}\right)-\left(v_{cz}\frac{\partial}{\partial z}v_{cz}\right)\right] \qquad \text{(C.7a)}$$

and the virtual volume coefficient can be defined as a function of the global dispersed phase fraction (Ruggles, et.al., 1988)

$$C_{vm} = 0.5\left(1+12\left(\bar{\alpha}_d\right)^2\right) \tag{C.7b}$$

C.1.3 Turbulence (Drew and Wood, 1985)

$$\underline{\underline{R}}_c = -\frac{1}{5}\alpha_d \rho_c \left|v_{cz} - v_{dz}\right|^2 \tag{C.8a}$$

$$\underline{\underline{R}}_d = \frac{\rho_d}{\rho_c}\underline{\underline{R}}_c \tag{C.8b}$$

C.1.4 Interfacial Pressure and Friction Factor

Friction Factor (Re > 3000) (Bird, 1960, Hestroni, 1982)

$$\tau_{kw} = \frac{\Delta p}{L} = 2\frac{\rho_k}{D_h} v_{kz}^2 f_{kt} \tag{C.9a}$$

$$f_{kt} = f_m f_k \tag{C.9b}$$

$$f_d \approx 1.2 f_c \tag{C.9c}$$

where f is defined by

$$\text{(Turbulent Re} > 3000) \quad f_k = \frac{0.0791}{\text{Re}^{1/4}} \tag{D.9d}$$

Interfacial Pressure (Stuhmiller, 1977, Drew and Wood, 1985)

$$p_{ki} = 2\sigma a_i - \frac{1}{4}\rho_c \left(v_{cz} - v_{dz}\right)^2 \tag{C.10a}$$

$$\text{(horizontal systems)} \qquad \rho g \cos(\theta) = 0 \tag{C.10b}$$

C.2 Boundary Conditions

C.2.1 Initial Linear Flowrates

$$V_{co} = \frac{Q_c}{A_T - A_d} \tag{C.11a}$$

$$V_{do} = \frac{Q_d}{A_d} \tag{C.11b}$$

C.2.2 Initial Phase Fraction and Interfacial Area Concentration

$$\alpha_{di} = \frac{\pi D_d^2}{4 A_T} \tag{C.12}$$

$$a_{ii} = \frac{\pi D_d dz}{A_T dz} = \frac{\pi D_d}{A_T} \tag{C.13}$$

C.2.3 Friction Factor Multiplier

$$f_m = 4074.2\left(\overline{\alpha}_d\right)^{2.4251} \tag{C.14}$$

C.3 Results

Table C.1 Results of Modeling 0.027" Injector Co-Current Jet Data

Co-Current Jet: 0.027" injector
Fluids: Continuous Phase - water/Dispersed Phase - kerosene

αd	Re	D32m/Do	D32c/Do	del D32/Do	We	We(-3/5)
0.091	6466	0.065	0.064	0.00015	564.1	0.022
0.091	4527	0.095	0.094	0.00099	276.7	0.034
0.091	2877	0.153	0.154	-0.00087	111.7	0.059
0.091	1870	0.305	0.249	0.05654	47.2	0.099
0.074	8066	0.055	0.061	-0.00575	853.9	0.017
0.074	5649	0.083	0.087	-0.00432	418.8	0.027
0.074	3590	0.138	0.143	-0.00452	169.1	0.046
0.074	2332	0.260	0.232	0.02767	71.4	0.077
0.057	10640	0.050	0.057	-0.00765	1444	0.013
0.057	9182	0.056	0.108	-0.05234	1076	0.015
0.057	4734	0.124	0.128	-0.00375	285.9	0.034
0.057	3076	0.210	0.205	0.00513	120.7	0.056
0.038	16240	0.038	0.053	-0.01475	3259	0.008
0.038	14020	0.047	0.060	-0.01286	2428	0.009
0.038	7226	0.101	0.110	-0.00892	645.2	0.021
0.038	4696	0.167	0.167	0.00000	272.5	0.035

Table C.2 Results of Modeling 0.041" Injector Co-Current Jet Data

Co-Current Jet: 0.041" injector
Fluids: Continuous Phase - water/Dispersed Phase - kerosene

αd	Re	D32m/Do	D32c/Do	del D32/Do	We	We(-3/5)
0.091	6466	0.176	0.171	0.00447	564.1	0.022
0.091	3843	0.292	0.277	0.01505	199.3	0.042
0.091	3394	0.368	0.316	0.05196	155.4	0.048
0.091	1870	0.726	0.584	0.14209	47.2	0.099
0.074	7463	0.159	0.166	-0.00604	730.9	0.019
0.074	5649	0.223	0.212	0.01082	418.8	0.027
0.074	3590	0.437	0.326	0.11088	169.1	0.046
0.074	2332	0.728	0.508	0.22020	71.4	0.077
0.057	10640	0.128	0.136	-0.00725	1444	0.013
0.057	9182	0.172	0.153	0.01874	1076	0.015
0.057	7450	0.208	0.183	0.02484	708.1	0.019
0.057	3076	0.647	0.432	0.21578	120.7	0.056
0.038	16240	0.072	0.116	-0.04328	3259	0.008
0.038	14020	0.090	0.129	-0.03921	2428	0.009
0.038	8524	0.178	0.190	-0.01207	897.9	0.017
0.038	4695	0.387	0.340	0.04690	272.5	0.035

C.4 Mathematica 2.2 Program

Hydrodynamic Model of Drop Formation in a Co-Current Jet Mixer

Test of interfacial area data on Lin's data for Co-Current Jet Mixer

Define System Constants:

Densities of the continuous and dispersed phases (g/cm3)

rhoc = 0.997

rhod = 0.825

Viscosities of the continuous and dispersed phases (poise)

muc = 0.8705

mud = 1.55

Surface Tension of the system water/kerosene

ST = 32.3

Width, height of the rectangular flow chamber, diameter of the dispersed phase inlet and length of the system (cm)

Wc = 0.5 2.54

Hc = 0.08 2.54

Diad = 0.027 2.54

L = 18 2.54

Area of the flow chamber, continuous and dispersed phase inlets (cm2)

area = Hc Wc

areac = area - 3.14159 (Diad/2)^2

aread = 3.14159 (Diad/2)^2

Calculate hydraulic diameter and initial phase fraction

Dh = area/(2 Hc + 2 Wc)

phidi = (3.14 Diad^2)/ (4 area)

Input volumetric flowrates and calculate initial final linear velocities

Qc = 9296

Qd = 367.2

Vco = (Qc/60)/areac

Vdo = (Qd/60)/aread

Vf = (((Vdo aread) + (Vco areac))/area)

Calculate average phase fractions

phido = (Vdo aread)/(Vf area)

phico = 1 - phido

Calculate average density and viscosity to check Re No.

rho = rhoc phico + rhod phido

mu = muc phico + mud phido

we = 1.748 10^-6 rho (Vf 60)^2

nre = 0.3388 rho (Vf 60)/mu

Calculate initial interfacial area concentration, friction multiplier, friction factors

and pressure drop

aio = (3.14159 Diad)/areac

fm = 4074.2 (phido)^2.4151

Define Parameters:

f = fm (0.0791/nre^0.25)

fd = f 1.2

delp = 2 rhoc/Dh Vf^2 f

Calculate wall drag, interfacial drag, virtual mass, interfacial pressure, bubble-induced

turbulence and interfacial work:

Fw = 2 rhoc/Dh Vc[z]^2 f

Fdw = 2 rhod/Dh Vd[z]^2 fd

fphid = (1 - phid[z])^2.25

Cd = 0.45 ((1 + 17.67 fphid^(6/7))/(18.67 fphid))^2

Cvm = 0.5 (1+12 (phido^2))

DynP = 0.25 rhoc (Vc[z] - Vd[z])^2

Fd = 3/8 phid[z] rhoc Cd ai[z] (Vc[z] - Vd[z])^2

Tzz = - 0.2 phid[z] rhoc (Vc[z]-Vd[z])^2

Fvm = phid[z] rhoc Cvm (Vd[z] Vd'[z]-Vc[z] Vc'[z])

Wi = -(D[phic[z] rhoc 1/2 Vc[z]^3,z] + D[phic[z] Tzz Vc[z],z]

- phic[z] Tzz Vc'[z] - Vc[z] phic[z] (delp - Fw)

+ Vc[z] (2 ST ai[z] - DynP) phic'[z])

Define Balance Equations:

Continuity Equations:

eqn1 = phid'[z] == (-phid[z]/Vd[z]) Vd'[z]

eqn2 = phic'[z] == (-phic[z]/Vc[z]) Vc'[z]

Momentum Equations:

eqn3 = Vd'[z] == (phid[z] (delp - Fdw) - (2 ST ai[z] - DynP) phid'[z]

- (rhod/rhoc) D[phid[z] Tzz,z] - Fvm

- Fd)/(rhod phid[z] Vd[z])

eqn4 = Vc'[z] == (phic[z] (delp - Fw) - (2 ST ai[z] - DynP) phic'[z]

+ D[phic[z] Tzz,z] + Fvm

+ Fd)/(rhoc phic[z] Vc[z])

eqn5 = ai'[z] == (1/ST Wi - ai[z] Vc'[z])/Vc[z]

Input Boundary Conditions and Solve:

sol = NDSolve[{eqn1,eqn2,eqn3,eqn4,eqn5,

phid[0] == phidi,

phic[0] == 1 - phidi,Vd[0] == Vdo,

Vc[0] == Vco, ai[0] == aio}, {phid[z],phic[z],Vd[z],Vc[z],ai[z]},

{z,0,L}, MaxSteps->5000]

Output Plot for the Interfacial Area Concentration

Plot[Evaluate[ai[z]/.sol],{z,0,15}, PlotRange->All,

AxesLabel->{"Length, cm","ai[z], 1/cm"}]

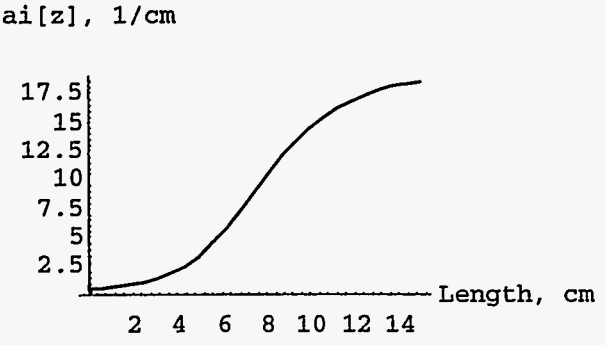

Output Plot for the Dispersed Phase Velocity

Plot[Evaluate[Vd[z]/.sol],{z,0,15}, PlotRange->All,

AxesLabel->{"Length, cm","Vd[z], cm/s"}]

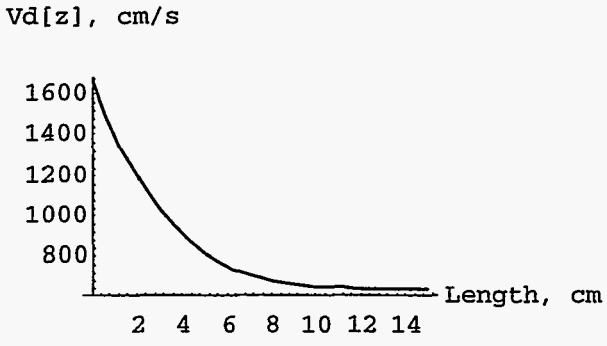

Output Plot for Continuous Phase Velocity:

Plot[Evaluate[Vc[z]/.sol],{z,0,15}, PlotRange->All,

AxesLabel->{"Length, cm","Vc[z], cm/s"}]

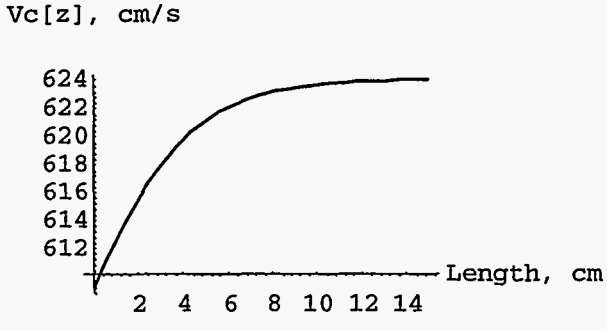

APPENDIX D

Reimus

Tee Mixer

D.1 Equation Summary

D.1.1 Model Equations

Mass:

Continuous

$$\frac{\partial}{\partial z}\alpha_c v_{cz} = 0 \tag{D.1}$$

Dispersed

$$\frac{\partial}{\partial z}\alpha_d v_{dz} = 0 \tag{D.2}$$

Momentum:

Continuous

$$\begin{aligned}
&\rho_c \alpha_c \frac{\partial}{\partial z} v_{cz} - \alpha_c \left(\frac{\partial}{\partial z} p - 2\frac{\rho_c}{D} v_{kz}^2 f_t \right) + \frac{\partial}{\partial z}\left(-\frac{1}{5}\alpha_d \rho_c \left(v_{cz} - v_{dz}\right)^2 \right) \\
&= -\left(2\sigma a_i - \frac{1}{4}\rho_c \left(v_{cz} - v_{dz}\right)^2 \right) \frac{\partial}{\partial z}\alpha_c - \frac{3}{8}\alpha_d \rho_c C_d a_i \left(v_{cz} - v_{dz}\right)^2 \\
&- C_{vm}\alpha_d \rho_c \left[\left(v_{dz} \frac{\partial}{\partial z} v_{dz} \right) - \left(v_{cz} \frac{\partial}{\partial z} v_{cz} \right) \right]
\end{aligned} \tag{D.3}$$

Dispersed

$$\rho_d\alpha_d\frac{\partial}{\partial z}v_{dz}-\alpha_d\left(\frac{\partial}{\partial z}p-2\frac{\rho_d}{D}v_{dz}^2f_t\right)-\frac{\rho_d}{\rho_c}\frac{\partial}{\partial z}\left(-\frac{1}{5}\alpha_d\rho_c\left(v_{cz}-v_{dz}\right)^2\right)$$
$$=-\left(2\sigma a_i-\frac{1}{4}\rho_c\left(v_{cz}-v_{dz}\right)^2\right)\frac{\partial}{\partial z}\alpha_d+\frac{3}{8}\alpha_d\rho_cC_da_i\left(v_{cz}-v_{dz}\right)^2 \qquad \text{(D.4)}$$
$$+C_{vm}\alpha_d\rho_c\left[\left(v_{dz}\frac{\partial}{\partial z}v_{dz}\right)-\left(v_{cz}\frac{\partial}{\partial z}v_{cz}\right)\right]$$

Interfacial Area:

$$\frac{\partial}{\partial z}\left(a_iv_{cz}\right)=-\rho_c\frac{\partial}{\partial z}\left(\alpha_c\frac{v_{cz}^3}{2}\right)-v_{cz}\left(\alpha_c\frac{\partial}{\partial z}p-2\frac{\rho_c}{D}v_{cz}^2f_t\right)$$
$$-\frac{\partial}{\partial z}\left[\left(-\frac{1}{5}\alpha_d\rho_c\left(v_{cz}-v_{dz}\right)^2\right)v_{cz}\right] \qquad \text{(D.5)}$$
$$-\left(-\frac{1}{5}\alpha_d\rho_c\left(v_{cz}-v_{dz}\right)^2\right)\frac{\partial}{\partial z}v_{cz}+v_{cz}\left(2\sigma a_i+\frac{1}{4}\rho_c\left(v_{cz}-v_{dz}\right)^2\right)\frac{\partial}{\partial z}\alpha_c$$

D.1.2 Equation Coefficients

Drag Coefficient (Lahey, 1990)

$$F_d=\frac{3}{8}\alpha_d\rho_cC_da_i\left|v_c-v_d\right|^2 \qquad \text{(D.6a)}$$

$$C_d=0.45\left(\frac{1+17.67\left[f\left(\alpha_d\right)\right]^{6/7}}{18.67f\left(\alpha_d\right)}\right)^2 \qquad \text{(D.6b)}$$

where $f(\alpha_d)$ is defined for drops in liquids as (Ishii, 1979)

$$f\left(\alpha_d\right)=\left(1-\alpha_d\right)^{2.25} \qquad \text{(D.6c)}$$

Virtual Mass (Lahey, 1991)

$$F_{vm}=C_{vm}\alpha_d\rho_c\left[\left(v_{dz}\frac{\partial}{\partial z}v_{dz}\right)-\left(v_{cz}\frac{\partial}{\partial z}v_{cz}\right)\right] \qquad \text{(D.7a)}$$

and the virtual volume coefficient can be defined as a function of the global dispersed phase fraction (Ruggles, et.al., 1988)

$$C_{vm} = 0.5\left(1+12\left(\overline{\alpha}_d\right)^2\right) \tag{D.7b}$$

D.1.3 Turbulence (Drew and Wood, 1985)

$$\underline{\underline{R}}_c = -\frac{1}{5}\alpha_d \rho_c \left|v_{cz} - v_{dz}\right|^2 \tag{D.8a}$$

$$\underline{\underline{R}}_d = \frac{\rho_d}{\rho_c}\underline{\underline{R}}_c \tag{D.8b}$$

D.1.4 Interfacial Pressure and Friction Factor

Friction Factor (Re > 3000) (Bird, 1960, Hestroni, 1982)

$$\tau_{kw} = \frac{\Delta p}{L} = 2\frac{\rho_k}{D_h} v_{kz}^2 f_{kt} \tag{D.9a}$$

$$f_{kt} = f_m f_k \tag{D.9b}$$

$$f_d \approx 1.2 f_c \tag{D.9d}$$

where f is defined by

$$\text{(Turbulent Re} > 3000) \quad f_k = \frac{0.0791}{\text{Re}^{1/4}} \tag{D.9c}$$

Interfacial Pressure (Stuhmiller, 1977, Drew and Wood, 1985)

$$p_{ki} = 2\sigma a_i - \frac{1}{4}\rho_c\left(v_{cz} - v_{dz}\right)^2 \tag{D.10a}$$

$$\text{(horizontal systems)} \qquad \rho g \cos(\theta) = 0 \tag{D.10b}$$

D.2 Boundary Conditions

D.2.1 Initial Linear Velocities

$$V_{doz} = \frac{Q_d}{A_d}\cot(\theta) \tag{D.11a}$$

$$V_{coz} = \frac{Q_c}{A_c}\cos(90^\circ - \theta) \tag{D.11b}$$

D.2.2 Contact Angle Theta

$$\theta = datafit \tag{D.12}$$

D.2.3 Estimating Initial Phase Fraction and Interfacial Area

$$\alpha_{di} = \cos(\theta) \tag{D.13}$$

$$a_{ii} = 100\alpha_d \tag{D.14}$$

D.2.4 Friction Factor Multiplier

$$f_m = 100\overline{\alpha}_d \tag{D.15}$$

D.3 Results

Table D.1 Results of Modeling 0.2 cm Diameter Tee Mixer Data

Tee Mixer: 0.2 cm diameter
Fluids: Continuous Phase - water/Dispersed Phase - kerosene

αd	Re	D32m/Do	D32c/Do	del D32/Do	We	We(-3/5)
0.1	31060	0.046	0.087	-0.0419	10860	0.0038
0.1	36460	0.038	0.063	-0.0248	16140	0.0030
0.1	43760	0.036	0.046	-0.0099	22540	0.0024
0.1	51060	0.034	0.036	-0.0019	29610	0.0021
0.06	29950	0.040	0.057	-0.0168	10030	0.0040
0.06	34600	0.032	0.039	-0.0079	14900	0.0031
0.06	42010	0.028	0.029	-0.0007	20800	0.0026
0.06	48700	0.026	0.022	0.0042	27340	0.0022
0.01	27620	0.045	0.043	0.0019	9119	0.0042
0.01	33140	0.030	0.029	0.0006	13550	0.0033
0.01	40230	0.022	0.021	0.0006	18920	0.0027
0.01	46630	0.018	0.016	0.0014	24860	0.0023

D.4 Mathematica 2.2 Program

Hydrodynamic Model of Drop Formation in a Tee Mixer

Test of interfacial area data on Reimus' data for a Tee Mixer

Define System Constants:

Densities of the continuous and dispersed phases (g/cm3)

rhoc = 0.9968

rhod = 0.826

Viscosities of the continuous and dispersed phases

muc = 0.008705

mud = 0.0154

Surface Tension of the system water/kerosene

ST = 32.6

Diameter of the inlet and outlet flow channels (cm)

Dia = 0.2

Diac = 0.2

Diad = 0.2

Radius, length and volume of the system (cm, cm3)

R = Dia/2

L = 21 2.54

Vol = 3.14159 Dia^2/4 L

Area of the inlet and outlet flow channels (cm2)

area = 3.14159 R^2

areac = 3.14159 R^2

aread = 3.14159 R^2

Input volumetric flowrates and calculate average phase fractions

Qc = 2280

Qd = 253.3

phido = N[Qd/(Qc + Qd)]

phico = 1-phido

Calculate average linear velocities (cm/s)

Vco = Qc/(60 area)

Vdo = Qd/(60 area)

Estimate contact angle and calculate initial linear velocities

theta = 89.827 (3.14159/180)

Vdi = Vdo Cot[theta]

Vci = Vco Cos[3.14159/2 - theta]

Estimate initial phase fractions and interfacial area concentration

phidi = Cos[theta]

phici = Cos[3.14159/2 - theta]

aio = 100 phido

Check final linear velocity and calculate We and Re No.

Vf = Vco + Vdo

we = rhoc Vco^2 Dia/ST

nre = rhoc Dia Vf/muc

Estimate friction factor multiplier and calculate friction factor and pressure drop

fm = 100 phido

f = fm (.0791/nre^0.25)

fd = f 1.207

delp = 2 rhoc/Dia Vf^2 f

Calculate wall drag, interfacial drag, virtual mass, interfacial pressure, bubble-induced turbulence and interfacial work:

```
Fw = 2 rhoc/Dia Vc[z]^2 f

Fdw = 2 rhod/Dia Vd[z]^2 fd

fphid = (1 - phid[z])^2.25

Cd = 0.45 ((1 + 17.67 fphid^(6/7))/(18.67 fphid))^2

Cvm = 0.5 (1+12 (phido^2))

DynP = .25 rhoc (Vc[z] - Vd[z])^2

Fd =  3/8 phid[z] rhoc Cd ai[z] (Vc[z] - Vd[z])^2

Tzz = -0.2 phid[z] rhoc (Vc[z]-Vd[z])^2

Fvm = phid[z] rhoc Cvm (Vd[z] Vd'[z]-Vc[z] Vc'[z])

Wi = -(D[phic[z] rhoc 1/2 Vc[z]^3,z] + D[phic[z] Tzz Vc[z],z]
   - phic[z] Tzz Vc'[z] - Vc[z] phic[z] (delp - Fw)
   + Vc[z] (2 ST ai[z] - DynP) phic'[z])
```

Define Balance Equations:

Continuity Equations:

```
eqn1 = phid'[z] == (-phid[z]/Vd[z]) Vd'[z]

eqn2 = phic'[z] == (-phic[z]/Vc[z]) Vc'[z]
```

Momentum Equations:

```
eqn3 = Vd'[z] == (phid[z] (delp - Fdw) - (2 ST ai[z] - DynP) phid'[z]
        + (rhod/rhoc) D[phid[z] Tzz,z] + Fvm
```

+ Fd)/(rhod phid[z] Vd[z])

eqn4 = Vc'[z] == (phic[z] (delp - Fw) - (2 ST ai[z] - DynP) phic'[z]

- D[phic[z] Tzz,z] - Fvm

- Fd)/(rhoc phic[z] Vc[z])

eqn5 = ai'[z] == (1/ST Wi - ai[z] Vc'[z])/(Vc[z])

Input Boundary Conditions and Solve:

sol = NDSolve[{eqn1,eqn2,eqn3,eqn4,eqn5,

phid[0] == phidi,phic[0] == phici, Vd[0] == Vdi,Vc[0] == Vci, ai[0] == aio},

{phid[z],phic[z],Vd[z],Vc[z],ai[z]}, {z,0,L}, MaxSteps->5000]

Output Plot of the Interfacial Area Concentration

Plot[Evaluate[ai[z]/.sol],{z,0,5}, PlotRange->All,

AxesLabel->{"Length, cm","ai[z], 1/cm"}]

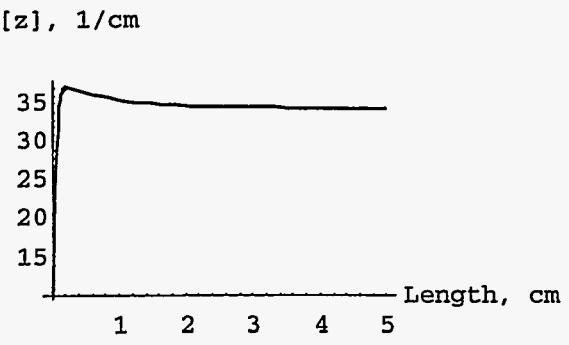

Output Plot of Dispersed Phase Velocity:

Plot[Evaluate[Vd[z]/.sol],{z,0,5}, PlotRange->All,

AxesLabel->{"Length, cm","Vd[z], cm/s"}]

Output Plot for Continuous Phase Velocity:

Plot[Evaluate[Vc[z]/.sol],{z,0,5}, PlotRange->All,

AxesLabel->{"Length, cm","Vc[z], cm/s"}]

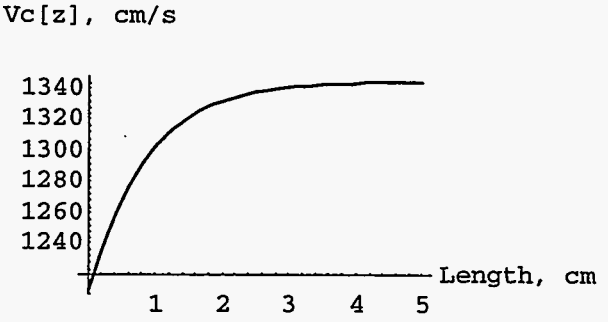

APPENDIX E

Results

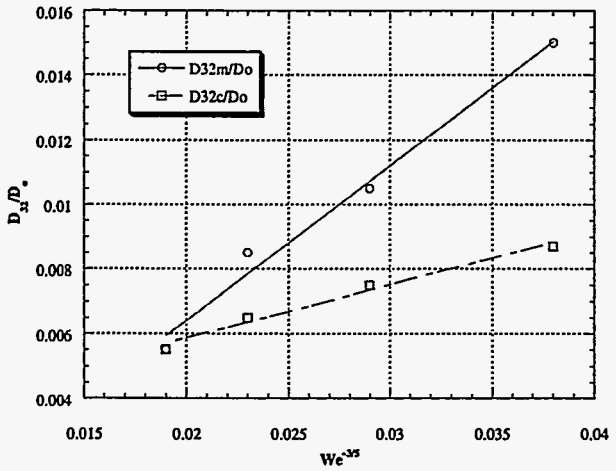

Figure E.1 Comparison of Data with the Model for a 1.91 cm Kenics Mixer

(12,000 < Re < 21,000 at a_d = 0.001)

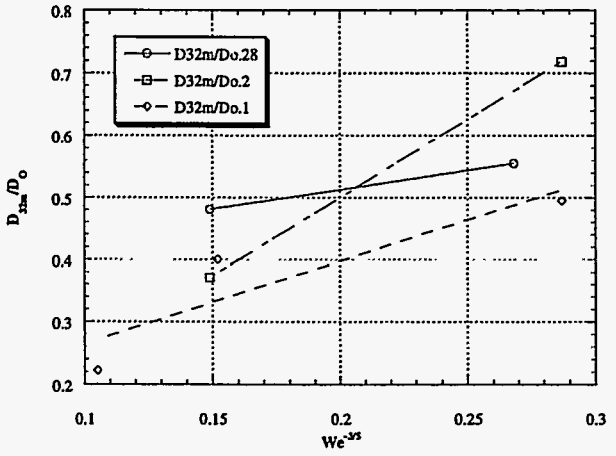

Figure E.2 Experimental Data for a 0.635 cm Diameter Kenics Mixer at Low Re

(1300 < Re <3100 and 0.1 < a_d < 0.28)

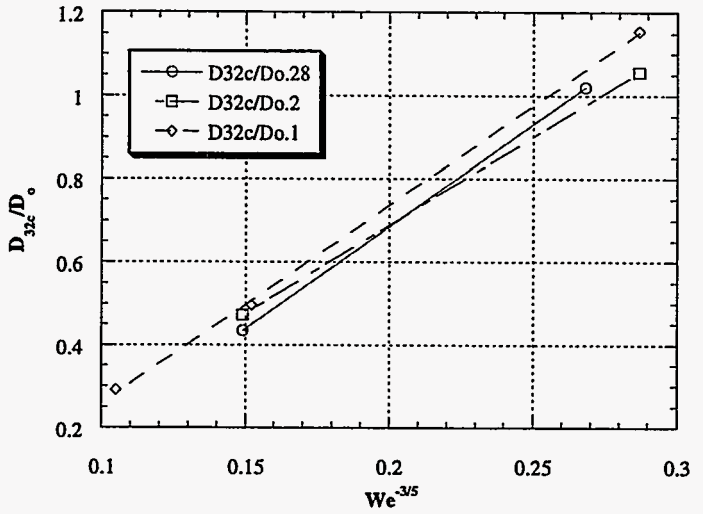

Figure E.3 Calculated Data for 0.635 cm Diameter Kenics Mixer

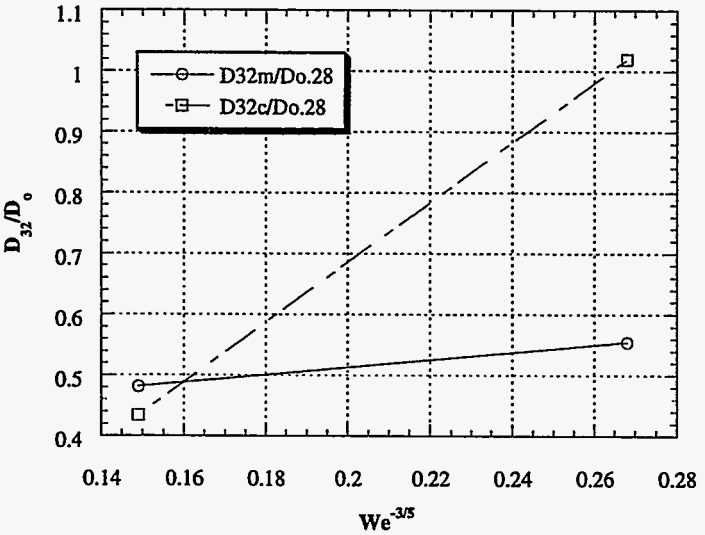

Figure E.4 Comparison of Experimental and Calculated Values for Drop Size at $a_d = 0.28$

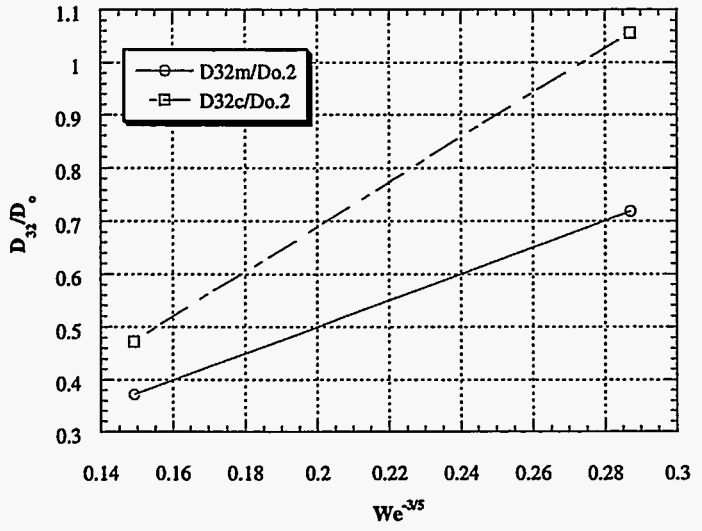

Figure E.5 Comparison of Experimental and Calculated Values for $a_d = 0.2$

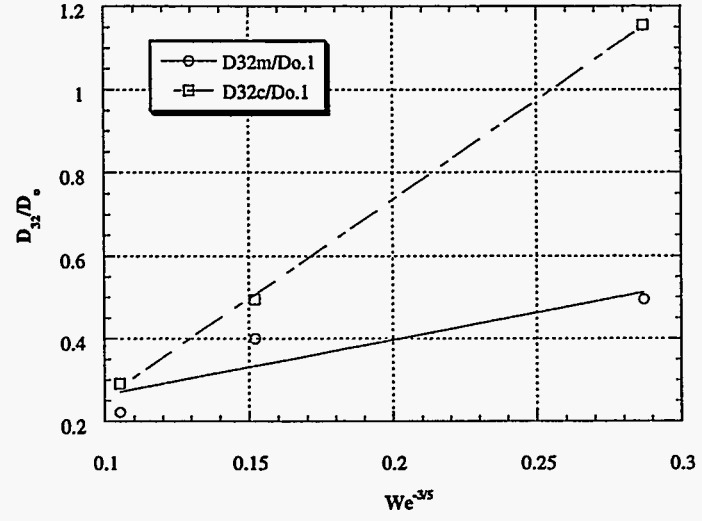

Figure E.6 Comparison of Experimental and Calculated Values for $a_d = 0.1$

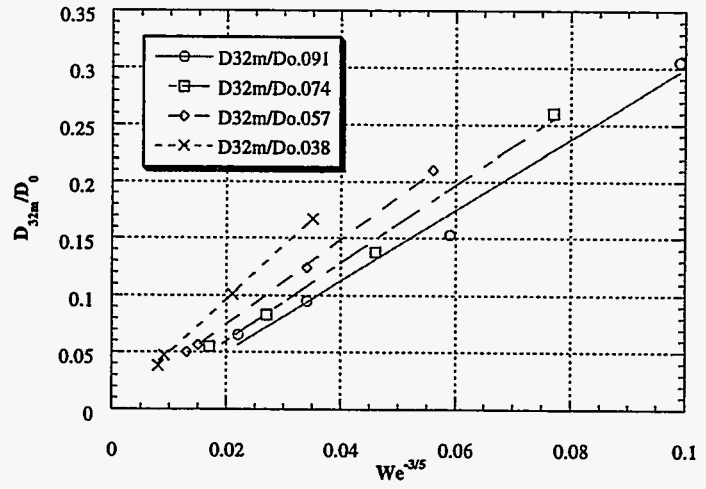

Figure E.7 Experimental Data for the 0.027" Injector

(2300 < Re < 16,300 and 0.038 < a_d < 0.091)

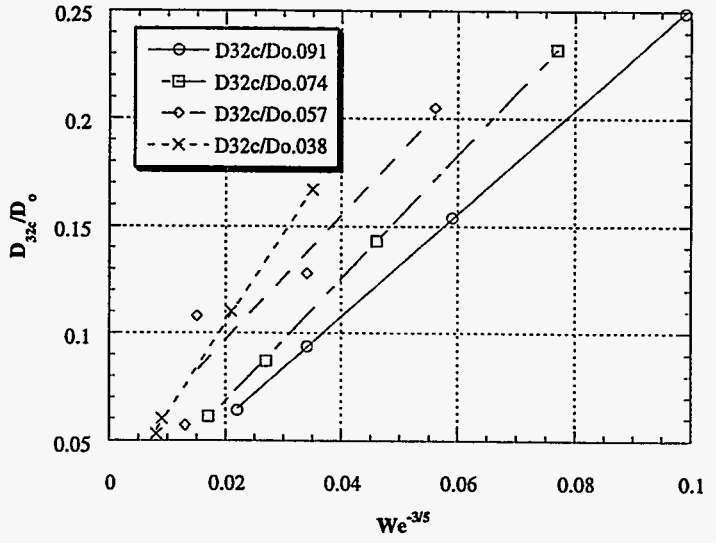

Figure E.8 Calculated Values for the 0.027" Injector

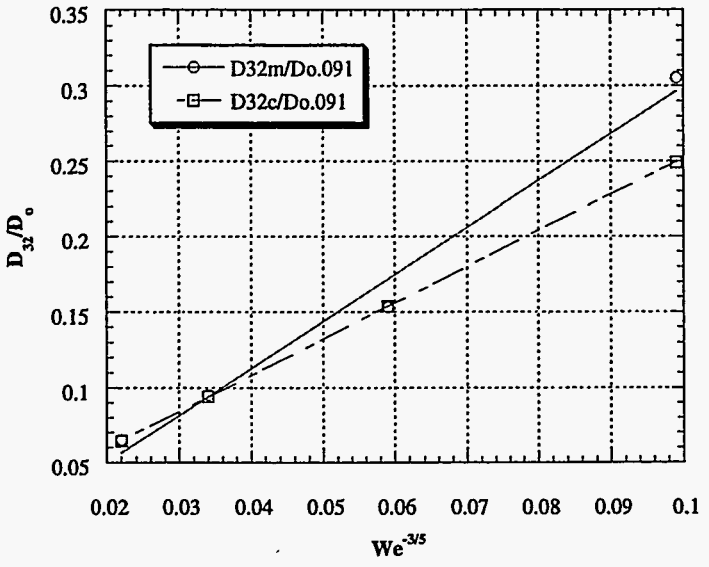

Figure E.9 Comparison of Experimental and Calculated Values for the 0.027" Injector at $a_d = 0.091$

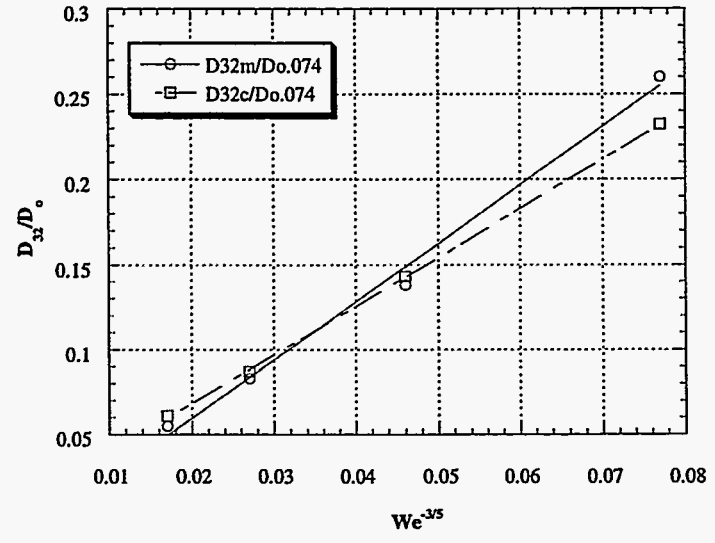

Figure E.10 Comparison of Experimental and Calculated Values for the 0.027" Injector at $a_d = 0.074$

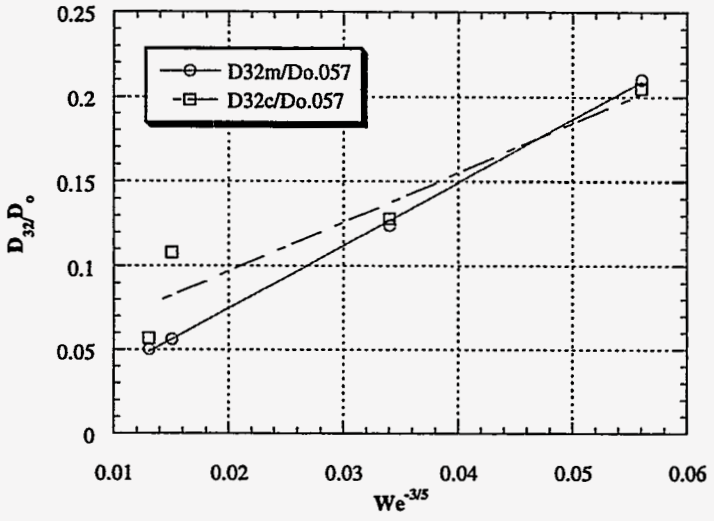

Figure E.11 Comparison of Experimental and Calculated Values for the 0.027" Injector at $a_d = 0.057$

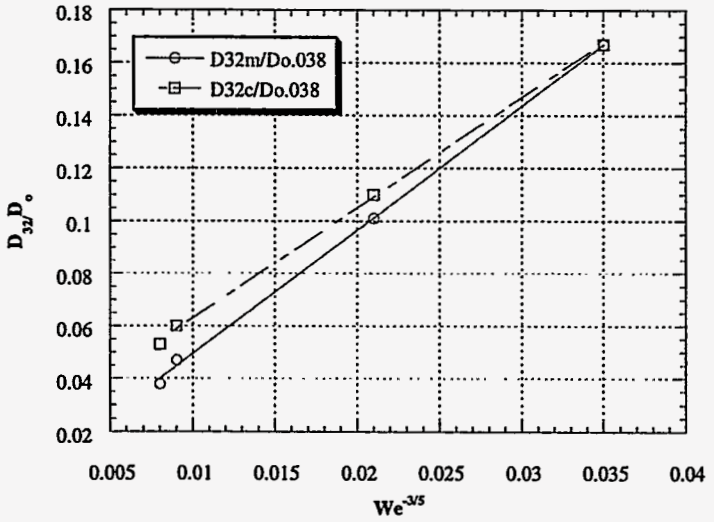

Figure E.12 Comparison of Experimental and Calculated Values for the 0.027" Injector at $a_d = 0.038$

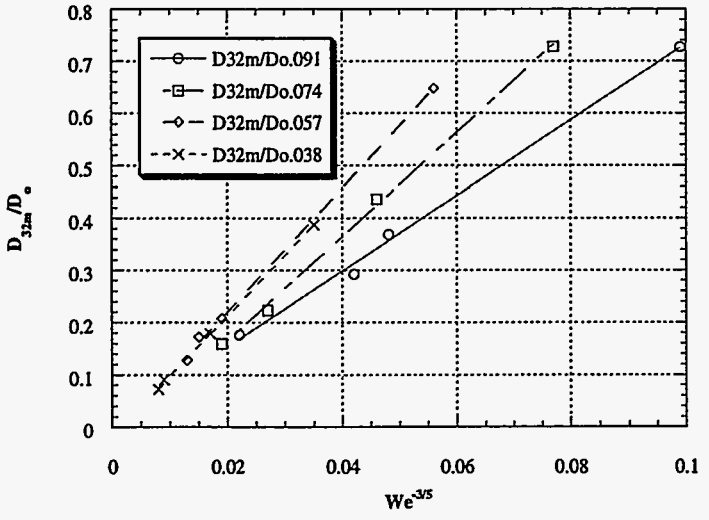

Figure E.13 Experimental Data for the 0.041" Injector

(2300 < Re < 16,300 and 0.038 < a_d < 0.091)

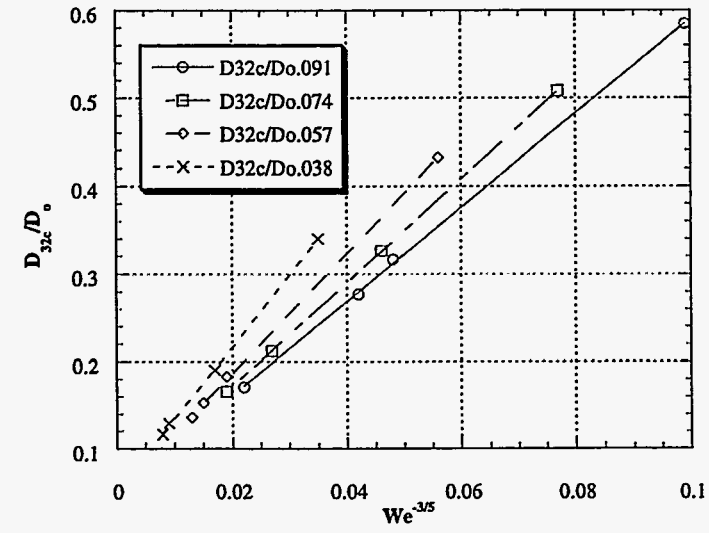

Figure E.14 Calculated Values for the 0.041" Injector

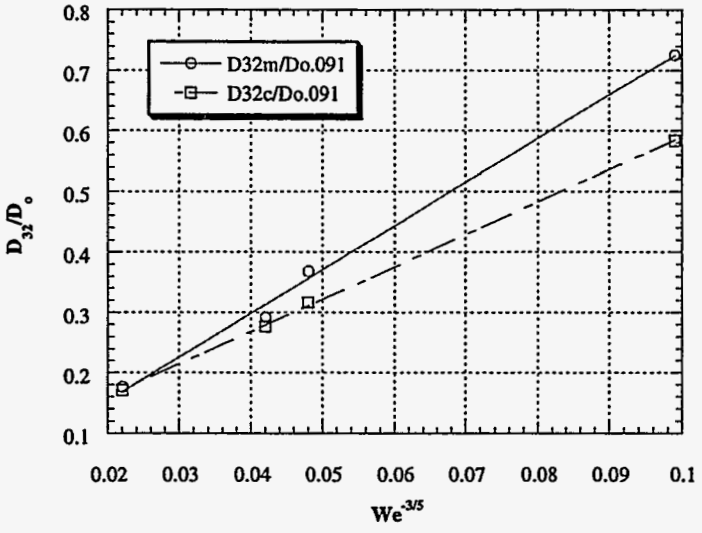

Figure E.15 Comparison of Experimental and Calculated Values for the 0.041" Injector at $a_d = 0.091$

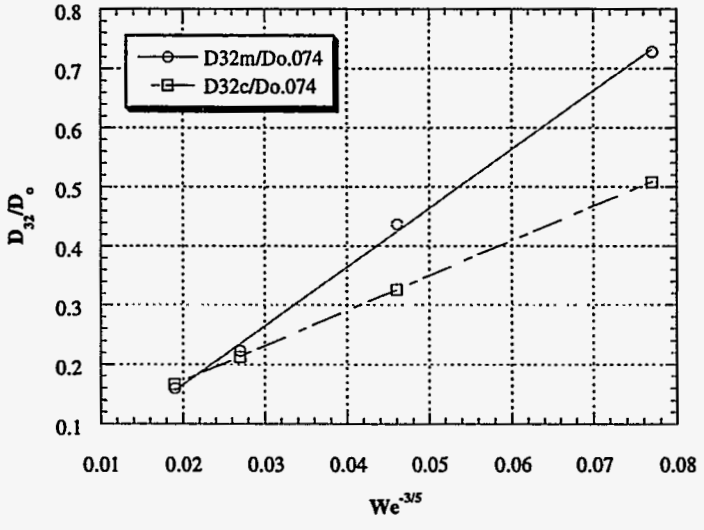

Figure E.16 Comparison of Experimental and Calculated Values for the 0.041" Injector at $a_d = 0.074$

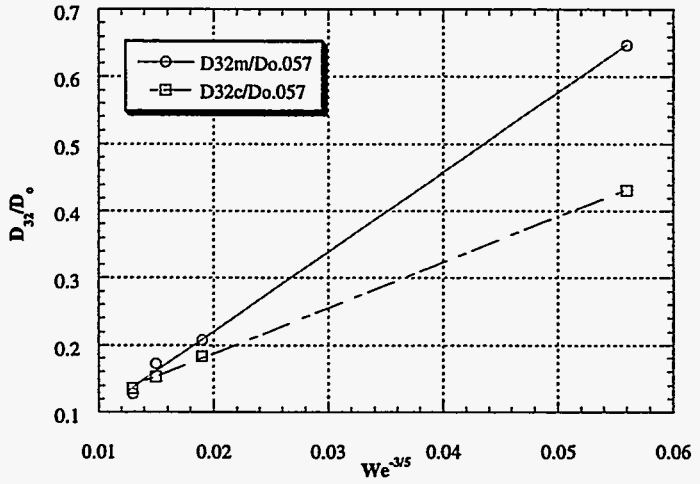

Figure E.17 Comparison of Experimental and Calculated Values for the 0.041" Injector at $a_d = 0.057$

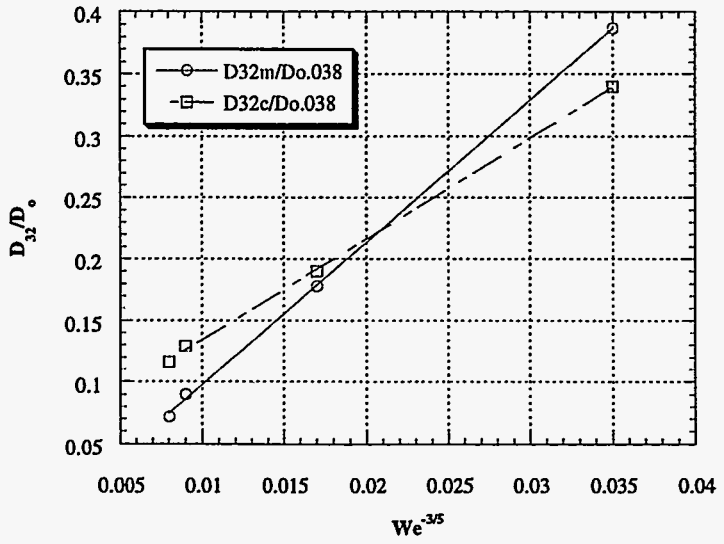

Figure E.18 Comparison of Experimental and Calculated Values for the 0.041" Injector at $a_d = 0.038$

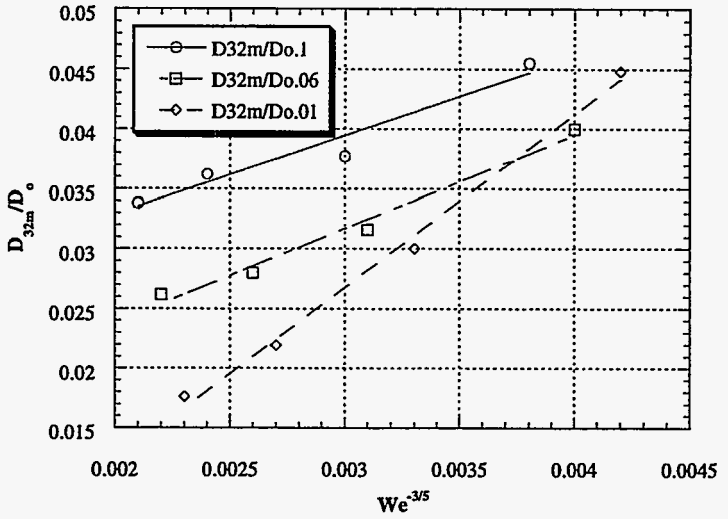

Figure E.19 Experimental Values for the 0.2 cm Tee Mixer

(27,000 < Re < 51,000 and 0.01 < a_d < 0.1)

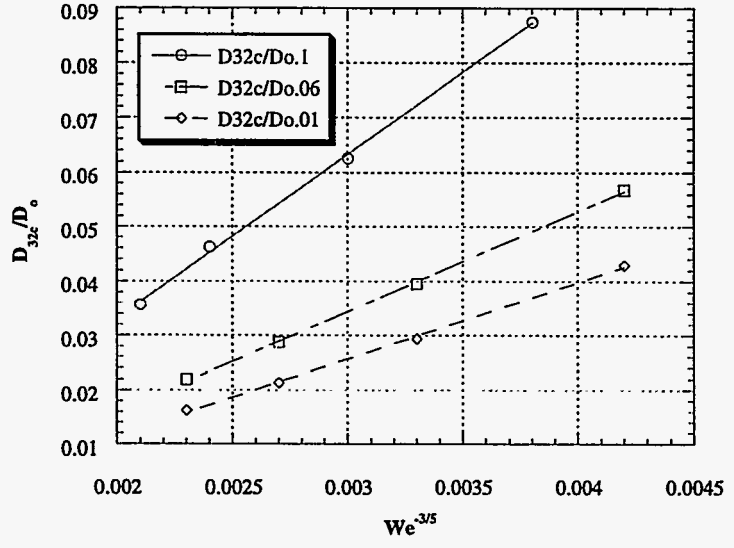

Figure E.20 Calculated Values for the 0.2 cm Tee Mixer

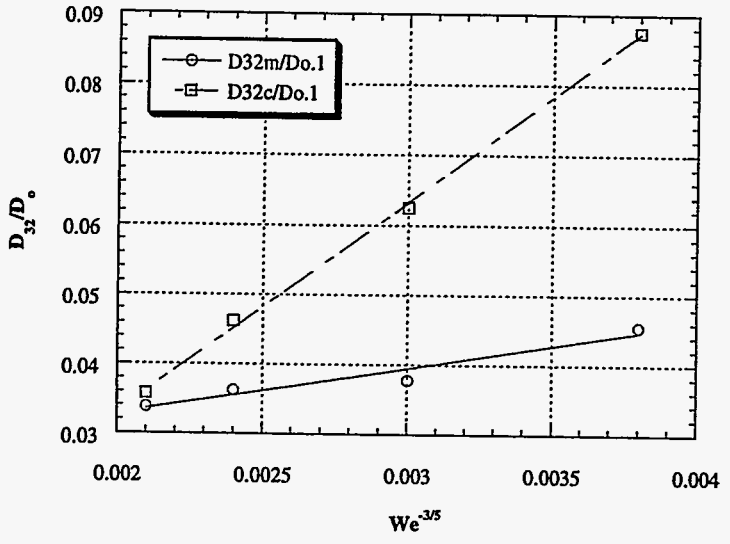

Figure E.21 Comparison of Experimental and Calculated Values for the 0.2 cm Tee at $a_d = 0.1$

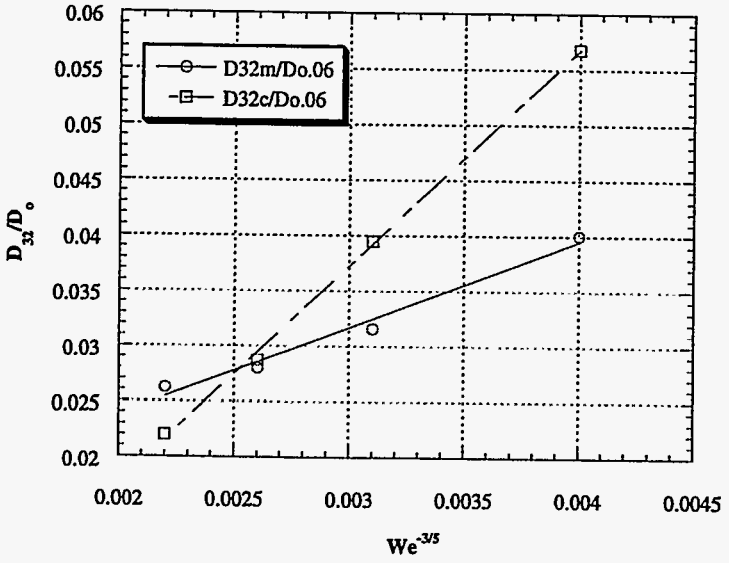

Figure E.22 Comparison of Experimental and Calculated Value for the 0.2 cm Tee at $a_d = 0.06$

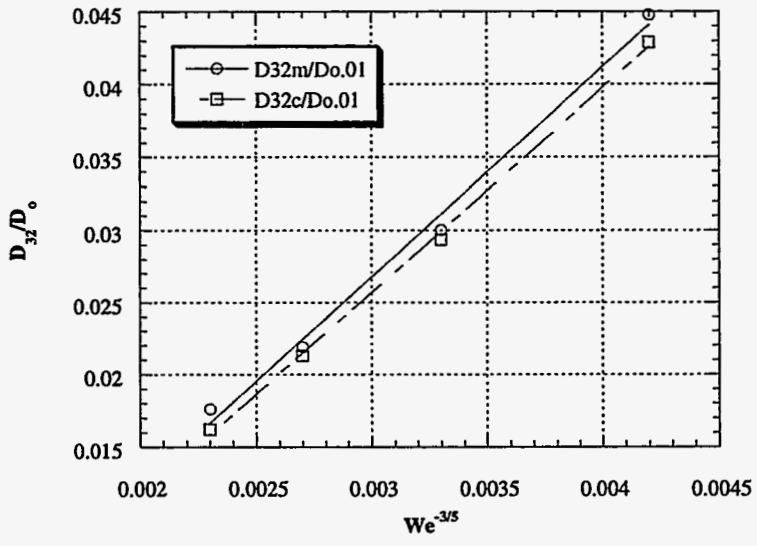

Figure E.23 Comparison of Experimental and Calculated Values for the 0.2 cm Tee at $a_d = 0.01$